High-Performance Computing in Biomedical Research

Edited by
Theo C. Pilkington
Bruce Loftis
Joe F. Thompson
Savio L-Y. Woo
Thomas C. Palmer
Thomas F. Budinger

CRC Press
Taylor & Francis Group
Boca Raton London New York

CRC Press is an imprint of the
Taylor & Francis Group, an **informa** business

CRC Press
Taylor & Francis Group
6000 Broken Sound Parkway NW, Suite 300
Boca Raton, FL 33487-2742

ISBN-13: 978-0-8493-4474-9 (hbk)

Visit the Taylor & Francis Web site at
http://www.taylorandfrancis.com

and the CRC Press Web site at
http://www.crcpress.com

Library of Congress Cataloging-in-Publication Data

High-performance computing in biomedical research/edited by Theo Pilkington ... [et al.].
p. cm.
ISBN 0-8493-4474-3
1. Medicine—Research—Data processing. 2. Medicine—Research-Computer simulation. 3. Supercomputers. I. Pilkington, Theo C.
[DNLM: 1. Biomedical Engineering. 2. Computers. 3. Diagnosis, Computer-Assisted. W 26.5 H638]
R853.D37H54 1993
610'.285—dc20
DNLM/DLC
for Library of Congress 92-20086
CIP

Library of Congress Card Number 92-20086

PREFACE

Advances in high-performance computing (HPC) can now provide the capabilities for highly sophisticated computer modeling of biomedical phenomena. Improvements in the speed of processors, programming, and graphics interfaces allow biomedical researchers to use computing power equivalent to the supercomputers of a few years ago to investigate research problems and to display complex data in understandable ways.

The purpose of the Cray Symposium on High-Performance Computing in Biomedical Research was to summarize the current status and project promising future potentials using examples of the best practice in research today. The Cray Symposium was held on October 14 and 15 on the campus of the North Carolina Supercomputing Center at Research Triangle Park, North Carolina. This research monograph is the proceedings of that symposium.

Although HPC in biomedical research cannot be comprehensively covered within the bounds of a single book, the editors selected representative areas which emphasize applications and the framework for the future. This monograph is divided into seven sections: (1) anatomical heart models and mechanics, (2) grids and bioelectric models, (3) inverse problems and computational methods, (4) distributed computing and biomechanics, (5) HPC and cardiac electrophysiology, (6) HPC and visualization, and (7) the future. It is to future high-performance computing and biomedical research that this monograph is dedicated.

Theo Pilkington
Bruce Loftis
Joe Thompson
Savio Woo
Thomas Palmer
Thomas Budinger

ACKNOWLEDGMENTS

This monograph and the associated symposium could not have been accomplished without substantial financial support from Cray Research, Inc. We are sincerely grateful to our friends Hugh Patrick, Cray Research Account Manager for North Carolina, and Eric Pitcher, Chuck Swanson, and Bill Samayoa from Cray Research headquarters in Eagan, Minnesota.

We gratefully acknowledge the support provided by Jeff Holtmeier and Sandy Pearlman at CRC Press and the help of Don Enichen, Business Manager at the North Carolina Supercomputing Center.

We appreciate the diligence and responsiveness of the reviewers of the manuscripts: Roger C. Barr, Craig J. Benham, John A. Board, John F. Dannenhoffer, Solomon R. Eisenberg, Carey E. Floyd, Jr., Boyd Gatlin, Ronald J. Jaszczak, Christopher R. Johnson, James P. Keener, Carl T. Kelley, Wanda Krassowska, L. Joshua Leon, Robert L. Lux, Lee Makowski, Barry S. Myers, Y. C. Pao, Shalom R. Rackovsky, Richard A. Robb, Bradley J. Roth, Tamar Schlick, Edward J. Shaughnessy, Mark F. Smith, Robert E. Smith, Joseph L. Steger, John E. Straub, and Jennifer S. Wayne.

And finally, we have been indeed fortunate to have assistance, nurturing, cajoling, encouragement, and superb administrative support from Martha Absher from the Engineering Research Center at Duke University.

EDITORS

Theo Pilkington, Ph.D., presently serves as Professor of Biomedical and Electrical Engineering and Director of the Duke–North Carolina National Science Foundation/Engineering Research Center (NSF/ERC) for Emerging Cardiovascular Technologies. Since 1963, he has been on the Duke faculty, where he was Founding Chairman of the Department of Biomedical Engineering. A North Carolina native, Dr. Pilkington received his B.E.E. from North Carolina State University in Raleigh in 1958 and his M.S. and Ph.D. (EE) degrees from Duke University in 1960 and 1963, respectively.

Dr. Pilkington currently serves on the AIMBE Fellows Selection Committee, the IEEE/EMBS Fellows Selection Committee, the IEEE Committee on Engineering Accreditation Activities, the *CRC Critical Reviews in Bioengineering* Editorial Board, and the Whitaker Foundation Scientific Advisory Committee. He has also served as Editor of *CRC Critical Reviews in Bioengineering* and *IEEE Transactions on Biomedical Engineering* and on the Editorial Board of the *Proceedings of the IEEE*. He has served as principal investigator on numerous grants, including a Cardiovascular Biomedical Engineering Training Grant, now in its 26th year of continuous NIH funding. He has served as an accreditation visitor or consultant to a large majority of the 22 accredited biomedical engineering programs, chaired the IEEE/ASME Committee that established Guidelines for Accreditation of Biomedical Engineering Programs, and was instrumental in establishing institutional commitment and critical faculty mass as requirements for biomedical engineering accreditation.

Honors include the ASEE Biomedical Engineering Educator of the Year Award, IEEE Centennial Medal, selection as an IEEE Fellow and as an AIMBE Founding Fellow, and his Ridge Woode Beagles winning the NBC Five Couple competition three years in a row (1985, 1986, and 1987).

Bruce Loftis, Ph.D., has a long history in high-performance computing and is now a Computational Scientist at the North Carolina Supercomputing Center. Dr. Loftis is also an Adjunct Professor in the Department of Operations Research at North Carolina State University.

He earned B.S. and M.S. engineering degrees from the University of Texas and a Ph.D. in water resources engineering from Colorado State University. Current research interests include modeling of environmental systems and high-performance numerical algorithms.

Joe F. Thompson, Ph.D., is currently Director of the NSF Engineering Research Center for Computational Field Simulation at Mississippi State University, where he is also a Distinguished Professor of Aerospace Engineering.

After receiving his undergraduate degree in physics with highest honors and his master's degree in aerospace engineering from Mississippi State University, Dr. Thompson joined the NASA Marshall Space Flight Center in Huntsville, Alabama, where he was involved in the Apollo space program. Following four years of teaching in the Department of Aerospace Engineering at Mississippi State University, Dr. Thompson pursued his Ph.D. in aerospace engineering at The Georgia Institute of Technology, where he was an NSF Science Faculty Fellow. Upon receiving his Ph.D. in 1971, he returned to MSU's Department of Aerospace Engineering and rose to full Professor in 1975, being named a Distinguished Professor in the department in 1988.

Aerodynamics and computational fluid dynamics have been Dr. Thompson's teaching areas, and his many years of research have been concentrated in numerical grid generation and its use in computational fluid dynamics. He has published numerous journal articles and conference presentations in the area of numerical grid generation and has been a consultant in this area for the aerospace, automotive, petroleum, nuclear, and civil engineering industries. In 1985, with colleagues, he authored a definitive text on numerical grid generation.

Dr. Thompson currently serves as senior associate editor for the journal *Applied Mathematics and Computation*, and he is associate editor for *Numerical Heat Transfer*. Among the honors and awards that have come his way are the Faculty Achievement Award for Teaching and Research at Mississippi State University in 1975, and in 1988, the Outstanding Faculty Award for the College of Engineering—one of his highest honors, for it was the result of the vote of his colleagues in the College.

He is a member of AIAA, SIAM, and the IEEE Computer Society and has served on the Fluid Dynamics Technical Committee of the AIAA. In 1992, Dr. Thompson received the Aerodynamics Award of the AIAA with the citation "for meritorious achievement in the field of applied aerodynamics recognizing notable contributions in numerical grid generation which have revolutionized computational aerodynamics for realistic configurations and complex flowfields."

Savio L-Y. Woo, Ph.D., is a Professor of Orthopaedic Surgery and Mechanical Engineering and Vice Chairman for Research, Department of Orthopaedic Surgery at the University of Pittsburgh. He is also Director of Research, Center for Sports Medicine and Rehabilitation, University of Pittsburgh.

Dr. Woo earned his B.S. in mechanical engineering from Chico State College, Chico, California in 1965 and an M.S. in mechanical engineering and Ph.D. in bioengineering from the University of Washington, Seattle in 1966 and 1971, respectively.

Dr. Woo is a member of the American Society of Biomechanics, the International Society of Biomechanics, the Society of Biomaterials, the American Orthopaedic Society for Sports Medicine, the Orthopaedic Research Society, the American Academy of Orthopaedic Surgeons, the American Institute of Medical and Biological Engineering (AIMBE), First World Congress in Biomechanics, Second World Congress in Biomechanics, and the International Society for Fracture Repair.

Among the awards he has received for his research are the American Academy of Orthopaedic Surgeons/Orthopaedic Research Society Elizabeth Winston Lanier Kappa Delta Award in 1983; the American Orthopaedic Society for Sports Medicine Excellence in Research Award in Basic Science in 1983, Sports Science in 1985, and Clinical Science in 1990; the Citation Award from the American College of Sports Medicine in 1988; and the O'Donoghue Award from the American Orthopaedic Society for Sports Medicine in 1990. He was elected to the Institute of Medicine of the National Academy of Sciences in 1991 and Founding Fellow, American Institute of Medical and Biological Engineering (AIMBE) in 1992.

Dr. Woo has presented over 400 invited lectures. He has published 130 research papers, 257 abstracts and extended abstracts, 50 book chapters, and has also edited 3 symposia proceedings and 4 books.

Dr. Woo's research has centered on the growth, development, healing, and aging of tendons, ligaments, and articular cartilage. This research includes the determination of nonlinear mechanical and viscoelastic properties, homeostatic responses, healing, and remodeling to various levels of applied stress and motion. One of his most important works, on the healing of the collateral ligaments secondary to knee injuries, has revolutionized the treatment of these ailments.

Thomas C. Palmer is a Scientific Visualization Specialist employed by Cray Research, Inc. and assigned to the North Carolina Supercomputing Center. Mr. Palmer earned a B.A. in economics from the University of North Carolina at Chapel Hill and an M.S. in computer science from UNC–Chapel Hill, with an emphasis on scientific visualization.

Recent notable accomplishments include generating the cover image for *Science* magazine's "Molecule of the Year." Current research interests include molecular graphics, programming languages for scientific visualization, the use of audio to augment visual display, and distributed visualization.

Thomas Budinger, M.D., Ph.D., is the Director of the Center for Functional Imaging, Lawrence Berkeley Laboratory, Henry Miller Professor of Medical Research at the University of California at Berkeley, and Professor of Radiology at the University of California at San Francisco.

Upon graduation from Regis College in 1954 with a B.S. degree in chemistry, Dr. Budinger obtained his M.S. degree from the University of Washington in 1957 in physical oceanography. He received his M.D. degree from the University of Colorado in 1964 and his Ph.D. degree in medical physics from the University of California at Berkeley in 1971.

Dr. Budinger is a past president and one of the founders of the Society of Magnetic Resonance in Medicine, a trustee for the Society of Nuclear Medicine, chair of IEEE Standards Subcommittee on Nonionizing Radiation, chair of the Committee on Nuclear Magnetic Resonance Safety for the American College of Radiology, and a member of the Scientific Review Committee for the Whitaker Foundation. His professional society memberships include the Society of Nuclear Medicine, American Association for Advancement of Sciences, Sigma Xi, Society of Magnetic Resonance in Medicine, North American Society for Cardiac Radiology, and Alpha Omega Alpha.

Dr. Budinger is a member of the Institute of Medicine of the National Academy of Sciences and his honors and awards include an award for his contribution on the NASA Apollo-Soyuz Project, American Nuclear Society Team Award for Special Achievement in Nuclear Technology for Medical Diagnostics, Louise and Lionel Berman Foundation Award for Scientific Contributions in the Peaceful Uses of Atomic Energy, Ernst Jung-Preis für Medizin, Jung-Stiftung für Wissenschaft und Forschung, Paul C. Aebersold Award for Basic Science from the Society of Nuclear Medicine, Distinguished Service Medal from the Society of Magnetic Resonance in Medicine, NIH Merit Award for his contributions in Alzheimer's research, and Distinguished Scientist Award from the Society of Nuclear Medicine.

Dr. Budinger has made a broad range of contributions to various scientific disciplines ranging from work in polar ice exploration and space exploration medicine to the development of advanced technologies in the imaging sciences for quantitatively studying the function of the human heart and brain in health and disease. Dr. Budinger has been the recipient of many grants from the National Institutes of Health, National Science Foundation, and the Department of Energy. He currently serves as Program Director of a Program Project Grant from the National Heart, Lung, and Blood Institute.

Dr. Budinger is the author of more than 300 papers and has been the author or co-author of 30 books. His current interests include mathematics, chemistry, and instrumentation involved in imaging biological function.

CONTRIBUTORS

John R. Baker
Department of Electrical Engineering and Computer Sciences and
Research Medicine and Radiation Biophysics Division
Lawrence Berkeley Laboratory
University of California at Berkeley
Berkeley, California

John A. Board, Jr.
Department of Electrical Engineering
Duke University
Durham, North Carolina

Richard C. Brower
Department of Electrical, Computer and Systems Engineering and
Department of Physics
Boston University
Boston, Massachusetts

Thomas F. Budinger
Department of Electrical Engineering and Computer Sciences and
Research Medicine and Radiation Biophysics Division
Lawrence Berkeley Laboratory
University of California at Berkeley
Berkeley, California

Piero Colli Franzone
Dipartimento di Informatica e Sistemistica
Universita di Pavia and Istituto di Analisi Numerica C.N.R.
Pavia, Italy

Timothy Cullip
Departments of Radiation Oncology and Computer Science
University of North Carolina at Chapel Hill
Chapel Hill, North Carolina

Edgard S. de Almeida
Department of Mechanical Engineering, Aeronautical Engineering, and Mechanics
Rensselaer Polytechnic Institute
Troy, New York

Charles DeLisi
Department of Bioengineering
Boston University
Boston, Massachusetts

Peter S. Donzelli
Department of Mechanical Engineering, Aeronautical Engineering, and Mechanics
Rensselaer Polytechnic Institute
Troy, New York

James Eason
National Science Foundation/ Engineering Research Center
Department of Biomedical Engineering
Duke University
Durham, North Carolina

Boyd Gatlin
NSF Engineering Research Center for Computational Field Simulation
Mississippi State University
Mississippi State, Mississippi

Julius Guccione
Department of Biomedical Engineering
Johns Hopkins University School of Medicine
Baltimore, Maryland

Luciano Guerri
Dipartimento di Informatica e Sistemistica
Universita di Pavia and Istituto di Analisi Numerica C.N.R.
Pavia, Italy

J. Francis Heidlage
Department of Pediatrics
Duke University Medical Center
Durham, North Carolina

Craig S. Henriquez
Department of Biomedical Engineering
Duke University
Durham, North Carolina

Nigel Hooke
Department of Computer Science
Duke University
Durham, North Carolina

Ronald H. Huesman
Research Medicine and Radiation
Biophysics Division
Lawrence Berkeley Laboratory
University of California at Berkeley
Berkeley, California

Ian W. Hunter
McGill University
Montreal, Quebec, Canada

Peter J. Hunter
University of Auckland
Auckland, New Zealand

Van L. Jacobson
Lawrence Berkeley Laboratory
University of California
Berkeley, California

William E. Johnston
Lawrence Berkeley Laboratory
University of California
Berkeley, California

Katherine M. Kavanagh
Department of Internal Medicine
University of Alberta
Edmonton, Alberta, Canada

George Koomullil
National Science Foundation/
Engineering Research Center
Department of Biomedical Engineering
Duke University
Durham, North Carolina

Ian J. LeGrice
University of Auckland
Auckland, New Zealand

Stewart C. Loken
Lawrence Berkeley Laboratory
University of California
Berkeley, California

Andrew McCulloch
Institute of Biomedical Engineering
University of California, San Diego
La Jolla, California

David M. McQueen
Courant Institute of Mathematical
Sciences
New York University
New York, New York and
The Geometry Center
University of Minnesota
Minneapolis, Minnesota

Poul M. F. Nielsen
University of Auckland
Auckland, New Zealand

Howard S. Oster
Department of Biomedical Engineering
Case Western Reserve University
Cleveland, Ohio

Thomas C. Palmer
Cray Research, Inc.
North Carolina Supercomputing Center
Research Triangle Park, North Carolina

Charles S. Peskin
Courant Institute of Mathematical Sciences
New York University
New York, New York and
The Geometry Center
University of Minnesota
Minneapolis, Minnesota

Theo Pilkington
National Science Foundation/Engineering Research Center
Department of Biomedical Engineering
Duke University
Durham, North Carolina

Andrew E. Pollard
Department of Biomedical Engineering
Tulane University
New Orleans, Louisiana

David W. Robertson
Lawrence Berkeley Laboratory
University of California
Berkeley, California

Jack Rogers
Institute for Biomedical Engineering
University of California, San Diego
La Jolla, California

Julian Rosenman
Departments of Radiation Oncology and Computer Science
University of North Carolina at Chapel Hill
Chapel Hill, North Carolina

Harry E. Rubash
Department of Orthopedic Surgery
University of Pittsburgh
Pittsburgh, Pennsylvania

Yoram Rudy
Department of Biomedical Engineering
Case Western Reserve University
Cleveland, Ohio

John Schmidt
National Science Foundation/Engineering Research Center
Department of Electrical Engineering
Duke University
Durham, North Carolina

Edward V. Simpson
Department of Medicine
Duke University
Durham, North Carolina

Bruce H. Smaill
University of Auckland
Auckland, New Zealand

William M. Smith
Departments of Medicine and Biomedical Engineering
Duke University
Durham, North Carolina

Patrick Smolinski
Department of Mechanical Engineering
University of Pittsburgh
Pittsburgh, Pennsylvania

Madison S. Spach
Department of Pediatrics
Duke University Medical Center
Durham, North Carolina

Robert L. Spilker
Department of Mechanical Engineering, Aeronautical Engineering, and Mechanics
Rensselaer Polytechnic Institute
Troy, New York

Joe F. Thompson
NSF Engineering Research Center for
Computational Field Simulation
Mississippi State University
Mississippi State, Mississippi

Brian L. Tierney
Lawrence Berkeley Laboratory
University of California
Berkeley, California

Natalia Trayanova
National Science Foundation/
Engineering Research Center
Department of Biomedical Engineering
Duke University
Durham, North Carolina

Lewis Waldman
Institute of Biomedical Engineering
University of California, San Diego
La Jolla, California

Nigel P. Weatherill
Department of Civil Engineering
University College of Swansea
Swansea, Wales

TABLE OF CONTENTS

Part I: Anatomical Heart Models and Mechanics

Chapter 1

AN ANATOMICAL HEART MODEL WITH APPLICATIONS TO MYOCARDIAL ACTIVATION AND VENTRICULAR MECHANICS

Peter J. Hunter, Poul M. F. Nielsen, Bruce H. Smaill, Ian J. LeGrice, and Ian W. Hunter

TABLE OF CONTENTS

ISBN 0-8493-4474-3

ABSTRACT

A three-dimensional finite element model of the mechanical and electrical behavior of the heart is being developed in a collaboration among Auckland University, New Zealand; the University of California at San Diego, U.S.; and McGill University, Canada.

The equations of continuum mechanics from the theory of finite deformation elasticity are formulated in a prolate spheroidal coordinate system and solved using a combination of Galerkin and collocation techniques. The finite element basis functions used for the dependent and independent variables range from linear Lagrange to cubic Hermite, depending on the degree of spatial variation and continuity required for each variable. Orthotropic constitutive equations derived from biaxial testing of myocardial sheets are defined with respect to the microstructural axes of the tissue at the Gaussian quadrature points of the model. In particular, we define the muscle fiber orientation and the newly identified myocardial sheet axis orientation throughout the myocardium using finite element fields with nodal parameters fitted by least-squares to comprehensive measurements of these variables. Electrical activation of the model is achieved by solving the FitzHugh–Nagumo equations with collocation at fixed material points of the anatomical finite element model. Electrical propagation relies on an orthotropic conductivity tensor defined with respect to the local material axes. The mechanical constitutive laws for the Galerkin continuum mechanics model are (1) an orthotropic "pole–zero" law for the passive mechanical properties of myocardium and (2) a Wiener cascade model of the active mechanical properties of the muscle fibers.

This chapter concentrates on two aspects of the model: first, grid generation, including both the generation of nodal coordinates for the finite element mesh and the generation of orthotropic material axes at each computational point, and, second, the formulation of constitutive laws suitable for numerically intensive finite element computations. Extensions to this model and applications to the mechanical and electrical function of the heart are described in Chapter 2 by McCulloch and co-workers.

I. INTRODUCTION

Two recent developments, one in numerical analysis and the other in computer hardware, have provided the tools for a powerful new approach to solving an age-old problem: How does the heart beat and what should be done when it fails? First, the development of the finite element method of numerical analysis has enabled the complex anatomy of the heart to be described mathematically in a form that can be coupled with well-established physical laws governing both the mechanics and the electrical activity of deformable excitable media. Second, computer workstations capable of solving the resulting equations and displaying the time-dependent three-dimensional modeling results are now available. When combined with currently available technology for clinically imaging the heart, these mathematical modeling tools offer exciting opportunities for real progress in the diagnosis and treatment of heart disease.

In this chapter, we argue that the problem of three-dimensional grid generation in cardiac modeling involves a great deal more than simply providing an accurate representation of the geometry of the heart. It is necessary to develop mathematical formulations that can incorporate appropriate descriptions of relevant cardiac anatomy at both the macroscopic and the microscopic levels. The electrical and mechanical properties of cardiac tissue are inhomogeneous and anisotropic, and the anisotropy is closely associated with the local organization of cardiac muscle cells. Although the muscular architecture of the heart is complex and spatially varying, it is nonetheless surprisingly well ordered, and we are developing a clear understanding of its hierarchical organization. As a result, it is possible to identify material axes for the formulation of constitutive laws based on local microstructure and to characterize the spatial variation of these material coordinate axes throughout the heart walls.

A solution of the governing equations on the computational heart mesh requires that the material constitutive laws be defined at the Gaussian quadrature or collocation points of the mesh. Thus, the spatially varying material coordinate axes needed to express the constitutive laws may be defined mathematically by finite element basis functions and nodal parameters in a manner completely analogous to the description of mesh geometry. The geometric, material, and dependent variables are given finite element bases appropriate to their degree of spatial nonuniformity. By using interpolation functions in the plane of the wall that are of different order from the transmural interpolation functions, the total number of degrees of freedom to achieve a given numerical accuracy is minimized.

We also consider the problem of finding suitable forms of constitutive law for the passive and active mechanical properties of myocardial tissue, based on these fitted material axes. The formulation of these laws is the most challenging problem facing cardiac modelers, and we consider it here only briefly and only to emphasize the requirements of the formulation in relation to large-scale numerical computation with the model.

The finite element heart model described here is developed further and used to examine some aspects of cardiac behavior by McCulloch and co-workers in Chapter 2.

II. PROLATE SPHEROIDAL COORDINATES

We begin our definition of the finite element model by introducing orthogonal prolate spheroidal coordinates that more closely match the geometry of the heart than rectangular Cartesian coordinates. A material point in the myocardium described by the coordinates (λ, μ, θ) has rectangular Cartesian coordinates

$$x = a \cosh \lambda \cos \mu,$$

$$y = a \sinh \lambda \sin \mu \cos \theta,$$

$$z = a \sinh \lambda \sin \mu \sin \theta,$$

where a is the location of the focus on the x-axis, as shown in Figure 1A. The λ-coordinate is directed transmurally, the μ-coordinate runs azimuthally from apex ($\mu = 0$) to base along an elliptical path, and the θ-coordinate is circumferential with $\theta = 0$ placed (arbitrarily) at the center of the right ventricular free wall.

By defining a finite element model of the heart geometry with prolate spheroidal coordinate parameters, the number of elements needed to represent the complex three-dimensional geometry is minimized, and a reasonable first-order (confocal ellipsoid) approximation to the left ventricle may be obtained with one element only. This ability to obtain accurate solutions with one or a few elements is particularly useful when establishing the validity of the numerical code by comparing finite element solutions of geometrically simple mechanics problems with known analytical solutions. Another reason for choosing prolate spheroidal coordinates in preference

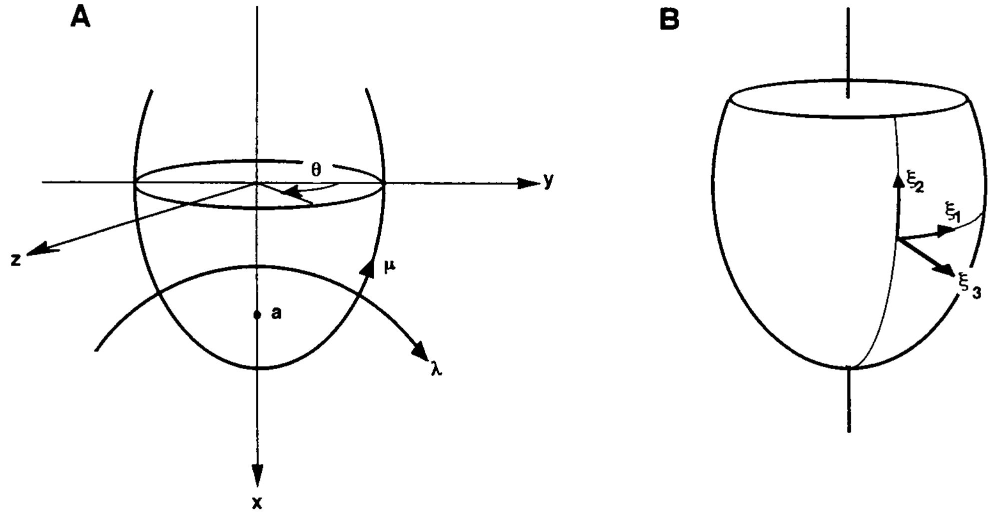

FIGURE 1. The cardiac prolate spheroid coordinate system. (A) The prolate spheroid coordinate system (λ, μ, θ) in relation to the rectangular coordinates (x, y, z); a is the focus. An ellipsoid of revolution about the x-axis is represented by λ = constant. (B) Element material coordinates (ξ_1, ξ_2, ξ_3) lie in the circumferential, azimuthal, and radial directions, respectively.

to rectangular coordinates is that the geometric nodal coordinates can then be found by a linear (rather than a nonlinear) least-squares data fitting procedure (see below). A further advantage will be apparent shortly when we use high-order (cubic Hermite) finite element basis functions for λ, to model the curved endocardial and epicardial ventricular surfaces, but we can limit μ and θ to low-order (linear Lagrange) basis functions. Finally, the prolate spheroidal focus parameter provides a convenient means of scaling the overall size of a model heart—for example, to compare the shapes of hearts of different weights.

III. FINITE ELEMENT BASIS FUNCTIONS

We adopt the standard piecewise polynomial approximation methods characteristic of the finite element method.[1] The value of some scalar variable u at the normalized element coordinates ξ_i ($0 < \xi_1, \xi_2, \xi_3 < 1$) is approximated by an interpolation of parameters defined at the element nodes. The element material coordinates ξ_1, ξ_2, and ξ_3 are chosen to lie in the circumferential, azimuthal, and transmural directions, respectively, as shown in Figure 1B. For linear interpolation, these parameters are simply the values of the variable u at the nodes of the element. Thus, a trilinear interpolation of the nodal values u_n ($n = 1, \ldots, 8$) is

$$\begin{aligned} u(\xi_1, \xi_2, \xi_3) = {} & L_1(\xi_1)L_1(\xi_2)L_1(\xi_3)u_1 + L_2(\xi_1)L_1(\xi_2)L_1(\xi_3)u_2 \\ & + L_1(\xi_1)L_2(\xi_2)L_1(\xi_3)u_3 + L_2(\xi_1)L_2(\xi_2)L_1(\xi_3)u_4 \\ & + L_1(\xi_1)L_1(\xi_2)L_2(\xi_3)u_5 + L_2(\xi_1)L_1(\xi_2)L_2(\xi_3)u_6 \\ & + L_1(\xi_1)L_2(\xi_2)L_2(\xi_3)u_7 + L_2(\xi_1)L_2(\xi_2)L_2(\xi_3)u_8, \end{aligned}$$

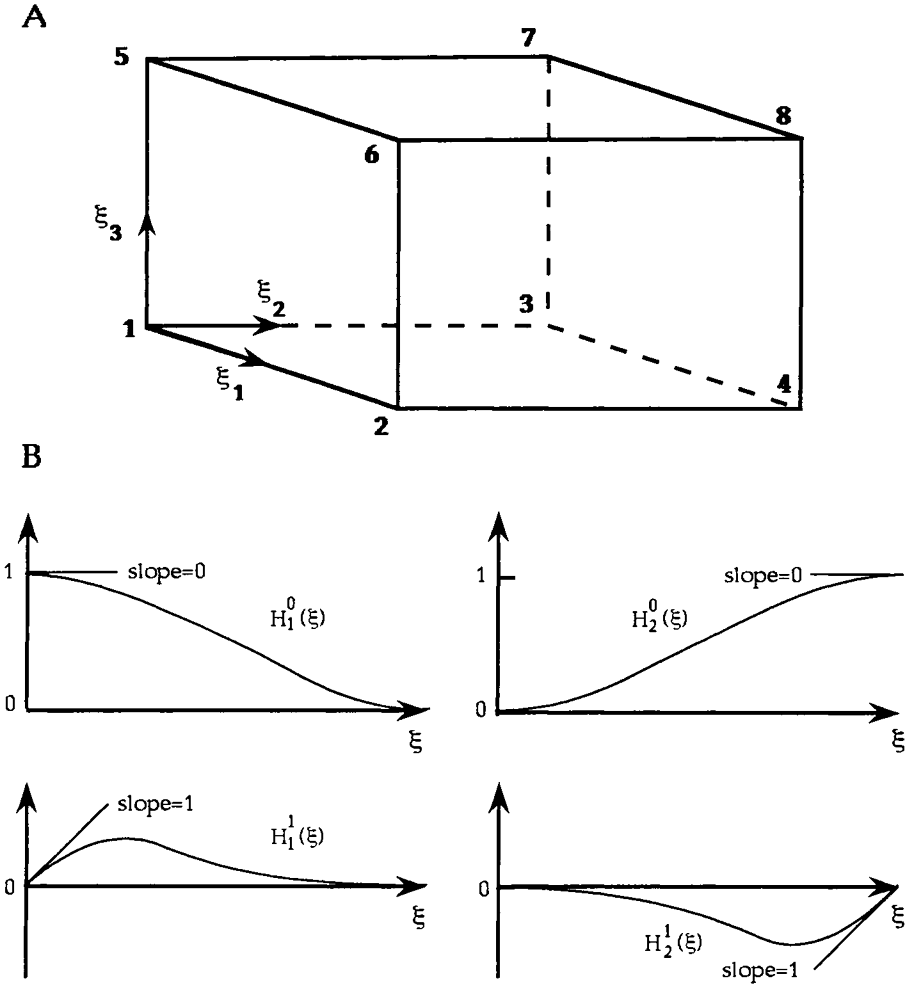

FIGURE 2. Finite element interpolation. (A) A three-dimensional cuboid in ξ_i-coordinate space ($0 < \xi_1, \xi_2, \xi_3 < 1$) with eight nodes at the vertices in the order shown. (B) One-dimensional cubic Hermite interpolation functions. The three-dimensional basis functions are formed from a tensor product of one-dimensional Lagrange or Hermite interpolants.

where $L_1(\xi) = 1 - \xi$ and $L_2(\xi) = \xi$ are one-dimensional linear Lagrange basis functions, and the nodes, located at the vertices of a three-dimensional cuboid, are numbered as shown in Figure 2A.

This trilinear Lagrange interpolation maintains the continuity of u throughout the mesh, but does not ensure the continuity of the spatial gradient of u. Continuity of gradient across element boundaries can be achieved with cubic Hermite basis functions and nodal parameters that include the derivatives of u with respect to the ξ_i-coordinates as well as the values of u itself. For example, a bicubic Hermite interpolation of u over the (ξ_1, ξ_2)-plane is given by

$$u(\xi_1, \xi_2) = H_1^0(\xi_1)H_1^0(\xi_2)u_1 + H_2^0(\xi_1)H_1^0(\xi_2)u_2$$

$$+ H_1^0(\xi_1)H_2^0(\xi_2)u_3 + H_2^0(\xi_1)H_2^0(\xi_2)u_4$$

$$+ H_1^1(\xi_1)H_1^0(\xi_2)\left(\frac{\partial u}{\partial \xi_1}\right)_1 + H_2^1(\xi_1)H_1^0(\xi_2)\left(\frac{\partial u}{\partial \xi_1}\right)_2$$

$$+ H_1^1(\xi_1)H_2^0(\xi_2)\left(\frac{\partial u}{\partial \xi_1}\right)_3 + H_2^1(\xi_1)H_2^0(\xi_2)\left(\frac{\partial u}{\partial \xi_1}\right)_4$$

$$+ H_1^0(\xi_1)H_1^1(\xi_2)\left(\frac{\partial u}{\partial \xi_2}\right)_1 + H_2^0(\xi_1)H_1^1(\xi_2)\left(\frac{\partial u}{\partial \xi_2}\right)_2$$

$$+ H_1^0(\xi_1)H_2^1(\xi_2)\left(\frac{\partial u}{\partial \xi_2}\right)_3 + H_2^0(\xi_1)H_2^1(\xi_2)\left(\frac{\partial u}{\partial \xi_2}\right)_4$$

$$+ H_1^1(\xi_1)H_1^1(\xi_2)\left(\frac{\partial^2 u}{\partial \xi_1 \partial \xi_2}\right)_1 + H_2^1(\xi_1)H_1^1(\xi_2)\left(\frac{\partial^2 u}{\partial \xi_1 \partial \xi_2}\right)_2$$

$$+ H_1^1(\xi_1)H_2^1(\xi_2)\left(\frac{\partial^2 u}{\partial \xi_1 \partial \xi_2}\right)_3 + H_2^1(\xi_1)H_2^1(\xi_2)\left(\frac{\partial^2 u}{\partial \xi_1 \partial \xi_2}\right)_4,$$

where the one-dimensional cubic Hermite basis functions, defined by

$$H_1^0(\xi) = 1 - 3\xi^2 + 2\xi^3, \qquad H_1^1(\xi) = \xi(\xi - 1)^2,$$

$$H_2^0(\xi) = \xi^2(3 - 2\xi), \qquad H_2^1(\xi) = \xi^2(\xi - 1),$$

are illustrated in Figure 2B.

The interpolation of the first derivatives $\partial u/\partial \xi_1$, $\partial u/\partial \xi_2$ and cross derivatives $\partial^2 u/\partial \xi_1 \partial \xi_2$ at the element nodes would ensure the continuity of $\partial u/\partial \xi_1$ and $\partial u/\partial \xi_2$ throughout the model if elements were evenly spaced. However, because ξ_1 is an element coordinate, the value of $\partial u/\partial \xi_1$ at one element vertex will not necessarily be the same as the value of $\partial u/\partial \xi_1$ at the vertex of an adjacent element that is associated with the same global node. We must therefore define the derivative of u with respect to some globally continuous parameter, such as arclength, at the global nodes. Thus, the derivative of u with respect to the arclength s_1 in the ξ_1 direction is $\partial u/\partial s_1$, and we define the element derivative $\partial u/\partial \xi_1$ by

$$\frac{\partial u}{\partial \xi_1} = \frac{\partial u}{\partial s_1} \cdot \frac{ds_1}{d\xi_1},$$

where $ds_1/d\xi_1$ is an element scaling factor that accounts for any differences in ξ_1 spacing with arclength in contiguous elements (notice that s_1, by definition, does not vary with ξ_2). A similar argument holds for ξ_2, giving

$$\frac{\partial u}{\partial \xi_2} = \frac{\partial u}{\partial s_2} \cdot \frac{ds_2}{d\xi_2}$$

and

$$\frac{\partial^2 u}{\partial \xi_1 \partial \xi_2} = \frac{\partial^2 u}{\partial s_1 \partial s_2} \cdot \frac{ds_1}{d\xi_1}\frac{ds_2}{d\xi_2}.$$

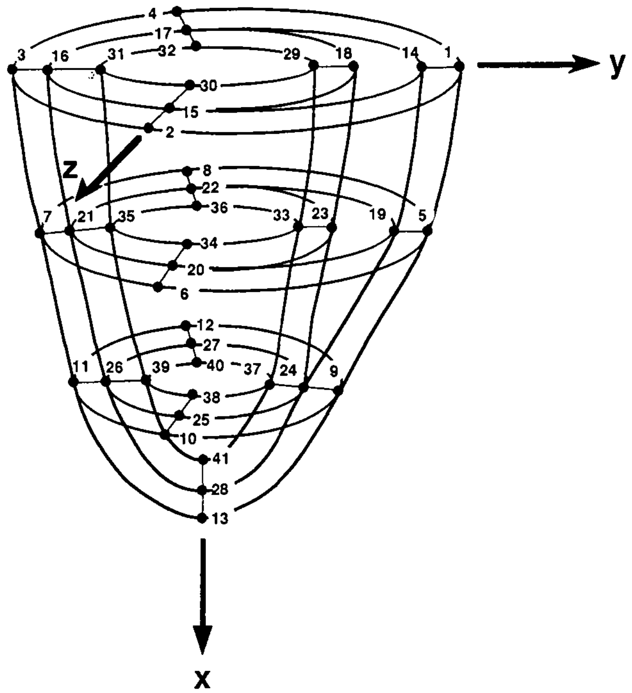

FIGURE 3. Schematic diagram of the finite element mesh. Node numbers are shown. The free wall of the right ventricle is represented by four elements (nodes 1, 2, 4, 5, 6, 8, 9, 10, 12, 14, 15, 17, 19, 20, 22, 24, 25, 27).

The parameters u, $\partial u/\partial s_1$, $\partial u/\partial s_2$, and $\partial^2 u/\partial s_1 \partial s_2$ defined at the nodes of the finite element mesh, together with the element scaling factors $ds_1/d\xi_1$, $ds_2/d\xi_2$ and the cubic Hermite interpolation functions given above, allow two-dimensional interpolation of u with C^1 continuity (continuity of gradient) across element boundaries. Tensor-product combinations of Lagrange and Hermite basis functions (e.g., bicubic Hermite in the (ξ_1, ξ_2)-plane and linear Lagrange in the ξ_3-direction, or bilinear Lagrange in the (ξ_1, ξ_2)-plane and cubic Hermite in the ξ_3-direction, etc.) can be used to provide a very flexible and powerful means of defining field variables over the myocardium.

IV. VENTRICULAR GEOMETRY

The first set of field variables that need to be defined at the nodes of the mesh are the geometric variables (λ, μ, θ). To model the complex shape of the endocardial and epicardial surfaces, we use a bicubic Hermite basis for λ in the (ξ_1, ξ_2)-wall plane and a linear Lagrange basis in the transmural ξ_3-direction. There would be no gain in accuracy by making λ cubic Hermite in the ξ_3-direction. Similarly, there is little to be gained by using cubic Hermite basis functions for μ and θ in any of the ξ_i-directions, and we therefore economize on the number of geometric parameters required to model the geometry of the heart by using trilinear bases for μ and θ.

The topology of the initial finite element mesh defining the heart geometry is shown in Figure 3. The mesh has four elements in the circumferential direction, three in the azimuthal direction, and two transmurally, giving a total of 24 elements and 41

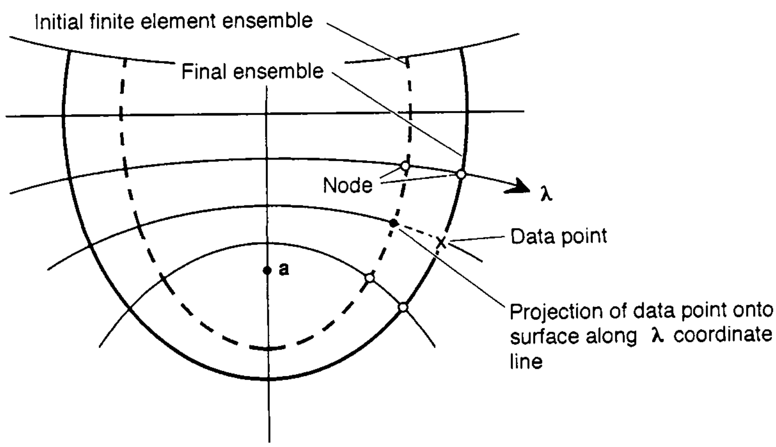

FIGURE 4. Schematic diagram of linear least-squares fit of finite element ensemble to geometric data in prolate spheroid coordinate system.

nodes. To fit the nodal parameters of the mesh to the measured geometry of the epicardial and endocardial surfaces of the heart, the nodal values of θ and μ are held fixed and the nodal values of λ, $\partial\lambda/\partial s_1$, $\partial\lambda/\partial s_2$, and $\partial^2\lambda/\partial s_1 \partial s_2$ are fitted using a least-squares algorithm.

The choice of a prolate spheroidal coordinate system for describing the geometry of the heart has a major benefit when fitting the nodal coordinates of the model to the surface measurements because only the radial λ-coordinate need enter the least-squares fitting procedure. Consider a data point d measured on the epicardial surface of the heart (see Figure 4). By assuming that the surface element coordinates (ξ_1^d, ξ_2^d), obtained from the orthogonal projection of data point d onto the model surface, do not change at all from their initial values, a linear-fitting procedure may be obtained by minimizing the sum (over the total number of data points n) of squares

$$S = \sum_d W_d\left(\lambda(\xi_1^d, \xi_2^d) - \lambda_d\right)^2, \tag{1}$$

where λ_d is the λ-coordinate of the measured point d, $\lambda(\xi_1^d, \xi_2^d)$ is the λ-coordinate of the projection of data point d onto the model surface *along lines of constant* μ *and* θ, and W_d is a weight associated with data point d. $\lambda(\xi_1^d, \xi_2^d)$ is given by a bicubic Hermite interpolation of the nodal parameters λ_n, $\partial\lambda_n/\partial s_1$, $\partial\lambda_n/\partial s_2$, and $\partial^2\lambda_n/\partial s_1 \partial s_2$, and the sum of squares is minimized with respect to these parameters.

Although minimizing the sum of squares given by Equation 1 is not the same as minimizing a Euclidean norm, the difference in fitting surface parameters is negligible in comparison with mean measurement error, and the computational cost of this linear fitting procedure is orders of magnitude less than the cost of the nonlinear procedure.[2]

The arclengths s_1 and s_2 are defined to be linear with respect to ξ_1 and ξ_2, respectively, in the initial unfitted finite element mesh and are not altered during the fitting procedure. Because θ and μ are constrained to be linear in ξ_1 and ξ_2 by the choice of basis function, ξ_1 and ξ_2 are linear in θ and μ and therefore cannot be linear in arclength on the fitted mesh. Thus, s_1 and s_2 should be interpreted, not as physical arclengths, but as arbitrary parameters specified along the ξ_1- and

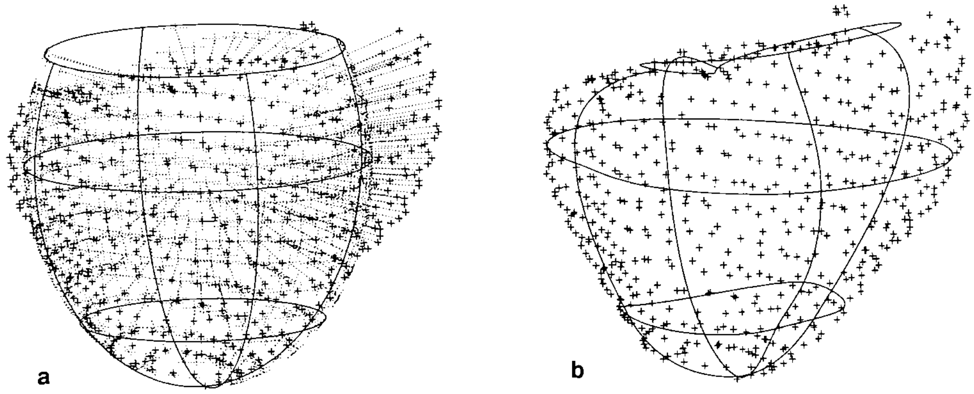

FIGURE 5. Least-squares fitting of finite element nodal λ parameters to epicardial geometry measurements. Data points projected onto (a) initial prolate spheroid and (b) optimized finite element surface mesh. The dotted line projections are from data points to sites on the mesh with the same μ, θ coordinates.

ξ_2-coordinate directions, respectively, which provide the connection between global derivatives and element derivatives in the cubic Hermite interpolation. They are arbitrary to the extent that they only appear in products such as $(\partial\lambda/\partial s_1)\cdot(ds_1/d\xi_1)$ and can therefore be scaled by an arbitrary multiplicative constant provided the scaling is applied consistently. If ξ_1-coordinate lines are to follow μ = constant trajectories and ξ_2-coordinate lines are to follow θ = constant trajectories, we could choose s_1 to be θ and s_2 to be μ. However, this is not possible here where, for example, the boundaries of the right ventricle are modeled by ξ_2-coordinate lines which vary with both θ and μ.

Fifty-two degrees of freedom are available as fitting parameters for the epicardial surface, whereas left and right endocardial surfaces are fitted using 52 and 44 parameters, respectively. The fitting procedure is illustrated in Figure 5, which shows the epicardial data points projected onto the epicardial surface mesh before (Figure 5a) and after (Figure 5b) fitting. The nodes defining the right ventricular boundaries (where free and septal endocardial surfaces become continuous) require special attention because there are surface data only to one side of these nodes. Because the surface derivatives at these sites are very sensitive to local surface irregularities, we allow λ at these nodes to enter the fit to the local surface data, but we fix the derivative at the adjacent epicardial value. This constraint is justified by the fact that the thin-walled right ventricle at its borders is parallel to the epicardium.

The full geometric model is obtained by combining the nodal information from the three surface fits as illustrated in Plates 1 and 2.* For this typical dog heart, the epicardial surface has been fitted to 803 measured coordinates, while the endocardial surfaces of the right and left ventricles are based on 770 and 846 data points, respectively. The time required to fit each of these surfaces is about 1 min on an 8MB VaxStation 3100. The use of four elements in the circumferential direction and three in the azimuthal direction provides a faithful representation of the epicardial surface with rms errors < 0.9 mm. Justification for the choice of the 12 surface elements for the epicardium is given in Figure 6 and Table 1. Increasing the number of elements gives little improvement, whereas reducing the number of elements or dropping to a bilinear basis significantly increases the error. However, the 12-element surface mesh

* Plates 1 and 2 appear following page 49.

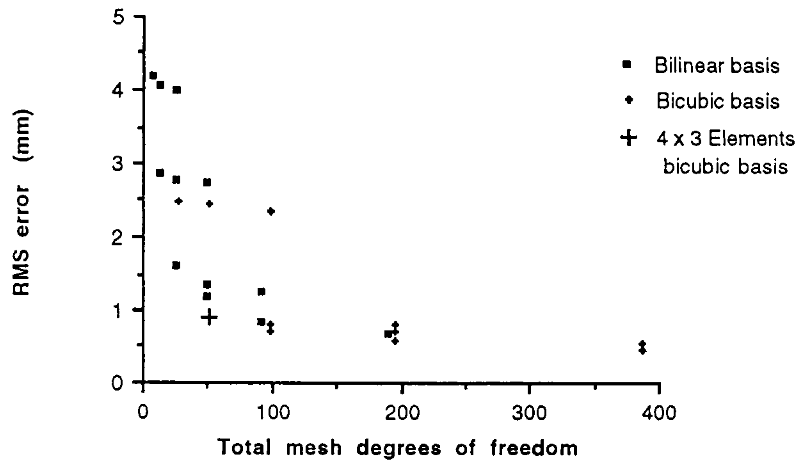

FIGURE 6. Root mean squared error of fit plotted against total number of degrees of freedom for various finite element meshes. The fitting errors are tabulated in Table 1. Note that the 4 × 3 bicubic mesh used in this study appears at the knee of the curve. Decreasing the number of degrees of freedom results in a marked increase in error; increasing the number of degrees of freedom reduces the error very little.

provides a less accurate representation of the convoluted endocardial surface of the left ventricle. We have found that increasing the number of elements to ten in the circumferential direction significantly reduces the fitting error for the left ventricular endocardium (from an rms error of 2.6 mm to < 1.8 mm) and gives a much better representation of the papillary muscles.[3] This detail can be seen in Figure 7 which shows ventricular cross sections at 12 axial locations.

Ventricular surface geometry has been fitted to a large number of dog hearts,[3] and this work demonstrates that shape and wall thickness are remarkably consistent for

TABLE 1
Root Mean Squared Error (mm) in Relation to Degrees of Freedom when Fitting Epicardial Geometry Using Bilinear or Bicubic Bases for Meshes of 2, 4, 8, 16 Elements Circumferentially and 3, 6, 12 Elements Axially

Number of axial elements		Number of circumferential elements 2	4	8	16
3	D.O.F. (bilinear)	7	13	25	49
	Error	4.19	2.86	1.61	1.19
	D.O.F. (bicubic)	27	51	99	195
	Error	2.48	0.89	0.75	0.71
6	D.O.F. (bilinear)	13	25	49	97
	Error	4.07	2.77	1.34	0.85
	D.O.F. (bicubic)	51	99	195	387
	Error	2.47	0.78	0.58	0.51
12	D.O.F. (bilinear)	25	49	97	193
	Error	4.01	2.75	1.25	0.69
	D.O.F. (bicubic)	99	195	387	
	Error	2.35	0.75	0.54	

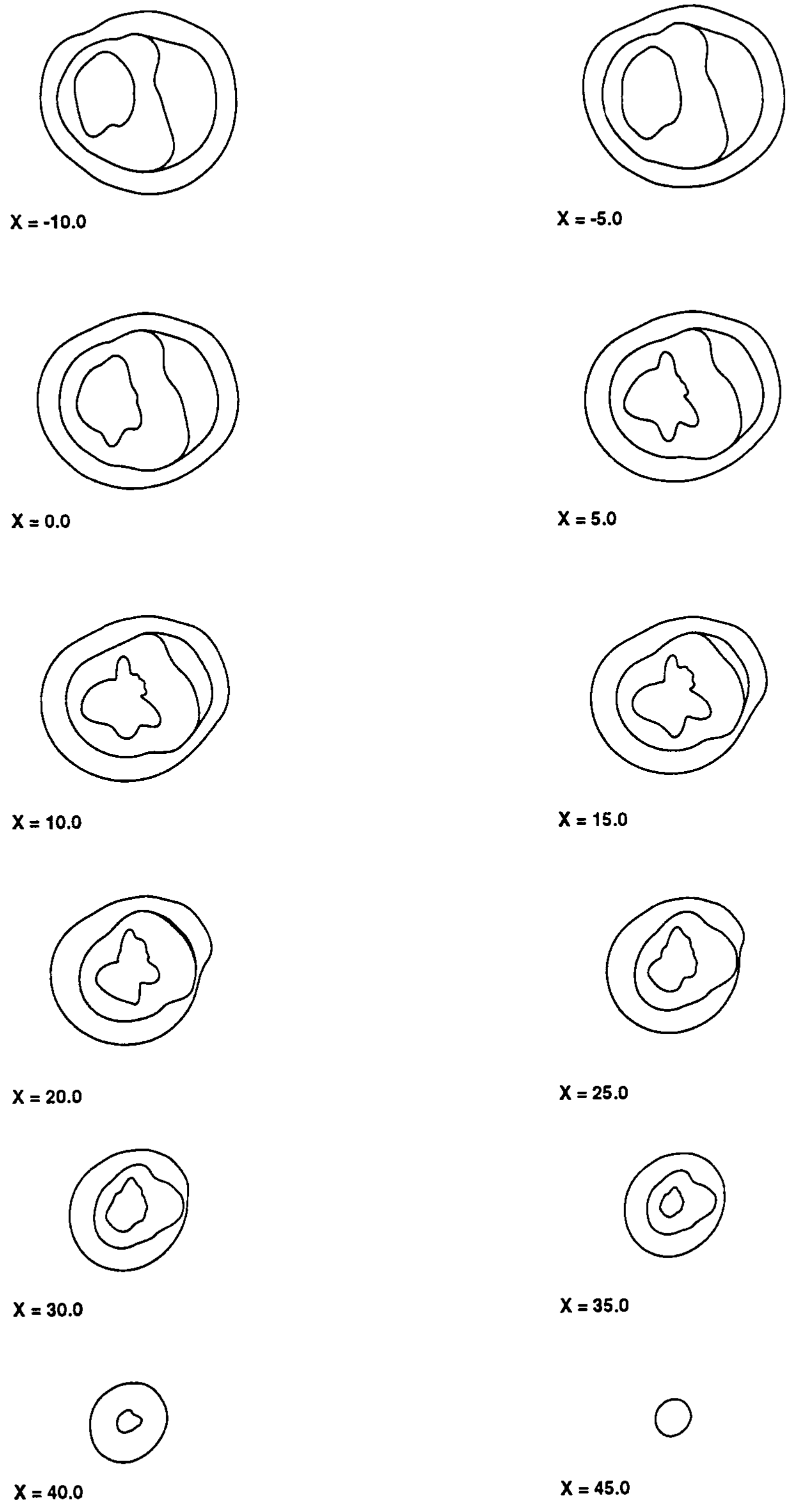

FIGURE 7. Ventricular cross sections from the finite element model at various axial locations (values given are in millimeters; 0 mm represents the equatorial plane). Note that all interelement boundaries appearing at the given axial location are drawn.

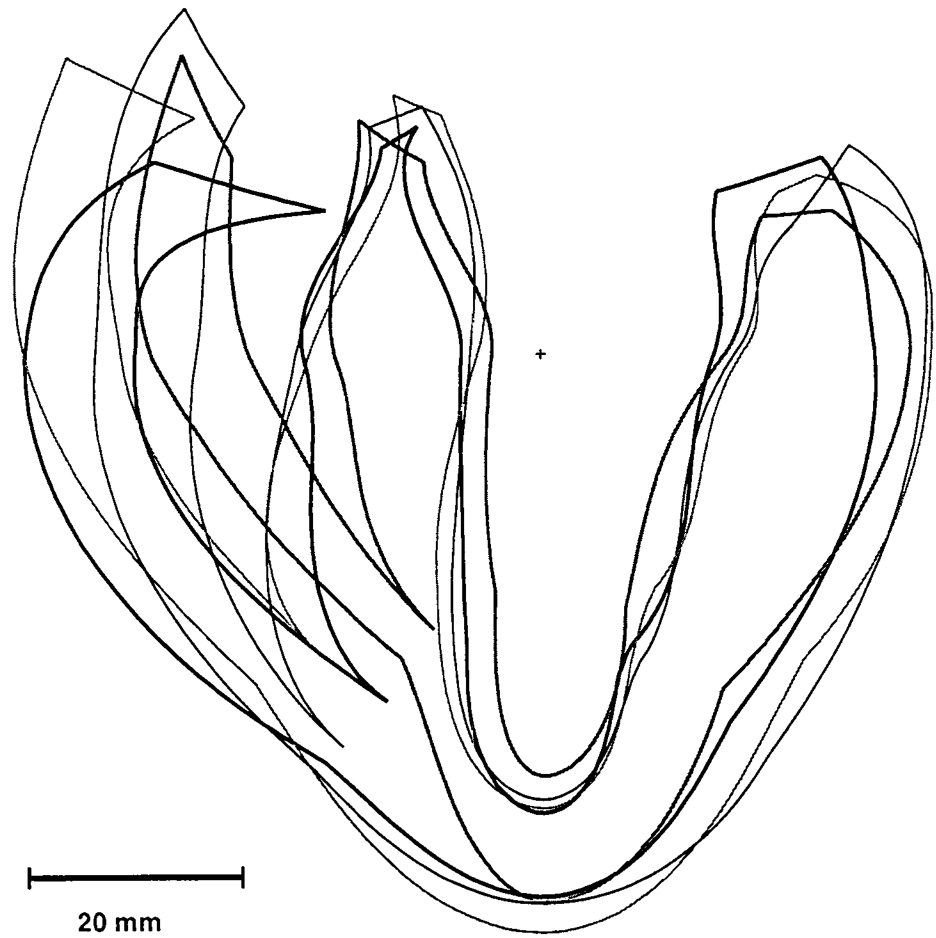

FIGURE 8. Coronal sections from four fitted dog hearts. Note the much greater variation in the position of the right ventricular free wall than in the left.

canine hearts fixed in an unloaded state. This is indicated in Figure 8, where coronal cross sections from the fitted models are compared for four hearts of similar weight. (Similar results are obtained when hearts of different sizes are normalized to the same focus parameter a.) The greatest shape variation occurs in the fixed position of the right ventricular free wall, which is to be expected because it is thinner and more flexible than the left ventricular free wall.

V. THE MUSCULAR ARCHITECTURE OF THE VENTRICLES

Cardiac muscle cells are roughly cylindrical in shape and form ordered arrays in which the axes of adjacent cells are parallel and for which a fiber orientation can be readily defined. The arrangement of muscle fibers within the ventricular wall has been the subject of continuing study over the years and an area of some controversy.[4] It is accepted that fiber orientation changes relatively smoothly through the ventricular wall: in the left ventricular free wall, for instance, muscle fibers that are oriented at about $-60°$ with respect to the circumferential direction at the epicardial surface are circumferentially aligned in the midwall and are nearly perpendicular to the circumferential direction at the endocardial surface.

For modeling purposes, it has generally been assumed that ventricular tissue is a continuum and that the material structure and properties are isotropic in the plane orthogonal to the local muscle fiber axis. Recent studies of cardiac microstructure have shown that this assumption is incorrect.[5,6] A schematic representation of our current understanding of the muscular architecture of ventricular tissue is given in Plate 3.* Muscle cells are arranged in layers or sheets that are on average four cells thick and are surrounded by a meshwork of connective tissue. Within a layer, cardiac muscle cells form a branching network in which each cell is tightly coupled to its neighbors via intercalated disk junctions, which provide electrical continuity. Adjacent cells are also tethered by a regular array of short interconnecting collagen fibrils. On the other hand, the coupling between neighboring layers is much less extensive. As can be seen in Plate 3, there is direct branching between layers, but this is relatively infrequent, particularly at the center of the ventricular wall. Layers are also interconnected by a network of collagen fibers, which are often long and convoluted.

The most interesting aspect of the laminar structure of ventricular tissue, from the perspective of computational mechanics, is the orientation of sheets with respect to the ventricular wall. In the midwall, the sheets are directed transmurally. In the longitudinal transmural section represented in Plate 3, the cut edges of the sheet reveal a series of cleavage planes, which run radially from the endocardial surface toward the epicardial surface. For a section cut tangential to the epicardial ventricular surface, however, the edges of the sheets define the fiber orientation. The local coordinate axes that we adopt to represent this structural anisotropy therefore consist of a unit vector aligned with the fiber orientation, a unit vector perpendicular to the fiber axis and lying in the plane of the sheet, and the unit normal to the sheet plane. These material axes can be specified at any point within the ventricular wall by appropriately identifying both the local fiber orientation and the local sheet orientation.

VI. MUSCLE FIBER ORIENTATIONS

The orientation of cardiac muscle fibers and the functional significance of the transmural fiber angle distributions have been studied and speculated upon for over a century. Early views of discrete layers[7,8] have given way to continuous distribution models.[9] We have recently published extensive measurements of muscle fiber orientations in the dog heart,[2] and a summary of these results, enhanced by more recent studies, is presented here. For details on the methods used to measure the fiber angles throughout the myocardium and for further information on the fitting procedures, see Reference 2.

To model the muscle fiber orientations, we assume that the fibers lie in (ξ_1, ξ_2)-coordinate planes and subtend an angle η with the (circumferential) θ-coordinate. (We later relax this assumption to allow the fibers to spiral from epicardium to endocardium at the left ventricular apex.) The "fiber angle" η is then given by an interpolation of nodal fiber field parameters at the same node positions used to define the geometry.

The basis functions used to interpolate η within an element are chosen to give a linear interpolation in ξ_1 and ξ_2 (in the plane of the wall; see Figure 1B) and a cubic

* Plate 3 appears following page 49.

Hermite interpolation in ξ_3 (transmurally). Like the geometric variable derivatives, the fiber angle cubic Hermite element derivative must be obtained from its global node counterpart by using an element scaling factor:

$$\frac{\partial \eta}{\partial \xi_3} = \frac{\partial \eta}{\partial s_3} \cdot \frac{ds_3}{d\xi_3}.$$

The nodal values of η and $\partial\eta/\partial s_3$ are fitted by least-squares to fiber angle measurements after the geometric fit, using a more refined mesh than that needed for the geometric data.

Because the measured fiber angles show rapid changes in the circumferential direction at the boundaries of the right ventricle, we use a 60-element, 99-node mesh obtained by subdividing the 24-element mesh used to fit the geometry. With this more refined mesh, having ten elements circumferentially, three axially, and two transmurally, it is found that linear interpolation in the (ξ_1, ξ_2)-coordinates and cubic Hermite interpolation in the ξ_3-coordinate provided sufficient degrees of freedom to represent the fiber field data with acceptable accuracy.

The three-dimensional fiber field parameters are found by first fitting the epicardial, left ventricular endocardial, and right ventricular endocardial surfaces with bilinear surface variation of the surface node η parameters and then fitting the transmural myocardial fiber measurements with the remaining interior node values of η together with the complete set of nodal derivatives $\partial\eta/\partial s_3$.

The surface fits are obtained by projecting the surface fiber angle measurements onto the adjacent fitted geometric surface. This strategy is required in order to obtain accurate epicardial and endocardial fits in regions where the fiber angle changes rapidly near the surface and the model geometry does not exactly match the real heart.

Fiber angle data are only unique within a principal angle range of 180°. It is sometimes necessary to adjust the principal angle of the data to ensure that the restricted principal value range does not produce artifactual discontinuities of fitted fiber angle for fiber angle data that are, in fact, varying smoothly around the ventricles and through the wall. Use of the conventional principal angle range for fiber orientation creates problems at the junction of the right ventricular free wall and the ventricular septum. In the right ventricular free wall, fiber orientation typically varies from $-60°$ at the epicardium to $+90°$ at the endocardium, whereas in the septal wall, the fiber angle ranges from about $-90°$ at the right ventricular endocardium to around $+80°$ at the left ventricular endocardium. On either side of the right ventricular border, therefore, the principal angle for endocardial fibers with a common orientation differs by 180°. To accommodate this abrupt change in principal value, three nodes are used at each of these right ventricular border sites, one for the right ventricular free wall, one for the septal wall, and one for the adjacent left ventricular free wall—the latter because there is, in fact, a real discontinuity in fiber angle due to the merging of right ventricular free wall and septal fibers with left ventricular fibers. This required two extra nodes at nine sites, giving a total of 117 nodes used in the fiber fits. We also localized the errors due to these discontinuities by decreasing the size of the elements at these sites.

Cardiac muscle fiber orientations have been systematically recorded throughout the ventricular walls of three hearts (at 9467, 9746, and 17,182 points) and fiber orientation fields have been fitted to these data.[3] Fitted fiber orientations for two of these hearts are compared in Figure 9b–h at the series of depths through the

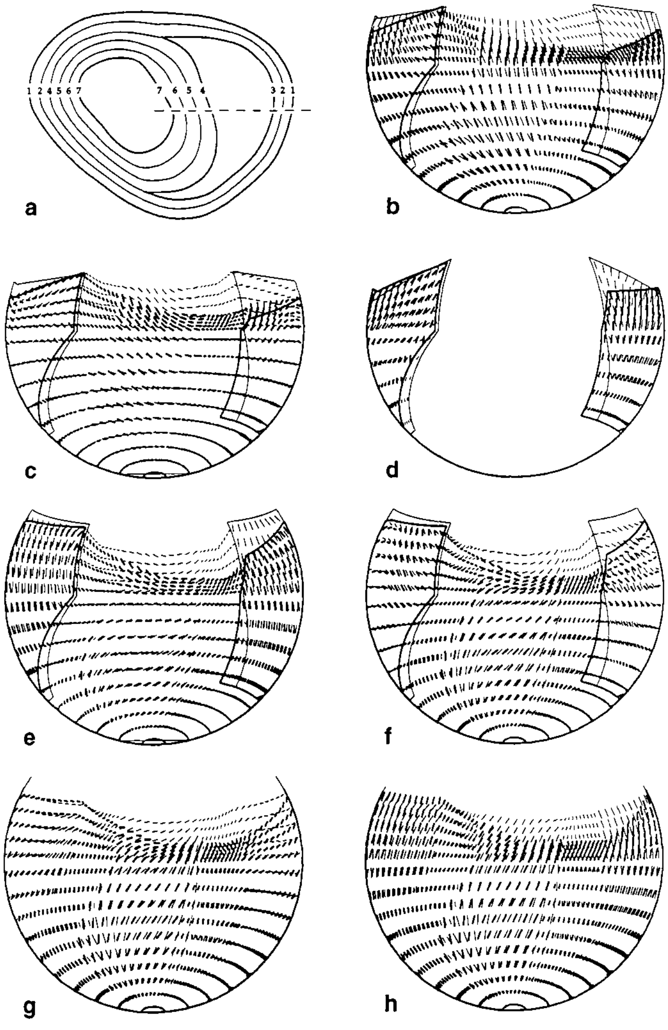

FIGURE 9. Intramural distributions of fitted myocardial fiber orientation for two hearts. Left and right ventricles are represented as a series of layers and fiber orientations at the surfaces are mapped into Hammer projections. (a) Transverse section through the ventricles indicating location of intramural surfaces. To visualize the Hammer projection, it may be imagined that the right ventricular free wall and interventricular septum are cut along the dotted line shown so that the shells can be opened and laid flat. (b)–(h) Fiber orientations at surfaces 1–7, respectively, the two hearts being distinguished by the thick and thin fiber direction vectors. Note that 3 shows the endocardial surface of the right ventricular free wall only, 4 incorporates the right endocardial surface of the interventricular septum with a left ventricular intramural surface, and 7 is the endocardial surface of the left ventricle.

ventricular walls indicated in Figure 9a. Fiber orientations in each of these surfaces are represented using the Hammer projection,[10] which preserves the left ventricular apex and opens the heart out flat from an imaginary cut through the midwall of the left ventricle. Note the variation in fiber angle through the left ventricular free wall from around $-60°$ with respect to the circumferential direction at the epicardial surface to around 80° at the endocardial surface. The model provides an accurate representation of the experimental fiber orientation field since fitting and measurement errors are of a similar magnitude.[2] Moreover, as shown in Figure 9, there is a high level of consistency between fitted orientation fields in different hearts defined relative to their measured and fitted geometry, and there are significant changes in the transmural variation of fiber orientation at different ventricular sites. Using the methods outlined here, it is possible to represent fiber orientation fields in a given heart for modeling purposes with a high degree of confidence.

The fiber distributions for one heart are shown in three-dimensional views in Plates 4 and 5.*

VII. MYOCARDIAL SHEET ORGANIZATION

Preliminary results have been obtained in an experimental program aimed at quantifying aspects of the laminar organization of cardiac muscle cells in ventricular myocardium.[11] This work has been carried out in dog hearts using light microscopy and scanning electron microscopy and demonstrates a significant transmural variation in the extent of coupling between adjacent sheets of muscle cells in the left ventricle. The density of branching between sheets was least, whereas the range of lengths of collagen fibers connecting neighboring layers was greatest in the center of the ventricular wall. However, the extent of transmural variation in laminar organization was very similar at different left ventricular sites. These results provide a possible structural basis for both anisotropic and inhomogeneous material properties in left ventricular myocardium.

Sheet orientations have also been systematically recorded in thick longitudinal transverse sections from dog hearts.[11] Typical results are presented in Figure 10. Sheet orientations are generally radial with respect to the ventricular surfaces, but in the subepicardial region they appear to turn through 90° to become tangent to the epicardial surface. Two areas which do not follow the standard pattern are around the bases of the left ventricular papillary muscles, where there is a complex interweaving of sheets from the papillary muscles with the dominant free wall pattern, and around the base of the left ventricular free wall, where the sheets angle up into the basal skeleton.

The details of the procedures for fitting the myocardial angle field are given in Reference 3. The basis function used for this field is linear in the ξ_1-coordinate and bicubic Hermite in the (ξ_2, ξ_3)-plane. The fitted myocardial sheet angles are illustrated in Figure 11 on sections corresponding to those shown in Figure 10.

VIII. PURKINJE FIBERS AND CORONARY VESSELS

The distribution of Purkinje fibers over the right and left ventricular endocardial surfaces is another important aspect of myocardial anatomy for electrical activation modeling. We have recorded these distributions on some of the canine hearts used in the fiber field studies.[6] A typical pattern is shown in Figure 12. For modeling purposes, we specify a set of endocardial Gauss points at which myocardial activation is initiated.

The question of oxygen delivery to the myocardium will need to be addressed

* Plates 4 and 5 appear following page 49.

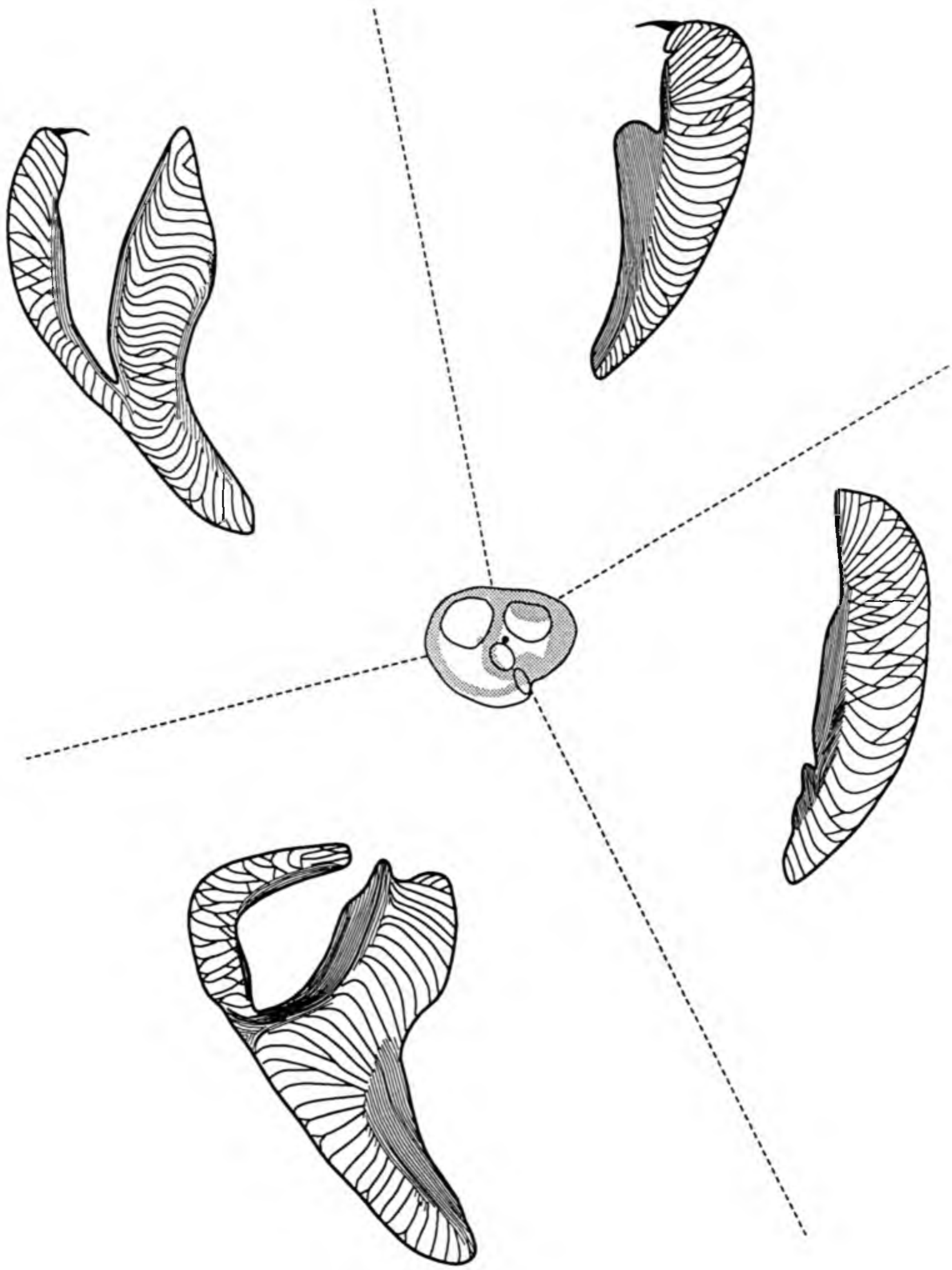

FIGURE 10. Coronal sections of the heart showing myocardial sheet orientations at four circumferential locations as indicated (sketched from original data).

within the framework of the continuum model of the heart described here. As a preliminary step to setting up a model of the coronary system, we have measured the location of the epicardial vessels. These are shown on the Hammer projection in Figure 13. One-dimensional linear elements are used to represent the coronary tree.

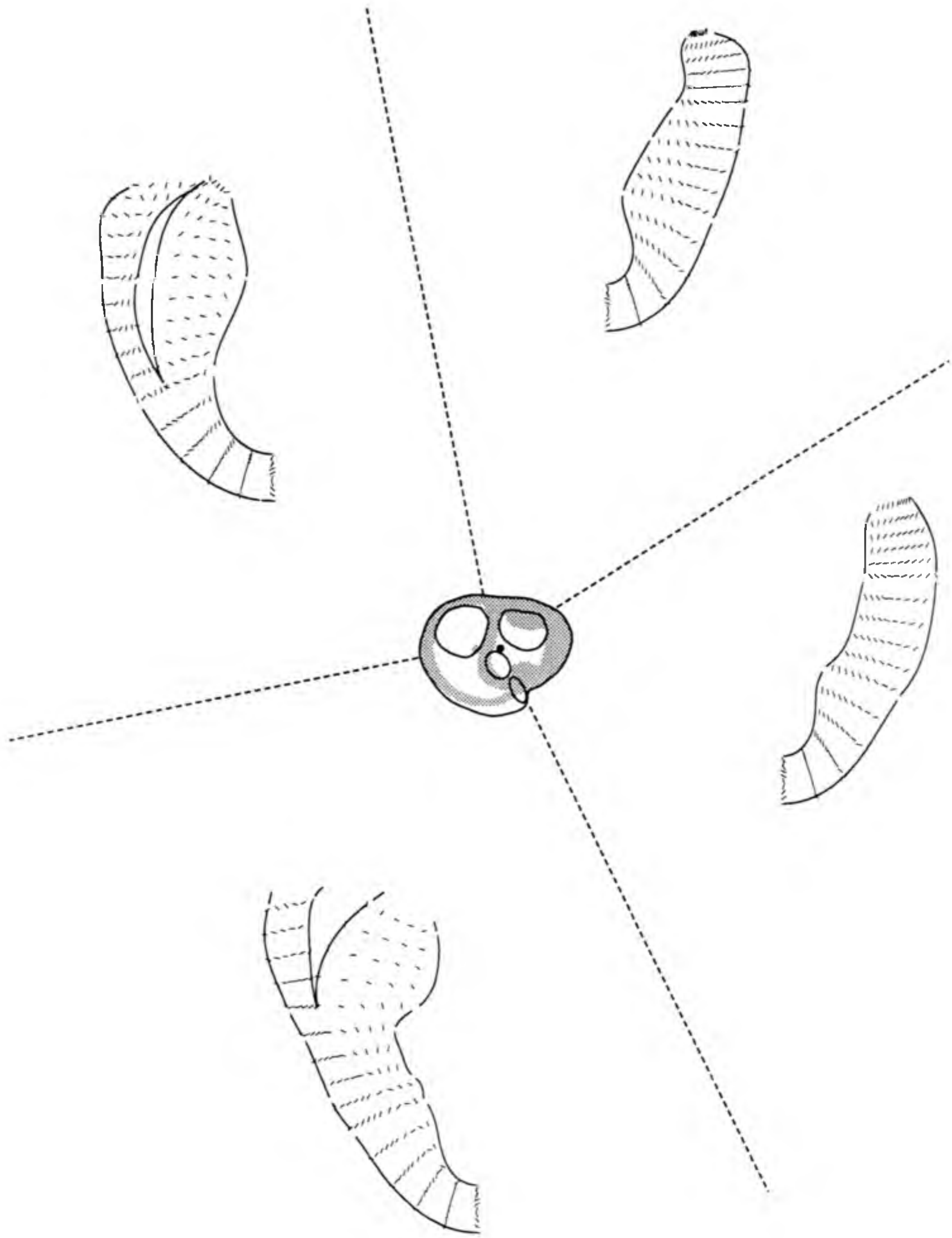

FIGURE 11. Fitted sheet vectors (i.e., drawn from the fitted finite element nodal sheet parameters) shown on planes normal to the wall at cross sections close to those shown in Figure 10.

IX. ORTHOTROPIC CONSTITUTIVE LAWS

The anatomical model of the heart described above has been used with the equations of finite elasticity theory to calculate the distributions of stress and strain throughout the myocardium and with the FitzHugh–Nagumo equations[12] and other ionic current models to calculate the electrical activation of cardiac muscle.

The equations of finite elasticity theory are cast in a Galerkin weighted residual

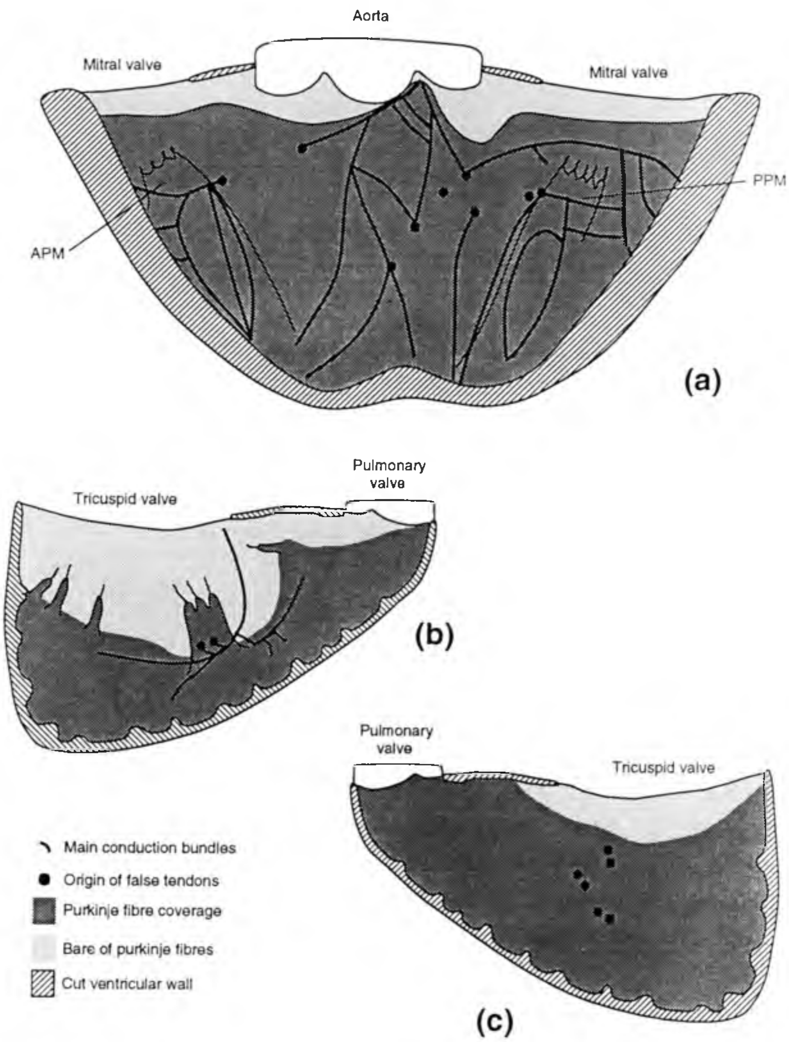

FIGURE 12. Purkinje fiber distributions on left and right ventricular endocardial surfaces.

form with displacement or deformed position as the dependent variable.[13,14] This yields a set of simultaneous algebraic equations, or ordinary differential equations if the problem is time dependent, in the nodal variables (displacements or positions). Element integrals are computed by Gaussian quadrature, and the "Gauss" points become the spatial locations at which the mechanical constitutive law—the experimentally determined relationship between stress and strain—is evaluated.

It is convenient to use collocation points generated at fixed ξ_i locations within the finite elements for solving the activation equations. When the coupled mechanical-electrical equations are solved together, the information on muscle activation can be computed at the Gauss points where the mechanical constitutive law is evaluated. Collocation is preferred to an integral formulation of the activation equations because this imposes fewer spatial continuity requirements on a field which is known to show very rapid changes over millimeter distances. The displacement field, on the other hand, has lower spatial gradients due to the extensive structural integrity of the

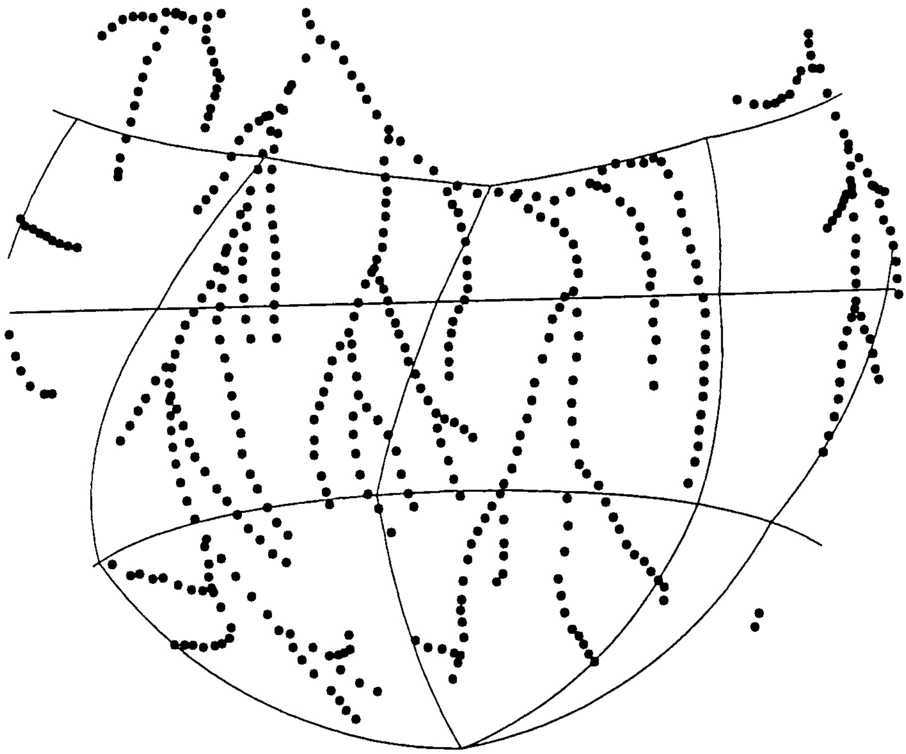

FIGURE 13. Epicardial coronary vessels shown on a Hammer projection. The points shown are original data points, not fitted representations.

tissue. Using a finite element basis for the displacement ensures that compatibility conditions on the displacement field are always met.[14]

To evaluate the constitutive laws at the Gauss points and collocation points of the anatomical model, a system of orthogonal material axes, based on the tissue microstructure, must be defined. The first axis is defined as the muscle fiber axis. The second axis is defined to lie in the plane of the myocardial sheet perpendicular to the fiber axis. The third axis is then defined to be orthogonal to these two—and thus transverse to the myocardial sheets.

The electrical conductivity of myocardial tissue has long been known to be anisotropic,[15] with the conductivity in the muscle fiber direction being two to three times that in the plane transverse to the fibers. We have recently proposed[6] that the conductivity tensor should be modeled as orthogonal rather than transversely isotropic, given the clear orthotropy of the tissue microstructure described in previous sections.

Thus, whichever model of electrical propagation is used, such as FitzHugh–Nagumo, Beeler–Reuter,[16] or diFrancesco–Noble,[17] the diffusive term $\nabla \cdot (\mathbf{D}\ \nabla u)$, where u is the transmembrane potential, incorporates a conductivity tensor **D**, which must be defined with respect to the material axes described here.

To use the anatomical model for studying the mechanics of the heart, a constitutive law relating the material stress and strain tensors at each Gauss point must be formulated. Two aspects of the mechanical properties need to be considered: the passive tissue properties and the active muscle tension development. A constitutive law for passive properties requires a fully three-dimensional relationship between the six components of stress and six components of strain, whereas the active muscle law requires only a one-dimensional relationship between the fiber strain and the active muscle tension (and, of course, time and the state of activation). To be used successfully in a large-scale numerical model, the constitutive relation must be efficient (i.e., not too time consuming to compute) and well conditioned (i.e., small changes in the input variables should not give unreasonably large changes in the output variables).

Because the composition of the tissue is too complex to be able to derive these laws from a knowledge of the mechanical properties and layout of the microstructural components, we instead propose simple empirical relationships guided by what knowledge of the microstructure we do have and then use biaxial testing to estimate the parameters. Furthermore, even if it were possible to derive the constitutive law from a detailed analysis of the tissue constituents, we may still require an equivalent simple computationally efficient relation to use in the numerical model. Three characteristic features of the mechanical properties of passive myocardium when loaded uniaxially or biaxially along the material axes[18,19] are as follows:

1. The stress–strain behavior along each of the three material axes is quite different.
2. The behavior along one axis is nearly independent of the degree of stretch along the other two axes.
3. The axial stress is very low at low axial strains, but rises rapidly as the strain approaches a characteristic limiting value for that axis.

These observations are encapsulated in the following pole–zero strain energy function for passive myocardium:[19]

$$W = k_1 \frac{e_{11}^2}{(a_1 - e_{11})^{\alpha_1}} + k_2 \frac{e_{22}^2}{(a_2 - e_{22})^{\alpha_2}} + k_3 \frac{e_{33}^2}{(a_3 - e_{33})^{\alpha_3}}$$

$$+ k_4 \frac{e_{12}^2}{(a_4 - e_{12})^{\alpha_4}} + k_5 \frac{e_{23}^2}{(a_5 - e_{23})^{\alpha_5}} + k_6 \frac{e_{31}^2}{(a_6 - e_{31})^{\alpha_6}},$$

where $e_{\alpha\beta}$ are the components of Green's strain tensor referred to material coordinates aligned with the structurally defined axes of the tissue; $a_1, \ldots, a_6$ are parameters expressing the limiting strain for a particular type of deformation (i.e., the strain energy becomes very large as e_{11} approaches a_1, etc.) and $a_1 > e_{11}$, $a_2 > e_{22}$, $a_3 > e_{33}$, $a_4 > e_{12}$, $a_5 > e_{23}$, $a_6 > e_{31}$; $\alpha_1, \ldots, \alpha_6$ are parameters expressing the curvature of the uniaxial stress–strain curves (partly a reflection of the distribution of unextended fiber lengths as more collagen fibers are recruited); and $k_1, \ldots, k_6$ are parameters giving the relative contribution of each strain energy term.

The last three terms express the contribution of material shear strain to the total strain energy. The Piola–Kirchhoff stress tensor is found from the derivatives of W with respect to the strain components (see Reference 14 for further details).

Three characteristic features of active tension development are as follows:

1. At fixed fiber extension ratio λ, the isometric tension $T_0(\lambda)$ is a function of the degree of activation of the myofilaments (primarily via intracellular $[Ca^{2+}]$).

2. When rapidly shortened from the isometric state to a new slightly lower fixed extension, the resulting tension change is large in comparison to the length change (e.g., a sudden length change of 0.5% can reduce the tension momentarily to zero) and shows a nonlinear dependence on the length change.
3. When shortening against a constant load, three rate constants are revealed, one slow (presumably associated with cross-bridge turnover) and two fast (possibly associated with cross-bridge head rotation).

These observations can be modeled by the following Wiener cascade model of the active properties in which a linear dynamic system is followed by a static nonlinearity:[13,14]

$$\frac{T/T_0 - 1}{T/T_0 + a} = \sum_{i=1}^{3} A_i \int_{-\infty}^{t} e^{-\alpha_i(t-\tau)} \dot{\lambda}(\tau)\, d\tau,$$

where $\lambda(\tau)$ is the muscle fiber extension ratio at some past time τ, $T_0 = T_0(\lambda)$ is the isometric tension (an empirically defined relation), T is the actively developed tension in the muscle fiber at current time t, $\alpha_1, \ldots \alpha_3$ are the rate constants of the linear dynamic system, $A_1, \ldots A_3$ are the associated weighting coefficients, and a is a parameter governing the shape of the static nonlinearity (see Reference 14 for further details).

These two constitutive models adequately describe the material properties of passive and active cardiac muscle, respectively, and are computationally efficient when used with the finite elasticity equations in the Galerkin finite element model.

X. SUMMARY

A numerical solution of the equations governing the electrical conductivity or mechanical function of the heart requires a mathematical model of the fibrous structure of the heart, as well as a computational grid conforming to the ventricular anatomy. In this paper, we have argued that the two requirements are intimately related and should be considered together. An orthogonal coordinate system, on which to base the constitutive laws of mechanics or electrical activation, was defined at each Gauss point of the finite element mesh using piecewise polynomial field descriptions of the muscle fiber direction and the myocardial sheet axis direction.

Prolate spheroidal coordinates were used to minimize the number of elements required to model the geometry of the heart and to simplify the geometric data fitting. Assuming finite element basis functions individually for each coordinate also helped to minimize the number of nodal degrees of freedom in the model. Thus, the radial coordinate λ was given a bicubic Hermite basis in the (ξ_1, ξ_2)-plane (plane of the wall) and a linear Lagrange basis in the ξ_3-direction (transmurally), whereas the azimuthal μ-coordinate and the circumferential θ-coordinate were given trilinear Lagrange bases.

Using these bases, a 60-element, 99-node mesh was found to give a good representation of heart geometry, and by fitting the fiber fields to the geometric model a consistent fiber pattern was shown to hold across several hearts, irrespective of size or shape. Detailed measurements and fitting of myocardial sheet geometry have only been carried out for one heart, but it is very likely that this too will conform to a standard description once normalized for heart geometry.

The muscle fiber axis direction and myocardial sheet axis direction, together with a third axis orthogonal to these two, provide an orthogonal coordinate system to which microstructurally based constitutive laws can refer. We briefly described three such laws, one for the electrical conductivity of the tissue, one for the mechanical properties of passive myocardium, and one for active muscle, and we emphasized the need for these laws to be defined with computational efficiency in mind, given the major (i.e., time-consuming) role they play in large-scale numerical studies with the model.

Other aspects of heart anatomy briefly considered were the density of myocardial sheet branching, the extent of the Purkinje fiber network, and a description of the coronary vasculature. All of these areas need further work to incorporate adequate descriptions into the modeling framework presented here.

We have shown that the geometric nodal parameters of the finite element model provide a convenient means of comparing different hearts from one species (so far, only dog). Clearly, the mesh generation and data fitting procedures described here need to be applied to other species as well, in particular, humans. It would also be very interesting to use the changes in nodal parameters to quantify both the growth of a heart from embryonic to adult form and some pathological conditions that affect the gross anatomy and fibrous structure of the heart.

Much work remains to be done in defining adequate constitutive laws for myocardial tissue and, in particular, how the constitutive laws are affected by changes in tissue microstructure. We have briefly commented on the formulation of separate electrical and mechanical constitutive laws, but in the future the coupling between electrical and mechanical events will also need to be described at a microstructural level via coupled constitutive laws. The viscoelastic and poroelastic properties of myocardial tissue are poorly understood aspects of ventricular mechanics that also await further elucidation.

Finally, a more complete model of the heart would need to consider both the atria and the pericardium, particularly if greater use is to be made of clinically obtained image data, because these structures appear to have an important role in the mechanics of the intact heart.

REFERENCES

1. Oden, J. T., *Finite Elements of Nonlinear Continua*, McGraw-Hill, New York, 1972.
2. Nielsen, P. M. F., LeGrice, I. J., Smaill, B. H., and Hunter, P. J., Mathematical model of geometry and fibrous structure of heart, *Am. J. Physiol.* 260 (*Heart Circ. Physiol.*, 29), H1365–H1378, 1991.
3. LeGrice, I. J., Hunter, P. J., and Smaill, B. H., A mathematical model of the heart incorporating a discrete laminar myocardium, *Circ. Res.*, in preparation for submission, 1992.
4. Streeter, D. D., Jr., Gross morphology and fiber geometry of the heart, in *Handbook of Physiology* Vol. 1 (*The Heart*), Sect. 2 (The Cardiovascular System), Berne, R. M., Sperelakis, N., and Geigert, S. R., Eds., Am. Physiol. Soc., Williams and Wilkins, Baltimore, MD, 1979, pp. 61–112.
5. Robinson, T. F., Cohen-Gould, L., and Factor, S. F., Skeletal framework of mammalian heart muscle, *Lab. Invest.*, 49, 482–498, 1983.
6. LeGrice, I. J., Smaill, B. H., and Hunter, P. J., Ventricular geometry and muscle fiber organization in the dog heart, *Am. J. Physiol.*, in preparation for submission, 1992.
7. MacCallum, J. B., On the muscular architecture and growth of the ventricles of the heart, *Johns Hopkins Hosp. Rep.*, 9, 307–335, 1900.
8. Mall, F. P., On the muscular architecture of the ventricles of the human heart, *Am. J. Anat.*, 11, 211–266, 1911.
9. Streeter, D. D., Jr. and Bassett, D. L., An engineering analysis of myocardial fiber orientation in pig's left ventricle in systole, *Anat. Rec.*, 155, 503–511, 1966.

10 Raisz, E., *Principles of Cartography*, McGraw-Hill, New York, 1962.
11 LeGrice, I. J., Smaill, B. H., Chai, L. Z., Edgar, S. G., Hunter, P. J., and Gavin, J. B., Cellular organization and connective tissue architecture in the heart: ventricular myocardium is not a continuum, *Cir. Res.*, in preparation for submission, 1992.
12 FitzHugh, R., Computation of impulse initiation and saltatory conduction in a myelinated nerve fiber, *Biophys. J.*, 2, 11–21, 1962.
13 Bergel, D. A., and Hunter, P. J., *Mechanics of the heart, in Quantitatiie Cardiovascular Studies: Clinical and Research Applications of Engineering Principles*, Wang, N. H. C., Gross, D. R., and Patel, D. J., Eds., University Park Press, Baltimore, MD, 1979, pp. 151–213.
14 Hunter, P. J. and Smaill, B. H., The analysis of cardiac function: a continuum approach, *Prog. Biophys. Molec. Biol.* 52, 101–164, 1989.
15 Roberts, D. E., Hersh, L. T., and Scher, A. M., Influence of cardiac fiber orientation on wavefront voltage, conduction velocity, and tissue resistivity in the dog, *Circ. Res.*, 44, 701–712, 1979.
16 Beeler, G. H. and Reuter, H., Reconstruction of the action potential of ventricular myocardial fibres, *J. Physiol. (London)*, 268, 177–210, 1977.
17 diFrancesco, D. and Noble, D., A model of cardiac electrical activity incorporating ionic pumps and concentration changes, *Philos. Trans. Roy. Soc. London Ser. B*, 307, 353–398, 1985.
18 Smaill, B. H. and Hunter, P. J., Structure and function of the diastolic heart: material properties of the passive myocardium, in *Theory of the Heart*, Glass, L., Hunter, P. J., and McCulloch, A. D., Eds., Springer-Verlag, Berlin, 1991.
19 Hunter, P. J., Smaill, B. H., and Hunter, I. W., A "pole-zero" constitutive law for myocardium, *ASME J. Biomech.*, submitted.
1 Argyris, J. H. and Kelsey, S., *Energy Theorems and Structural Analysis*, Butterworths, London, 1960.
2 Arts, T., Veenstra, P. C., and Reneman, R. S., Epicardial deformation and left ventricular wall mechanics during ejection in the dog, *Am. J. Physiol.*, 243, H379–H390, 1982.
3 Bailie, A. H., Mitchell, R. H., and Anderson, J. M., A computer model of re-entry in cardiac tissue, *Comput. Biol. Med.*, 20, 47–54, 1990.
4 Beeler, G. W. and Reuter, H., Reconstruction of the action potential of ventricular myocardial fibers, *J. Physiol. (London)*, 268, 177–210, 1977.
5 Bergel, D. A. and Hunter, P. J., *The mechanics of the heart, in Quantitatiie Cardiovascular Studies*, Hwang, N. H. C., Gross, D. R., and Patel, D. I., Eds., University Park Press, Baltimore, 1979, pp. 151–213.
6 Beyar, R. and Sideman, S., The dynamic twisting of the left ventricle: A computer study, *Ann. Biomed. Eng.*, 14, 547–563, 1986.
7 Bluhm, W. F. and McCulloch, A. D., A fading memory model for cardiac muscle, *FASEB J.*, 6(4), A983, 1992.
8 Bogen, D. K., Rabinowitz, S. A., Needleman, A., McMahon, T. A., and Abelmann, W. H., An analysis of the mechanical disadvantage of myocardial infarction in the canine left ventricle, *Circ. Res.*, 47, 728–741, 1980.
9 Broyden, C. G., The convergence of a class of double rank minimization algorithms, *J. Inst. Math. Appl.*, 6, 76–90, 1970.
10 Chen, P.-S., Wolf, P. D., Dixon, E. G., et al., Mechanism of ventricular vulnerability to single premature stimuli in open-chest dogs, *Circ. Res.*, 62, 1191–1209, 1988.
11 Courtemanche, M., Skaggs, W., and Winfree, A. T., Stable three-dimensional action potential circulation in the FitzHugh–Nagumo model, *Physica D*, 41, 173–182, 1990.
12 Dahlquist, G. and Bjorck, A., *Numerical Methods*, Prentice-Hall, Englewood Cliffs, NJ, 1974.
13 Demer, L. L. and Ying, F. C. P., Passive biaxial mechanical properties of isolated canine myocardium, *J. Physiol.*, 339, 615–630, 1983.
14 Demiray, H., Large deformation analysis of some basic problems in biophysics. *Bull. Math. Biol.*, 38, 701–712, 1976.
15 Feit, T. S., Diastolic pressure-volume relations and distribution of pressure and fiber extension across the wall of a model left ventricle, *Biophys. J.*, 28, 143–166, 1979.
16 FitzHugh, R. A., Impulses and physiological states in theoretical models of nerve membrane, *Biophys. J.*, 1, 445–466, 1961.
17 Fletcher, R. A., A new approach to variable metric algorithms, *Comput. J.*, 13, 317–322, 1970.
18 Flynn, M. J., Some computer organizations and their effectiveness, *IEEE Trans. Comput.*. C-21(9). 948–960, 1972.
19 Frazier, D. W., Wolf, P. D., Wharton, J. M., Tang, A. S. F., Smith, W. M., and Ideker, R. E., Mechanism for electrical initiation of reentry in normal canine myocardium, *J. Clin. Invest.*, 83, 1039–1052, 1989.
20 Gallivan, K., Plemmons, R., and Sameh, A., Parallel algorithms for dense linear algebra computations, *SIAM Rev.*, 31, 54–135, 1990.
21 Gerhardt, M., Schuster, H., and Tyson, J. J., A cellular automaton model of excitable media including curvature and dispersion, *Science*, 247, 1563–1566, 1990.
22 Gill, P. E., Murray, W., and Wright, M. H., *Practical Optimization*, Academic, London, 1981.
23 Glantz, S. A., Misbach, G. A., Moores, W. Y., et al., The pericardium substantially affects the left ventricular diastolic pressure-volume relationship in the dog, *Circ. Res.*, 42, 433–441, 1978.
24 Goldfarb, D., A family of variable metric methods derived by variational means, *Math. Comput.*, 24, 23–26, 1970.
25 Guccione, J. M. and McCulloch, A. D., Mechanics of active contraction in cardiac muscle. I. Constitutive relations for fiber stress that describe deactivation, *ASME J. Biomech. Eng., in press*, 1993.

26 Guccione, J. M. and McCulloch, A. D., Mechanics of active contraction in cardiac muscle. II. Cylindrical models of the systolic left ventricle, *ASMEJ. Biomech. Eng., in press*, 1993.
27 Guccione, J. M., McCulloch, A. D., and Waldman, L. K., Passive material properties of intact ventricular myocardium determined from a cylindrical model, *ASME J. Biomech. Eng.*, 113, 42–55, 1991.
28 Gubko, F. P. and Petrov, A. A., Mechanism of the formation of closed pathways of conduction in excitable media, *Biofizika*, 17, 261–270, 1972.
29 Gulrajani, R. M., Models of the electrical activity of the heart and computer simulation of the electrocardiogram, *CRC Crit. Rev. Biomed. Eng.*, 16, 1–66, 1988.
30 Hamid, M. S., Sabbah, H. N., and Stein, P. D., Determination of left ventricular wall stress during isometric contraction using finite elements, *Comput. Structures*, 24, 589–594, 1986.
31 Hansen, D. E., Sarris, G. E., Niczyporuk, M. A., Derby, G. C., Cahill, P. D., and Miller, D. C., Physiologic role of the mitral apparatus in left ventricular regional mechanics, contraction synergy, and global systolic performance, *J. Thorac. Cardiovasc. Surg.*, 97, 521–533, 1989.
32 Heath, M. T., Ng, E., and Peyton, B. W., Parallel algorithms for sparse linear systems, *SIAM Rev.*, 33, 420–460, 1991.
33 Heethaar, R. M., Pao, Y. C., and Ritman, E. L., Computer aspects of three-dimensional finite element analysis of stresses and strains in the intact heart, *Comput. Biomed. Res.*, 10, 271–285, 1977.
34 Horowitz, A., Sheinman, I., and Lanir, Y., Nonlinear incompressible finite element for simulating loading of cardiac tissue. II. Three dimensional formulation for thick ventricular wall segments, *J. Biomech. Eng.*, 110(1), 62–68, 1988.
35 Humphrey, J. D. and Yin. F. C. P., Biaxial mechanical behavior of excised epicardium, *ASME J. Biomech. Eng.*, 110, 349–351, 1988.
36 Humphrey, J. D. and Yin, F. C. P., Constitutive relations and finite deformations of passive cardiac tissue. II. Stress analysis in the left ventricle, *Circ. Res.*, 65, 805–817, 1989.
37 Hunter, P. J., McCulloch, A. D., Nielsen, P. M. F., and Smaill, B. H., *A finite element model of passive ventricular mechanics, in Computational Methods in Bioengineering*, Spilker, R. L. and Simon, B. R., Eds., vol. BED-9, ASME, Chicago, 1988, pp. 387–397.
38 Huyghe, J. M. R. J., *Eindhoven University*, The Netherlands, 1986.
39 Irons, B. M., A frontal solution program, *Int. J. Numer. Methods Eng.*, 2, 5–32, 1970.
40 Janz, R. F. and Grimm, A. F., Deformation of the diastolic left ventricle. I. Nonlinear elastic effects, *Biophys. J.*, 13, 689–704, 1973.
41 Janz, R. F., Kubert, B. R., Moriarty, T. F., and Grimm, A. F., Deformation of the diastolic left ventricle. II. Nonlinear geometric effects, *J. Biomech.*, 7, 509–516, 1974.
42 Janz, R. F. and Waldron, R. J., Predicted effect of chronic apical aneurysms on the passive stiffness of the human left ventricle, *Circ. Res.*, 42, 255–263, 1978.
43 Keener, J. P., *Wave propagation in myocardium, in Theory of Heart: Biomechanics, Biophysics and Nonlinear Dynamics of Cardiac Function*, Glass, L., Hunter, P. J., and McCulloch, A. D., Eds., Springer-Verlag, New York, 1991, pp. 405–436.
44 Kogan, B. Y., Karplus, W. J., and Pang, A. T., Simulation of nonlinear distributed parameter systems on the connection machine, *Simulation*, 55(N5), 271–281, 1990.
45 Lab, M. J. and Holden, A. V., Mechanically induced changes in electrophysiology: Implications for arrhythmia and theory, in *Theory of Heart: Biomechanics, Biophysics and Nonlinear Dynamics of Cardiac Function*, Glass, L., Hunter, P. J., and McCulloch, A. D., Eds., Springer-Verlag, New York, 1991, pp. 561–581.
46 Le Tallec, P., Compatibility condition and existence results in discrete finite incompressible elasticity, *Comput. Methods Appl. Math. Eng.*, 27, 239–259, 1981.
47 Lee, M. C., Fung, Y. C., Shabetai, R., and LeWinter, M. M., Biaxial mechanical properties of human pericardium and canine comparisons, *Am. J. Physiol.*, 253, H75–H82, 1987.
48 Leon, L. J. and Roberge, F. A., Directional characteristics of action potential propagation in cardiac muscle, *Circ. Res.*, 69, 378–395, 1991.
49 Lesh, M. D., Pring, M., and Spear, J. F., Cellular uncoupling can unmask dispersion of action potential duration in ventricular myocardium, *Circ. Res.*, 65, 1426–1440, 1989.
50 McCulloch, A. D., Guccione, J. M., Rogers, J. M., and Hunter, P. J., Three-dimensional finite element analysis of stress and activation in the heart, in *Proc. ASCE*, 1991, pp. 514–581.
51 McCulloch, A. D. and Hunter, P. J., Finite element modeling of left ventricular mechanics, in *Proceedings of the First World Congress of Biomechanics*, La Jolla, CA, 1990, p. 32.
52 McCulloch, A. D. and Omens, J. H., Factors affecting the regional mechanics of the diastolic heart, in *Theory of Heart: Biomechanics, Biophysics and Nonlinear Dynamics of Cardiac Function*, Glass, L., Hunter, P. J., and McCulloch, A. D., Eds., Springer-Verlag, New York, 1991, pp. 87–119.
53 McCulloch, A. D., Smaill, B. H., and Hunter, P. J., Regional left ventricular epicardial deformation in the passive dog heart, *Circ. Res.*, 64, 721–733, 1989.
54 Mirsky, I., Ventricular and arterial wall stresses based on large deformation analyses, *Biophys. J.*, 13, 1141–1157, 1973.
55 Moe, G. K., Reinboldt, W. C., and Abildskov, J. A., A computer model of atrial fibrillation, *Am. Heart J.*, 67, 200–220, 1964.
56 Needleman, A., Rabinowitz, S. A., Bogen, D. K., and McMahon, T. A., A finite model of infarcted left ventricle, *J. Biomech.*, 16, 45–58, 1983.

57 Nielsen, K., *Ada in Distributed Real-Time Systems*, 1st ed., McGraw-Hill, New York, 1990, p. 371.
58 Nielsen, P. M. F., Le Grice, I. J., Smaill, B. H., and Hunter, P. J., Mathematical model of geometry and fibrous structure of the heart, *Am. J. Physiol.*, 260(Heart Circ. Physiol. 29), H1365–H1378, 1991.
59 Ohayon, J. and Chadwick, R., Theoretical analysis of the effects of a radial activation wave and twisting motion on the mechanics of the left ventricle. *Biorheology*, 25(3), 435–447, 1988.
60 Omens, J. H., May, K. D., and McCulloch, A. D., Transmural distribution of finite strain in the isolated arrested canine left ventricle, *Am. J. Physiol.*, 261 (Heart Circ. Physiol. 30), H918–H928, 1991.
61 Panda, S. C. and Natarajan, R., Finite-element method of stress analysis in the human left ventricular layered wall structure, *Med. Biol. Eng. Comput.*, 15, 67–71, 1977.
62 Perl, M., Horowitz, A., and Sideman, S., Comprehensive model for the simulation of left ventricle mechanics, *Med. Biol. Eng. Comput.*, 2, 145–149, 1986.
63 Pinto, J. G. and Fung, Y. C., Mechanical properties of the heart muscle in the passive state, *J. Biomech.*, 6, 597–616, 1973.
64 Plonsey, R. and Barr, R. C., Current flow patterns in two-dimensional anisotropic bisyncytia with normal and extreme conductivities, *Biophys. J.*, 45, 557–571, 1984.
65 Pogwizd, S. M. and Corr, P. B., Mechanisms underlying the development of ventricular fibrillation during early myocardial ischemia, *Circ. Res.*, 66, 672–695, 1990.
66 Restivo, M., Craelius, W., Gough, W. P., and El-Sherif, N. A., A logical state model of reentrant ventricular activation, *lEEE Trans. Biomed. Eng.*, 37, 344–353, 1990.
67 Ritman, E. L., Heethaar, R. M., Robb, R. A., and Pao, Y. C., Finite element analysis of myocardial diastolic stress and strain relationships in the intact heart, *Eur. J. Cardiol.*, 1, 105–119, 1978.
68 Rogers, J. M. and McCulloch, A. D., A collocation/Galerkin finite element model of the electrical activity of the heart, *Adi. Bioeng.*, BED-20, 591–594, 1991.
69 Rudy, Y. and Quan, W.-L., A model study of the effects of discrete cellular structure on electrical propagation in cardiac tissue, *Circ. Res.*, 61, 815–823, 1987.
70 Shanno, D. F., Conditioning of quasi-Newton methods for function minimization, *Math. Comput.*, 34, 647–657, 1970.
71 Shibata, N., Chen, P.-S., Dixon, E. G., et al., Influence of shock strength and timing on induction of ventricular arrhythmias in dogs, *Am. J. Physiol.*, 255, H891–H901, 1988.
72 Slinker, B. K., Goto, Y., and LeWinter, M. M., Systolic direct ventricular interaction affects left ventricular contraction and relaxation in the intact dog circulation, *Circ. Res.*, 65, 307–315, 1989.
73 Smith, J. M. and Cohen, R. J., Simple finite-element model accounts for a wide range of cardiac dysrhythmias, *Proc. Natl. Acad. Sci. USA*, 81, 233–237, 1984.
74 Streeter, D. D., Jr. and Hanna, W. T., Engineering mechanics for successive states in canine left ventricular myocardium. I. Cavity and wall geometry, *Circ. Res.*, 33, 639–655, 1973.
75 Streeter, D. D., Jr. and Hanna, W. T., Engineering mechanics for successive states in canine left ventricular myocardium. II. Fiber angle and sarcomere length, *Circ. Res.*, 33, 656–664, 1973.
76 Suga, H. and Sagawa, K., Instantaneous pressure-volume relationships and their ratio in the excised supported canine left ventricle, *Circ. Res.*, 35, 117–126, 1974.
77 ter Keurs, H. E. D. J., Rijnsburger, W. H., Van Heuningen, R., and Nagelsmit, M. J., Tension development and sarcomere length in rat cardiac trabeculae: Evidence of length-dependent activation, *Circ. Res.*, 46, 703–713, 1980.
78 Takor, N. V. and Eisenman, L. N., Three-dimensional computer model of the heart: Fibrillation induced by extrastimulation, *Comput. Biomed. Res.*, 22, 532–545, 1989.
79 Tozeren, A., Static analysis of the left ventricle, *J. Biomech. Eng.*, 105, 39–46, 1983.
80 Tozeren, A., Continuum rheology of muscle contraction and its application to cardiac contractility, *Biophys. J.*, 47, 303–309, 1985.
81 Turner, M. J., Clough, R. W., Martin, H. C., and Topp, L. J., Stiffness and deflection analysis of complex structures, *J. Aero. Sci.*, 9, 805–823, 1956.
82 Van Capelle, F. J. L. and Durrer, D., Computer simulation of arrhythmias in a network of coupled excitable elements, *Circ. Res.*, 47, 454–466, 1980.
83 Vawter, D. L., Poisson's ratio and incompressibility, *ASME J. Biomech. Eng.*, 105, 194–195, 1983.
84 Waldman, L. K., Fung, Y. C., and Coveil, J. W., Transmural myocardial deformation in the canine left ventricle: Normal in vivo three-dimensional finite strains, *Circ. Res.*, 57, 152–162, 1985.
85 Waldman, L. K., Nossan, D., Villarreal, F., and Coveil, J. W., Relation between transmural deformation and local myofiber direction in canine left ventricle, *Circ. Res.*, 63, 550–562, 1988.
86 Winfree, A. T., Electrical instability in cardiac muscle: Phase singularities and rotors, *J. Theor. Biol.*, 138, 353–405, 1989.
87 Yettram, A. L., Vinson, C. A., and Gibson, D. G., Effect of myocardial fibre architecture on the behaviour of the human left ventricle in diastole, *J. Biomed. Eng.*, 5, 321–328, 1983.
88 Yin, F. C. P., Ventricular wall stress, *Circ. Res.*, 49, 829–842, 1981.
89 Yin, F. C. P., Strumpf, R. K., Chew, P. H., and Zeger, S. L., Quantification of the mechanical properties of noncontracting canine myocardium under simultaneous biaxial loading, *J. Biomech.*, 20, 577–589, 1987.
90 Zienkeiwicz, O. C. and Morgan, K., *Finite Elements and Approximations*, University of Wales, Swansea, UK, 1982.
91 Zitelli, T., McCulloch, A. D., Chen, P.-S., and Waldman, L. K., Distribution of electromechanical function in the beating dog heart, *FASEB J.*, 6(4), 1232, 1992.

1 Peskin, C. S., Flow Patterns Around Heart Valves: A Digital Computer Method for Solving the Equations of Motion, *Ph.D. thesis, Albert Einstein College of Medicine*, 1972 (available from University Microfilms, 72–30, 378).
2 Peskin, C. S., Numerical analysis of blood flow in the heart, *J. Comput. Phys.*, 25, 220–252, 1977.
3 Peskin, C. S. and McQueen, D. M., A three-dimensional computational method for blood flow in the heart. I. Immersed elastic fibers in a viscous incompressible fluid, *J. Comput. Phys.*, 81, 372–405, 1989.
4 McQueen, D. M. and Peskin, C. S., A three-dimensional computational method for blood flow in the heart. II. Contractile fibers, *J. Comput. Phys.*, 82, 289–297, 1989.
5 Peskin, C. S. and McQueen, D. M., Computational biofluid dynamics, *Contemp. Math., in press*, 1992.
6 Chorin, A. J., Numerical solution of the Navier-Stokes equations, *Math. Comp.*, 22, 745–762, 1968.
7 Chorin, A. J., On the convergence of discrete approximations to the Navier-Stokes equations, *Math. Comp.*, 23, 341–353, 1969.
8 McQueen, D. M., Peskin, C. S., and Yellin, E. L., Fluid dynamics of the mitral valve: Physiological aspects of a mathematical model, *Am. J. Physiol.*, 242, H1095–H1110, 1982.
9 Printz, B. F., Peskin, C. S., Yellin, E. L., and Teichholz, L. E., Effects of mitral apparatus geometry on mitral flow and leaflet motion: A computer study, *J. Am. Coll. Cardiol., submitted.*
10 Meisner, J. S., McQueen, D. M., Ishida, Y., Vetter, H. O., Bortolotti, U., Strom, J. A., Frater, R. W. M., Peskin, C. S., and Yellin, E. L., Effects of timing of atrial systole on LV filling and mitral valve closure: Computer and dog studies. *Am. J. Physiol.*, 249, H604–H619, 1985.
11 Peskin, C. S. and McQueen, D. M., Modeling prosthetic heart valves for numerical analysis of blood flow in the heart, *J. Comput. Phys.*, 37, 113–132, 1980.
12 McQueen, D. M. and Peskin, C. S., Computer-assisted design of pivoting-disc prosthetic mitral valves, *J. Thoracic Cardiovasc. Sarg.*, 86, 126–135, 1983.
13 McQueen, D. M. and Peskin, C. S., Computer-assisted design of butterfly bileaflet valves for the mitral position, *Scand. J. Thoracic Cardiovasc. Surg.*, 19, 139–148, 1985.
14 McQueen, D. M. and Peskin, C. S., *Curved butterfly bileaflet prosthetic cardiac valve*, U.S. Patent Number 5026391, 1991.
15 McQueen, D. M. and Peskin, C. S., *A heart valve prothesis*, European Patent Publication Number EP 0 211 576 B1, 1990.
16 Thomas, C. E., The muscular architecture of the ventricles of hog and dog hearts, *Am. J. Anatomy*, 101, 17–57, 1957.
17 Streeter, D. D., Jr., Spotnitz, H. M., Patel, D. P., Ross, J., Jr., and Sonnenblick, E. H., Fiber orientation in the canine left ventricle during diastole and systole, *Circ. Res.*, 24, 339–347, 1969.
18 Streeter, D. D., Jr., Powers, W. E., Ross, M. A., and Torrent-Guasp, F., Three-dimensional fiber orientation in the mammalian left ventricle wall, in *Cardiovascalar System Dynamics*, Baan, J., Noordergraaf, A., and Raines, J., Eds., MIT Press, Cambridge, MA, 1978, pp. 73–84.
19 Peskin, C. S. and McQueen, D. M., Mechanical equilibrium determines the fractal fiber architecture of the aortic heart valve leaflets, *Am. J. Physiol., submitted.*
20 Buttke, T. F., A numerical study of superfluid turbulence in the self-induction approximation, *J. Comput. Phys.*, 76, 301–326, 1988.
21 Sauren, A. A. H. J., The Mechanical Behavior of the Aortic Valve, *Ph.D. thesis*, Eindhoven Technical University, The Netherlands, 1981.
22 Peskin, C. S., Fiber architecture of the left ventricular wall: An asymptotic analysis, *Commun. Pure Appl. Math.*, 42, 79–113, 1989.
1 Thompson, J. F., Warsi, Z. U. A., and Mastin, C.W., *Numerical Grid Generation: Foundations and Applications*, North-Holland, Amsterdam, 1985.
2 Thompson, J. F., Grid generation, in *Handbook of Numerical Heat Transfer*, Minkowycz, W. J., Sparrow, E. M., Schneider, G. E., and Pletcher, R. H., Eds., Wiley, New York, 1988, ch. 21.
3 Thompson, J. F., Warsi, Z. U. A., and Mastin, C. W., Boundary-fitted coordinate systems for numerical solution of partial differential equations—A review, *J. Computat. Phys.*, 47, 1, 1982.
4 Thompson, J. F., Grid generation techniques in computational fluid dynamics, *AIAA J.*, 22, 1505, 1984.
5 Thompson, J. F., A survey of dynamically-adaptive grids in the numerical solution of partial differential equations, *Appl. Numer. Math.*, 1, 3, 1985.
6 Eiseman, P. R., Grid generation for fluid mechanics computations, *Annu. Rev. Fluid Mechanics*, vol. 17, 1985.
7 Thompson, J. F., A survey of composite grid generation for general three-dimensional regions, in *Numerical Methods for Engine-Airframe Interpolation*, Murthy, S. N. B. and Paynter, G. C., Eds., AIAA, New York, 1986.
8 Thompson, J. F. and Steger, J. L., Eds., *Three Dimensional Grid Generation for Complex Configurations—Recent Progress*, AGARD-AG No. 309, AGARD, NATO, 1988.
9 Thompson, J. F., Some current trends in numerical grid generation, in *Numerical Methods for Fluid Dynamics III*, Morton, K. W. and Baines, M. J., Eds., Oxford University Press, 1988, p. 87.
10 Thompson, J. F., Ed., *Numerical Grid Generation*, North-Holland, Amsterdam, 1982 (also published as vols. 10 and 11 of Appl. Math. Computat., 1982).
11 Smith, R. E., Ed., *Numerical Grid Generation Techniques, NASA Conf. Publ. 2166*, NASA Langley Research Center, 1980.
12 Ghia, K. H. and Ghia, U., Eds., Advances in Grid Generation, FED—vol. 5, *Applied Mechanics, Bioengineering, and Fluids Engineering Conference*, ASME, New York, 1983.

13 Hauser, J. and Taylor, C., Eds., Numerical Grid Generation in Computational Fluid Dynamics, *Proc. 1st Int. Conf*, Pineridge Press, Swansea, Wales, UK, 1986.
14 Sengupta, S., Hauser, J., Eiseman, P. R., and Thompson, J. F., Eds., *Numerical Grid Generation in Computational Fluid Dynamics 1988, Proceedings of.the Second International Conference*, Pineridge Press, Swansea, Wales, UK, 1988.
15 Arcilla, A. S., Hauser, J., Eiseman, P. R., and Thompson, J. F., Eds., Numerical Grid Generation in Computational Fluid Dynamics and Related Fields, *Proc. 3rd Int. Conf*, North-Holland, Amsterdam, 1991.
16 Thompson, J. F., A composite grid generation code for 3D regions—The EAGLE code, *AIAA J.*, 26, 915, 1988.
17 Thompson, J. F., Lijewski, L. E., and Gatlin, B., Efficient application techniques of the EAGLE grid code to complex missile configurations, in *AIAA 27th Aerospace Sciences Meeting*, Reno, NV, 1989, AIAA-89-0361.
18 Gatlin, B., Thompson, J. F., Yoon, Y. H., Luong, P., Ganapathiraju, D., and Wolverton, M. K., Extensions to the EAGLE grid code for quality control and efficiency, in *AIAA 29th Aerospace Sciences Meeting*, Reno, NV, 1991, AIAA-91-0148.
19 Soni, B. K., Thompson, J. F., Stokes, M., and Shih, M., GENIE: EAGLE-VIEW and TIGER: General and special purpose graphically interactive grid system, in *AIAA 30th Aerospace Sciences Meeting*, Reno, NV, 1992, AIAA-92-0071.
20 Sorenson, R. L., Three-dimensional elliptic grid generation about fighter aircraft for zonal finite-difference computations, in *AIAA 24th Aerospace Sciences Meeting*. Reno, NV, 1987, AIAA-86-0429.
21 Sorenson, R. L., Three-dimensional zonal grids about arbitrary shapes by Poisson's equation, in *Numerical Grid Generation in Computational Fluid Dynamics 1988, Proc. 2nd lnt. Conf.*, Sengupta, S., et al., Eds., Pineridge Press, Swansea, Wales, UK, 1988, pp. 75–84 (also published as NASA TN-101018, 1988).
22 Sorenson, R. L., *The 3DGRAPE.Book: Theory, Users' Manual, Examples, NASA TM-10224*, 1989.
23 Sorenson, R. L. and McCann, K. M., A method for interactive specification of multiple-block topologies, in *AIAA 29th Aerospace Sciences Meeting*, Reno, NV, 1991, AIAA-91-0147.
24 Sorenson, R. L. and McCann, K. M., A method for interactive specification of multiple-block topologies, in *Numerical Grid Generation in Computational Fluid Dynamics and Related Fields, Proc. 3rd lnt. Conf.*, Arcilla, A. S. et al., Eds., North-Holland, Amsterdam, 1991, p. 731.
25 Steinbrenner, J. P., Karman, S. L., Jr., and Chawner, J. R., Generation of multiple block grids for arbitrary 3D geometries, in *Three Dimensional Grid Generation for Complex Configurations–Recent Progress*, AGARD-AG No. 309, AGARD, NATO, 1988, p. 40.
26 Steinbrenner, J. P., Enhancements to the GRIDGEN system for increased user efficiency and grid quality, in *AIAA 30th Aerospace Sciences Meeting*, Reno, NV, 1992, AIAA-92-0662.
27 Soni, B. K., Two- and three-dimensional grid generation for internal flow applications of computational fluid dynamics, in *AIAA 17th Fluid Dynamics, Plasma Dynamics, and Laser Conference*, Cincinnati, 1985, AIAA-85-1526.
28 Soni, B. K., GENIE: Generation of computational geometry-grids for internal/external flow configurations, in *Numerical Grid Generation in Computation Fluid Dynamics 1988, Proc. 2nd lnt. Conf.*, Sengupta, S. et al., Eds., Pineridge Press, Swansea, Wales, UK, 1988, p. 915.
29 Benek, J. A., Buning, P. G., and Steger, J. L., *A 3d chimera grid embedding technique*, 1985, AIAA-85-1523.
30 Benek, J. A., Donegan, T. L., and Suhs, N. E., *Experience with three-dimensional composite grids, in Three Dimensional Grid Generation for Complex Configurations—Recent Progress*, Thompson, J. F. and Steger, J. L., Eds., AGARD-AG No. 309, AGARD, NATO, 1988, p. 124.
31 Thompson, J. F. and Mastin, C. W., Order of difference expressions curvilinear coordinate systems, *J. Fluids Eng.*, 50, 215, 1983.
32 Thompson, J. F., A general three-dimensional elliptic grid generation system on a composite block structure, *Comput. Methods Appl. Mech. Eng.*, 64, 377, 1987.
33 Vinokur, M., On one-dimensional stretching functions for finite-difference calculations, *J. Computat. Phys.*, 50, 215, 1983.
34 Gordon, W. J. and Thiel, L. C., Transfinite mappings and their application to grid generation, in *Numerical Grid Generation*, Thompson, J. F., Ed., North-Holland, Amsterdam, 1982.
35 Brackbill, J. U. and Saltzman, J. S., Adaptive zoning for singular problems in two-dimensions, *J. Computat. Phys.*, 46, 948, 1986.
36 Anderson, D. A., Equidistribution schemes, Poisson generation, and adaptive grids, *Appl Math. Computat.*, 24, 211, 1987.
37 Eiseman, P. R., Adaptive grid generation, *Comput. Methods Appl. Mech. Eng.*, 64, 321, 1987.
38 Warsi, Z. U. A. and Thompson, J. F., Application of variational methods in the fixed and adaptive grid generation, *Comput. Math. Appl.*, 19, 31–41, 1990.
39 Kim, J. K. and Thompson, J. F., Three-dimensional adaptive grid generation on a composite block grid, *AIAA J.*, 28, 420, 1990.
40 Tu, Y. and Thompson, J. F., Three-dimensional solution—Adaptive grid generation on composite configurations, *AIAA J.*, 29, 2025, 1991.
41 Luong, P., Thompson, J. F., and Gatlin, B., Adaptive EAGLE: Solution-adaptive and quality-enhancing multi-block grids for arbitrary domains, in *AIAA 10th Computational Fluid Dynamics Conference*, Honolulu, 1991, AIAA-91-1593CP.
42 Baker, T. J., Developments and trends in three-dimensional mesh generation, *Appl. Numer. Methods*, 5, 275–309, 1989.

43 George, P. L., *Automatic Mesh Generation*. Wiley, New York, 1991.
44 Thacker, W. C., A brief review of techniques for generating irregular computational grids, *Int. J. Numer. Method Eng.*, 15, 1335–1341, 1980.
45 Aho, A., Hopcroft, J., and Ullman, J., *Data Structures and Algorithms*. Addison-Wesley, Reading, MA, 1983.
46 Lohner, R., Some useful data structures for the generation of unstructured grids, *Commun. Appl. Numer. Methods*, 4, 123–135, 1988.
47 Dirichlet, G. L., Über die Reduction der positiven quadratischen formen mit drei underestimmten ganzen Zahlen, *Z. Reine Angew. Math.*, 40(3), 209–227. 1850.
48 Voronoi, G., Nouvelles applications des paramètres continus à la théorie des formes quadratiques. Recherches sur les parallelloedres primitifs, *J. Reine Angew. Math.*, vol. 134, 1908.
49 Delaunay, B., Sur la sphere vide, *Bull. Acad. Sci. URSS, Class. Sei. Nat.*, pp. 793–800, 1934.
50 Preparata, F. P. and Shamos, M. I., *Computational Geometry, An Introduction*. Springer-Verlag, Berlin, 1985.
51 Watson, D. F., Computing the n-dimensional Delaunay tessellation with applications to Voronoi polytopes, *Comput. J.*, 24(2), 167–172, 1981.
52 Green, P. J. and Sibson, R., Computing Dirichlet tessellations in the plane, *Comput. J.*, 21(2), 168-173, 1978.
53 Bowyer, A., Computing Dirichlet tessallations, *Comput. J.*, 24, 162–166, 1981.
54 Weatherill, N. P. and Hassan, O., *A fast implementation of the Bowyer algorithm for Delaunay triangulations, to be published*, 1992.
55 Baker, T. J., Automatic mesh generation for complex three-dimensional regions using a constrained Delaunay triangulation, *Eng. Comput.*, 5, 161–175, 1989.
56 George, P. L., Hecht, F., and Saltel, E., Automatic mesh generation with specified boundary, *Computat. Methods Appl. Mech. Eng.*, 1990.
57 Childs, P. N. and Weatherill, N. P., Generation of unstructured grids within a hybrid multiblock environment, in *Proc. 3rd Int. Conf. Numerical Grid Generation*, Elsevier, Amsterdam, 1991.
58 Jameson, A., Baker, T. J., and Weatherill, N. P., Calculation of inviscid transonic flow over a complete aircraft, in *AIAA 24th Aerospace Sciences Meeting*, Reno, NV, 1986, AIAA 86-0103.
59 Weatherill, N. P., A method for generating irregular computational grids in multiply connected planer domains, *Int. J. Numer. Methods Fluids*, 8, 181–197, 1988.
60 Baker, T. J., Three dimensional mesh generation by triangulation of arbitrary point sets, *Appl. Numer. Math.*, 2, 1, 1986.
61 Baker, T. J., Shape reconstruction and volume meshing for complex solids, *Int. J. Numer. Methods Eng.*, 32, 665–675, 1991.
62 George, P. L. and Hermeline, F., Delaunay's mesh of a convex polyhedron in dimension d. Application for arbitrary polyhedra, *Int. J. Numer. Methods Eng.*, 1991.
63 Lo, S. H., A new mesh generation scheme for arbitrary planer domains, *Int. J. Numer. Methods Eng.*, pp. 1403–1426, 1985.
64 Lohner, R. and Parikh, P., Three-dimensional grid generation by the advancing-front method, *Int. J. Numer. Methods Fluids*, 8, 1135–1149, 1988.
65 Peraire, J., Peiro, J., Formaggia, L., Morgan, K., and Zienkiewicz, O. C., Finite element Euler computations in three dimensions, *Int. J. Numer. Methods Eng.*, 26, 2135–2159, 1988.
66 Yerri, M. A. and Shephard, M. S., Automatic 3D mesh generation by the modified octree technique, *Int. J. Numer. Methods Eng.*, 20, 1965–1990, 1984.
67 Weatherill, N. P., Mixed structured-unstructured meshes for aerodynamic flow simulation, *Aeronaut. J.*, 94(934), 111–123, April 1990.
68 Weatherill, N. P. and Natakusumah, D. J., The simulation of potential flow around multiple bodies using overlapping connected meshes, *Appl. Math. Computat.*, 46(1), 1–22, 1991.
69 Weatherill, N. P., Grid generation, *VKI Lecture Series Notes*, 1990–10, 1990.
70 Shephard, M. S. and Weatherill, N. P., Eds., Special Volume on Grid Adaption, *J. Numer. Methods Eng.*, vol. 32, September 1991.
71 Zienkiewicz, O. C. and Zhu, H., *Int. J. Numer. Methods Eng.*, vol. 32, September 1991.
72 Evans, A., Marchant, M. J., Szmelter, J., and Weatherill, N. P., Adaptivity for compressible flow computations using point embedding on 2D structured multiblock grids, *Int. J. Numer. Methods Eng.*, vol. 32, 1991.
73 Peraire, J., Vahdati, M., Morgan, K., and Zienkiewicz, O. C., Adaptive remeshing for compressible flow computations, *J. Computat. Phys.*, 72(2), 449–466, 1987.
74 Steger, J. L., Grid generation with hyperbolic partial differential equations for application to complex configurations, in *Numerical Grid Generation in Computational Fluid Dynamics and Related Fields, Proc. 3rd Int. Conf.*, Arcilla, A. S. et al., Eds., North-Holland, Amsterdam, 1991.
75 Eiseman, P. R., Coordinate generation with precise controls over mesh properties, *J. Computat. Phys.*, 47, 331, 1982.
76 Eiseman, P. R., High level continuity for coordinate generation with precise controls, *J. Computat. Phys.*, 47, 352, 1982.
1 Mirowski, M., The automatic implantable cardioverter-defibrillation: an overview, *J. Am. Coll. Cardiol.*, 6, 461–466, 1985.
2 Hoffman, B. F., Suckling, E. E., and Brooks, C. McC., Vulnerability of the dog ventricle and effects of the defibrillation, *Cire. Res.*, 3, 147–151, 1955.

3 Geddes, L. A., Tacker, W. A., Rosborough, J., Moore, A. G., Câbler, P., Bailey, M., McCrady, J. D., and Witzel, D., The electrical dose for ventricular defibrillation with electrodes applied directly to the heart, *J. Thorac. Cardiocasc. Surg*., 68, 593–602, 1974.
4 Geddes, L. A. and Bourland, J. D., Theoretical considerations and practical applications, *Med. Biol. Eng. Comp*., 23, 131–137, 1985.
5 Lepeschkin, E., Jones, J. L., Rush, S., and Jones, R. E., Local potential gradients as a unifying measure for thresholds of stimulation, standstill, tachyarrhythmia and fibrillation appearing after strong capacitor discharges, *Adr. Cardiol*., 21, 268–278, 1978.
6 Geddes, L. A., Niebauer, M. J., Babbs, C. F., and Bourland, J. D., Fundamental criteria underlying the efficacy and safety of defibrillating current waveforms, *Med. Biol. Eng. Comput*., 23, 122–130, 1985.
7 Deale, O. C. and Lerman, B. R., Intrathoracic current flow during transthoracic defibrillation in dogs, *Circ. Res*., 67(6), 1405–1419, 1990.
8 Lerman, B. R. and Deale, O. C., Relation between transcardiac and transthoracic current during defibrillation in humans, *Circ. Res*., 67(6), 1420–1426, 1990.
9 Karlon, W. J., Eisenberg, S. R., and Lehr, J. L., Defibrillation current density distributions: a three-dimensional finite element model of the canine thorax, *Proc. Int. Conf. IEEE/EMBS*, 13(2), 770–771, 1991.
10 Karlon, W. J., Defibrillation Current Density Distributions: A Three-Dimensional Finite Element Model of the Canine Thorax, *M.S. thesis*, Boston University, 1991.
11 Claydon, F. J., Hilger, A. L., Morrow, M. N., and Pilkington, T. C., Examining the fraction of intrathoracic current that enters the heart during transthoracic defibrillation, *Proc. Int. Conf. IEEE/EMBS*, 13(2), 778–779, 1991.
12 Claydon, F. J., Pilkington, T. C., Tang, A. S. L., Morrow, M. N., and Ideker, R. E., A volume conductor model of the thorax for the study of defibrillation fields, *IEEE Trans. Biomed. Eng*., 35, 981–992, 1988.
13 Johnson, C. R. and MacLeod, R. S., Computer models for calculating transthoracic current flow, *Proc. Int. Conf. IEEE/EMBS*, 13(2), 768–769, 1991.
14 Blilie, D. E., Fahy, J. B., Chan, C., Ahmed, M., and Kim, Y., Efficient solution of three-dimensional finite element models for defibrillation and pacing applications, *Proc. Int. Conf. IEEE/EMBS*, 13(2), 772–773, 1991.
15 Plonsey R. and Fleming, D. G., *Bioelectric Phenomena*, McGraw-Hill, New York, 1969.
16 Pilkington, T. C. and Plonsey, R., *Engineering Contributions to Biophysical Electrocardiography*, IEEE Press, New York, 1982.
17 Plonsey, R., Laws governing current flow in the volume conductor, in *The Theoretical Basis af Electrocardiology*, Nelson, C. V. and Geselowitz, D. B., Eds., Clarendon Press, Oxford. 1976, pp. 165–174.
18 Warsi, Z. U. A., Tensors and Differential Geometry Applied to Analytic and Numerical Grid Generation, *Report No. MSSU-EIRS-81-1*, Mississippi State University, 1981.
19 Thompson, J. F., Warsi, Z. U. A., and Mastin, C. W., *Numerical Grid Generation Foundations and Applications*, North-Holland, New York, 1985.
20 Anderson, D. A., Tannehill, J. C., and Pletcher, R. H., *Computational Fluid Mechanics and Heat Transfer*, Hemisphere, New York, 1984.
21 Burnett, D. S., *Finite Element Analysis*, Addison-Wesley, Reading, MA, 1988.
22 Ramsey, M., III, Comparison of Epicardial Potentials with Measured and Simulated Torso Potentials for Ventricular Depolarization and Repolarization in *the Dog, Ph.D. dissertation*, Duke University, 1974.
23 Faux, I. D. and Pratt, M. J., *Computational Geometry for Design and Manufacture*, Ellis Horwood Ltd., London, 1979.
24 Farin, G., *Curi es and Surfaces for Computer Aided Geometric Design*, Academic Press, San Diego, 1988.
25 Thompson, J. F. and Gatlin, B., *Program EAGLE User's Manuals*, Vols. II and III, AFATL-TR-88-117, Air Force Armament Laboratory, Eglin AFB,October 1988.
26 Soni, B. K., Thompson, J. F., Stokes, M., and Shi, M. S., GENIE + +, EAGLEView, and TIGER: General and Special Purpose Graphically Interactive Grid Systems, Paper No. AIAA-92-0071, *AIAA*, 1992.
27 Fuchs, H., Kedem, Z. M., and Uselton, S. P., Optimal surface reconstruction from planar contours, *Comm. ACM*, 20(10), 693–702, 1977.
28 Weatherill, N. P., A method for generating irregular computational grids in multiply connected planar domains, *Int. J. Numer. Methods Fluids*, 8, 181–197, 1988.
29 Frey, W. H., Selective refinement: a new strategy for automatic node placement in graded triangular meshes, *Int. J. Numer. Methods Eng*., 24, 2183–2200, 1987.
30 Schmidt, J., Eason, J., and Pilkington, T., Adaptive grid generation, *submitted.*
31 Watt, A., *Fundamentals af Three-Dimensional Computer Graphics*, Addison-Wesley, Wokingham, England, 1989, pp. 162–165.
32 Rush, S., Abildskov, J., and McFee, R., Resistivity of body tissues at low frequencies, *Circ. Res*., 12, 40–50, 1963.
1 Rudy, Y. and Plonsey, R., A comparison of volume conductor and source geometry effects on body surface and epicardial potentials, *Circ. Res*., 46, 282–291, 1980.
2 Barr, R. C., Ramsey. III. M., and Spach, M. S., Relating epicardial to body surface potential distributions by means of transfer coefficients based on geometry measurements, *IEEE Trans. Biomed. Eng*., BME-24, 1–11, 1977.
3 Barr, R. C. and Spach, M. S., Inverse solutions directly in terms of potentials, in *The Theoretical Basis af. Electrocardiology*, Nelson, C. V. and Geselowitz, D. B., Eds., Clarendon Press, Oxford. 1976. p.294.
4 Martin, R. O. and Pilkington, T. C., Unconstrained inverse electrocardiography: Epicardial potentials. *IEEE Trans. Biomed. Eng*., BME-19(4), 276, 1972.

5 Martin, R. O., Pilkington, T. C., and Morrow, M. N., Statistically constrained inverse electrocardiography, *IEEE Trans. Biomed. Eng.*, BME-22, 487, 1975.
6 Barr, R. C. and Spach, M. S., Inverse calculation of QRS-T epicardial potentials from body surface potential distributions for normal and ectopic beats in the intact dog, *Circ. Res.*, 1(42), 661, 1978.
7 Mirvis, D. M., Ed., *Body Surface Electrocardiographic Mapping*, Kluwer, Boston, 1988.
8 van Dam, R. Th. and van Oosterom. A., Eds., *Electrocardiographic Body Surface Mapping*, Martinus Nijhoff, Dordrecht, 1986.
9 De Ambroggi, L., Musso, E., and Taccardi, B., Body-surface mapping in comprehensive electrocardiology: Theory and practice, in *Health and Disease*, Vol. 2, Macfarlane, P. W. and Veitch Lawrie, T. D., Eds., Pergamon Press, Oxford, 1989, pp. 1015–1050.
10 Tikhonov, A. N. and Arsenin, V. Y., *Solution of Ill-Posed Problems*, Wiley, New York, 1977.
11 Groetsch, C. W., The theory of Tikhonov regularization of Fredholm equations of the first kind, in *Advanced Research Notes in Mathematics*, Vol. 105, Pitman Advanced Publishing Program, Boston, 1984.
12 Payne, L. E., Improved stability estimates for classes of ill-posed Cauchy problems, *Appl. Anal.*, 19, 63, 1973.
13 Rudy, Y. and Messinger-Rapport, B. J., The inverse problem in electrocardiography: Solutions in terms of epicardial potentials, *CRC Crit. Rev. Biomed. Eng.*, 16, 215–268, 1988.
14 Messinger-Rapport, B. J. and Rudy, Y., Regularization of the inverse problem in electrocardiography: A model study, *Math Biosci.*, 89, 79–118, 1988.
15 Messinger-Rapport, B. J. and Rudy, Y., Computational issues of importance to the inverse recovery of epicardial potentials in a realistic heart-torso geometry, *Math. Biosci.*, 97, 85–120, 1989.
16 Messinger-Rapport, B. J. and Rudy, Y., Noninvasive recovery of epicardial potentials in a realistic heart-torso geometry: Normal sinus rhythm, *Circ. Res.*, 66, 1023–1039, 1990.
17 Oster, H. S. and Rudy, Y., The use of temporal information in the regularization of the inverse problem of electrocardiography, *IEEE Trans. Biomed. Eng.*, 39, 65–75, 1992.
18 Huebner, K. H. and Thornton, E. A., *The Finite Element Method for Engineers*, 2nd ed., Wiley, New York, 1982.
19 Brebbia, C. A., Telles, J. C. F., and Wrobel, L. C., *Boundary Element Techniques: Theory and Applications in Engineering*, Springer-Verlag, Berlin, 1984.
20 Cruse, T. A., An improved boundary-integral equation method for three dimensional elastic stress analysis, *Comput. Struct.*, 4, 741–754, 1974.
21 Foster, M., An application of the Weiner-Kolmogorov smoothing theory to matrix inversion, *J. Soc. Ind. Appl. Math.*, 9(3), 387–392, 1961.
22 Strand, O. N. and Westwater, E. R., Minimum RMS estimation of the numerical solution of a Fredholm integral equation of the first kind, *SIAM J. Numer. Anal.*, 5(2), 287–295, 1968.
23 Wahba, G., Practical approximate solutions to linear operator equations when the data are noisy, *SIAM J. Numer. Anal.*, 14, 651, 1977.
24 Colli Franzone, P., Guerri, L., Taccardi, B., and Viganotti, C., Finite element approximation of regularized solution of the inverse potential problem of electrocardiography and applications to experimental data, *Calcolo*, XXII(I), 91–186, 1985.
25 Twomey, S., On the numerical solution of Fredholm integral equations of the first kind by the inversion of the linear system produced by quadrature, *J. ACM*, 10, 97–101, 1963.
1 Andrews, H. C. and Hunt, B. C., *Digital Image Restoration*, Prentice-Hall, Englewood Cliffs NJ, 1977.
2 Baker, J. R. and Budinger, T. F., Advanced models for medical imaging, in *High Speed Computing: Scientific Applications and Algorithm Design*, University of Illinois Press, Urbana, IL, 1987, pp. 221–226.
3 Hanson, K. M., Bayesian and related methods in image reconstruction from incomplete data, in *Image Recovery: Theory and Application*, Stark, H., Ed., Academic Press, Orlando, FL, 1987, pp. 79–123.
4 Baker, J. R., Spatially Variant Tomographic Imaging: Estimation, Identification, and Optimization. *Ph.D. dissertation LBL-31561*, University of California, Berkeley, 1991.
5 Luenberger, D. G., Optimization by vector space methods, in *Decision and Control*, Howard, R. A., Ed., Wiley, New York, 1969.
6 Bellini, S., Piacentini, M., Cafforio, C., and Rocca, F., Compensation of tissue absorption in emission tomography, *IEEE Trans. Acoust., Speech, Signal Processing*, ASSP-27(3), 213–218, 1979.
7 Jaszczak, R. J. and Colemen, R. E., Single photon emission computed tomography (SPECT) principles and instrumentation, *Invest. Radiol.*, 20, 897–910, 1985.
8 Huesman, R. H., Salmeron, E. M., and Baker, J. R., Compensation for crystal penetration in high resolution positron tomography, *IEEE Trans. Nucl. Sei.*, NS-36, 1100–1107, 1989.
9 Radon, J., Über die bestimmung von funktionen durch ihre integralwert längs gewisser mannig- faltigkeiter. *Berichte Sächsische Akademie der Wissenschaften*, 69, 262–267, 1917.
10 Cormack, A. M., Representation of a function by its line integrals, with some radiological applications, *J. Appl. Phys.*, 34(9), 2722–2727, 1963.
11 Cormack, A. M., Representation of a function by its line integrals, with some radiological applications II, *J. Appl. Phys.*, 35(10), 2908–2913, 1964.
12 Deans, S. R., *The Radon Transform and Some of Its Applications*, Wiley, New York,1983.
13 Goitein, M., Three-dimensional density reconstruction from a series of two-dimensional projections. *Nucl. Instmm. Methods*, 101, 509–518, 1972.
14 Hsieh, R. C. and Wee, W. G., On methods of three-dimensional reconstruction from a set of radioisotope scintigrams, *IEEE Trans. Syst., Man, Cybem.*, SMC-6(12), 854–862, 1976.

15 Budinger, T. F., Gullberg, G. T., and Huesman, R. H., Emission computed tomography, in *Image Reconstruction from Projections*. Vol. 32, Hermann, G. T., Ed., Springer-Verlag, New York, 1979, pp. 147–246.
16 Wood, S. L., A System Theoretic Approach to Image Reconstruction, *Ph.D. dissertation*,May1978.
17 Levitan, E. and Herman, G. T., A maximum a posteriori probability expectation algorithm for image reconstruction in emission tomography, *IEEE Trans. Med. Imaging*, MI-6, 185–192, 1987.
18 Leahy, R. M. and Goutis, C. E., An optimal technique for constraint-based image restoration and reconstruction, *IEEE Trans. Acoust., Speech, Signal Processing*, ASSP-34(6), 1629–1642, 1986.
19 Leahy, R., Hebert, T. J., and Lee, R., Applications of Markov random fields in medical imaging, *Prog. Clin. Biol. Res.*, 363, 1–14, 1991.
20 Gordon, R., Bender, R., and Herman, G. T., Algebraic reconstruction techniques (ART) for threedimensional electron microscopy and x-ray photography, *J. Theoret. Biol.*, 29, 471–481, 1970.
21 Golub, G. H. and Reinsch, C., Singular value decomposition and least squares solutions, *Numer. Math.*, 14, 403–420, 1970.
22 Lawson, C. L. and Hanson, R. J., *Solving Least Squares Problems*, Prentice-Hall, Englewood Cliffs, NJ, 1974.
23 Golub, G. H. and Van Loan, C. F., *Matrix Computations*, Vol. 3, Johns Hopkins University Press, Baltimore, 1983.
24 Buonocore, M. H., Brody, W. R., and Macovski, A., A natural pixel decomposition for two dimensional image reconstruction, *IEEE Trans. Biomed. Eng.*, BME-28(2), 69–78, 1981.
25 Marr, R. B., On the reconstruction of a function on a circular domain from a sampling of its line integrals, *J. Math. Anal. Appl.*, 45, 357–374, 1974.
26 Moore, E. H., *Bull. Am. Math. Soc.*, 26, 394–395, 1920.
27 Penrose, R., A generalized inverse for matrices, *Cambridge Philos. Soc.*, 51, 406–413, 1955.
28 Strang, G., *Linear Algebra and Its Applications*, Academic Press, Orlando, FL, 1980.
29 Floyd, C. E., Jaszcak, R. J., and Colemen, R. E., Image resampling on a cylindrical sector grid, *IEEE Trans. Med. Imaging*, MI-5(3), 128–131, 1986.
30 Trussell, H. J., Orun-Ozturk, H., and Civanlar, M. R., Errors in reprojection methods in computerized tomography, *IEEE Trans. Med. Imaging*, MI-6, 220–227, 1987.
31 Knuth, D. E., *The Art of Computer Programming*, Vol. 1, Addison Wesley, Reading, MA,1981.
32 Davis, P. J., *Circulant Matrices*, Wiley, New York, 1979.
33 Brigham, E. O., *The Fast Fourier Transform*, Prentice-Hall, Englewood Cliffs, NJ, 1974.
34 Bracewell, R. N., Fourier techniques in two dimensions, in *Fourier Techniques and Applications*, Vol. 3, Part 1, Price, J. R., Ed., Plenum Press, New York, 1985, pp. 45–71.
35 Baker, J. R., Macrotasking the singular value decomposition of block circulant matrices on the Cray-2, in *Proc. Supercomputing '89*, Reno, NV, 1989, pp. 243–247.
36 Zenios, S. A. and Censor, Y., Parallel Computing with Block-Iterative Image Reconstrution Algorithms, Medical Imaging Processing Group, *Technical Report MIPG136*, Department of Radiology, University of Pennsylvania, Philadelphia,October 1988.
37 Herman, G. T., Odhner, D., Toennies, K. D., and Zenios, S. A., A Parallelized Algorithm for Image Reconstruction from Noisy Projections, *Medical Imaging Processing Group Technical Report MIPG155*, Department of Radiology, University of Pennsylvania, Philadelphia,September 1989.
38 Quinn, M. J., *Designing Efficient Algorithms for Parallel Computers*, McGraw-Hill, New York, 1987.
39 Buneman, O., Vector FFT for the Cray-2, *NMFECC (National Magnetic Fusion Energy Computing Center) Buffer*, 10(11), 10–11, 1986.
40 Despain, A. M., Very fast Fourier transform algorithms for hardware implementation, *IEEE Trans. Compute* C-28(5), 333–341, 1979.
41 Mundie, D. A. and Fisher, D. A., Parallel processing in Ada, *Computer*, 19(8), 20–25, 1986.
42 Mirin, A., Parallelization of a 3-d MHD code. Part I. Methodology and results, *NMFECC (National Magnetic Fusion Energy Computing Center) Buffer*, 11(7), 14–6, 1987.
43 Mirin, A., Parallelization of a 3-d MHD code. Part II. Analysis of multiprocessing efficiency on the Cray-2, *NMFECC (National Magnetic Fusion Energy Computing Center) Buffer*, 11(8), 11–13, 1987.
44 Patton, P. C., Multiprocessors: Architectures and applications, *Computer*, 18(6), 29–40, 1985.
45 Gelernter, D., Domesticating parallelism, *Computer*, 19(8), 12–16, 1986.
1 Beguelin, A., Dongarra, J., Geist, G., Manchek, R., and Sunderam, V., Graphical development tools for network-based concurrent supercomputing, in *Proc. Supercomputing VI Conf*, pp. 435–444.
2 Birns, P., Brown, P., and Muster, J., *UNIX for People*, Prentice-Hall, Englewood Cliffs, NJ, 1984.
3 Catlett, C., In search of gigabit applications, *IEEE Commun. Mag.*,April 1992.
4 Cline, H., Lorensen, W., Ludke, S., Crawford, C., and Teeter, B., Two algorithms for the threedimensional reconstruction of tomograms, *Med. Phys.*,May 1988.
5 Comer, D., *Internetworking with TCP/IP*, 2nd ed., Prentice-Hall, Englewood Cliffs, NJ, 1991.
6 Corbin, J., *The Art of Distributed Applications: Programming Techniques for Remote Procedure Calls*, Springer-Verlag, Berlin, 1990.
7 Cysper, R., *Communications for Cooperating Systems: OSI, SNA, and TCP/IP*, Addison-Wesley, Reading, MA, 1991.
8 Grand Challenges: High Performance Computing and Communications—The FY 1992 U.S. Research and Development Program, a Report by the Committee on Physical, Mathematical, and Engineering Sciences, *Federal Coordinating Council for Science, Engineering, and Technology, and Office of Science and Technology Policy.*

9 Foley, J., van Dam, A., Feiner, S., and Highes, J., *Computer Graphics: Principles and Practice*, 2nd ed., Addison-Wesley, Reading, MA, 1990.
10 Gigabit network testbeds, *IEEE Comput.*, 23(9), 1990.
11 *Mass Storage System Reference Model: Version 4 (May, 1990)*, Coleman, S. and Miller, S., Eds., developed by the IEEE Technical Committee on Mass Storage Systems and Technology.
12 Lee, E., Chen, P., Hartman, J., Chervenak Drapeau, A., Miller, E., Katz, R., Gibson, G., and Patterson, D., RAID-II: A Scalable Storage Architecture for High-Bandwidth Network File Service, Report No. UCB/CSD 92/672, *Computer Science Division (EECS)*, University of California, Berkeley,February 1992.
13 Jacobson, V. and Braden, R., Proposed Standard TCP Extensions for Long-Delay Paths, *ARPANet Working Group Requests for Comment RFC1072*, DDN Network Information Center, Menlo Park, CA,October 1988.
14 Jacobson, V., Congestion avoidance and control, in *Proc. ACM SIGCOMM '88 Workshop*, Stanford, CA,August 1988.
15 Jacobson, V., Braden, R., and Zhang, L., Proposed Standard TCP Extension for High-Speed Paths, *ARPANet Working Group Requests for Comment RFC1185*, DDN Network Information Center, Menlo Park, CA,October 1988.
16 Libes, D. and Ressler, S., *Life With Unix*, Prentice-Hall, Englewood Cliffs, NJ, 1989.
17 Markoff, J., Creating a giant computer highway—Robert Kahn's vision of a national network of information begins to take hold, *New York Times (Business Section)*, Sunday,September 2, 1990.
18 Narten, T., Internet routing, *Comput. Commun. Rer.*, 19(4), 1989 (Proc. ACM SIGCOMM 89 Workshop, September 1989).
19 Rasure, J. and Williams C., An integrated data flow visual language and software development environment, *J. Visual Languages Comput.*, 2(3), 217–246, 1991. (For more information, send e-mail to http://khoros-request@chama.eece.unm.edu.)
20 Schneider, M., Pittsburgh's not-so-odd couple, *Supercomput. Rer.*,August 1991.
21 Stevens, W., *Unix Network Programming*, Prentice-Hall, Englewood Cliffs, NJ, 1990.
22 *The Unix System: A Sun Technical Report*, Sun Microsystems, 1985 (part 800-1419-02).
23 Sequoia 2000: A Multimedia Large Capacity Object Server,M. Stonebraker, Computer Science Division, *University of California, Berkeley, and J. Dozier, Center for Remote Sensing and Environmental Optics*, University of California, Santa Barbara, Project Directors.
24 Sunderam, V., PVM: A framework for parallel distributed computing, *Concurrency: Practice and Experience*, 2(4), 315–339, 1990. (For more information, send the following message by e-mail to https://netlib@ornl.gov. Message: "send index from pvm," or send e-mail to https://pvm@msr.epm.ornl.gov.)
25 Upson, C. et al., The application visualization system: A computational environment for scientific visualization, *IEEE Comput. Graphics Applications*, pp. 30-42,July 1989. (For more information, contact Advanced Visualization Systems, Inc. at (617) 890-4300.)
1 Arnoczky, S. P., Structure and function of the knee meniscus, in *Biomechanics of Diarthrodial Joints*, Mow, V. C., Rateliffe, A., and Woo, S. L.-Y., Eds., Springer-Verlag, New York, 1990, pp. 177–190.
2 Wainwright, S. A., Biggs, W. D., Currey, J. D., and Gosline, J. M., *Mechanical Design in Organisms*, Princeton University Press, 1982.
3 Arnoczky, S. A., Adams, M., DeHaven, K., Eyre, D. R., and Mow, V. C., Meniscus, in *Injury and Repair of the Musculoskeletal Soft Tissue*, Woo, S. L.-Y. and Buckwalter, J. A., Eds., American Academy of Orthopaedic Surgeons, Chicago, 1988, pp. 483–537.
4 Kelly, M. A., Fithian, D. C., Chern, K. Y., and Mow, V. C., Structure and function of the meniscus: Basic clinical implications, in *Biomechanics of Diarthrodial Joints*, Mow, V. C., Rateliffe, A., and Woo. S. L.-Y., Eds., Springer-Verlag, New York, 1990, pp. 191–211.
5 Hayes, W. C., Keer, L. M., Herrmann, G., and Mockros, L. F., A mathematical analysis for indentation tests of articular cartilage, *J. Biomech.*, 5, 541–551, 1972.
6 Fung, Y. C., *Biomechanics, Mechanical Properties of Lining Tissue*, Springer-Verlag, New York, 1981.
7 Mow, V. C., Kuei, S. C., Lai, W. M., and Armstrong, C. G., Biphasic creep and stress relaxation of articular cartilage in compression: Theory and experiments, *J. Biomech. Eng.*, 102, 73–83, 1980.
8 Armstrong, C. G., Lai, W. M., and Mow, V. C., An analysis of the unconfined compression of articular cartilage, *J. Biomech. Eng.*, 106, 165–173, 1984.
9 Mow, V. C., Holmes, M. H., and Lai, W. M., Fluid transport and mechanical properties of articular cartilage: A review, *J. Biomech.*, 17, 377–394, 1984.
10 Mak, A. F., Lai, W. M., and Mow, V. C., Biphasic indentation of articular cartilage. Part I. Theoretical analysis, *J. Biomech.*, 20, 703–714, 1987.
11 Hou, J. S., Holmes, M. H., 1 .ai, W. M., and Mow, V. C., Boundary conditions at the cartilage-synovial fluid interface for joint lubrication and theoretical verifications, *J. Biomech. Eng.*, 111(1), 78–87, 1989.
12 Fithian, D. C, Kelly, M. A., and Mow, V. C., Material properties and structure-function relationships in the menisci, *Clin. Orthopaed. Rel. Res.*, 252, 19–31, 1990.
13 Lai, W. M., Mow, V. C., and Roth, V., Effects of nonlinear strain dependent permeability and rate of compression on the stress behavior of articular cartilage, *J. Biomech. Eng.*, 103, 61–66, 1981.
14 Holmes, M. H., Lai, W. M., and Mow, V. C., Singular perturbation analysis of the nonlinear, flow-dependent compressive stress relaxation behavior of articular cartilage, *J. Biomech. Eng.*, 107, 206–218, 1985.
15 Mak, A. F., The apparent viscoelastic behavior of articular cartilage—The contributions from the intrinsic matrix viscoelasticity and interstitial fluid flows, *J. Biomech. Eng.*, 108, 123–130, 1980.

16 Holmes, M. H., Finite deformation of soft tissue: Analysis of a mixture model in uni-axial compression, *J. Biomech. Eng.*, 108, 372–381, 1986.
17 Mow, V. C., Kwan, M. K., Lai, W. M., and Holmes, M. H., A finite deformation theory for nonlinearly permeable cartilage and other soft hydrated connective tissues, in *Frontiers in Biomechanics*, Woo, S. L.-Y., Schmid-Schonbein, G., and Zweifach, B., Eds., Springer-Verlag, New York, 1986, pp. 153–179.
18 Kwan, M. K., Lai, W. M., and Mow, V. C., A finite deformation theory for cartilage and other soft hydrated connective tissues, *J. Biomech.*, 23, 145–155, 1990.
19 Lai, W. M., Hou, J. S., and Mow, V. C., A triphasic theory for the swelling and deformational behaviors of articular cartilage, *J. Biomech. Eng.*, 113(3), 245–258, 1991.
20 Bowen, R. M., Incompressible porous media models by use of the theory of mixtures, *Int. J. Eng. Sci.*, 18, 1129–1148, 1980.
21 Mow, V. C., Zhu, W., and Ratcliffe, A., Biomechanical properties of articular cartilage and the meniscus, in *Basic Orthpaedic Biomechanics*, Mow, V. C. and Hayes, W. C., Eds., Raven Press, New York, 1991.
22 Ateshian, G. A., Soslowsky, L. J., Froimson, M. I., Kelly, M. A., and Mow, V. C., Determination of patellofemoral contact areas from stereophotogrammetric models of joint surfaces, in *Biomechanics Symposium*, ASME, New York, 1989.
23 Ateshian, G., Soslowsky, L., and Mow, V., Quantitation of articular surface topography and cartilage thickness in knee joints using stereophotogrammetry, *J. Biomech.*, 24(8), 761–776, 1991.
24 Blankevoort, L., Kuiper, J., Huiskes, R., and Grootenboer, H., Articular contact in a three-dimensional model of the knee, *J. Biomech.*, 24(11), 1019–1032, 1991.
25 Ghaboussi, J. and Wilson, E. L., Variational formulation of dynamics of fluid-saturated porous elastic solids, *J. Eng. Mech. Dir. ASCE*, 98(EM4), 947–963, 1972.
26 Ghaboussi, J. and Dikman, S. U., Liquefaction analysis of horizontally layered sands, *J. Geotech. Dir. ASCE*, GT3, 341–356, 1978.
27 Zienkiewicz, O. C. and Bettes, P., Soils and other saturated media under transient, dynamic conditions; General formulation and the validity of various simplifying assumptions, in *Soil Mechanics—Transient and Cyclic Loads*, Pande, G. N. and Zienkiewicz, O. C., Eds., Wiley, New York, 1982, pp. 1–16.
28 Zienkiewicz, O. C. and Shiomi, T., Dynamic behavior of saturated porous media—the generalized Biot formulation and its numerical solution, *Int. J. Anal. Methods Geomech.*, 8(1), 71–96, 1984.
29 Simon, B. R., Wu, J. S. S., and Zienkiewicz, O. C., Evaluation of higher order, mixed, and Hermitian finite element procedures for the dynamic analysis of saturated porous media using one-dimensional models, *Int. J. Numer. Anal. Methods Geomech.*, 10, 483–499, 1986.
30 Simon, B. R., Wu, J. S. S., Zienkiewicz, O. C., and Paul, D. K., Evaluation of U-W and U-P finite element methods for the dynamic response of saturated porous media using one-dimensional models, *Int. J. Numer. Methods Eng.*, 10, 461–482, 1986.
31 Biot, M. A., General theory of three-dimensional consolidation, *J. Appl. Phys.*, 12, 155–164, 1941.
32 Simon, B. R., et al., Structural models for human spinal motion segments based on a poroelastic view of the intervertebral disk, *Biomech. Eng.*, 107, 327–335, 1985.
33 Simon, B. R. and Gaballa, M., Finite strain poroelastic finite element models for large arterial cross sections, in *Computational Methods for Bioengineering*, Spilker, R. L. and Simon, B. R., Eds., ASME, New York, 1988.
34 Prevost, J. H., Nonlinear transient phenomena in saturated porous media, *Comput. Methods Appl Mech. Eng*, 20, 3–18, 1982.
35 Prevost, J. H., Non-linear transient phenomena in soil media, in *Mechanics of Engineering Materials*, Desai, C. S. and Gallagher, R. H., Eds., Wiley, New York, 1984, pp. 515–533.
36 Prevost, J. H., Wave propagation in fluid-saturated porous media: An effective finite element procedure, *Soil Dynamics Earthquake Eng.*, 4(4), 183–202, 1985.
37 Oomens, C. W. J., Van Campen, D. H., and Grootenboer, H. J., A mixture approach to the mechanics of skin, *J. Biomech.*, 20(9), 877–885, 1987.
38 Wayne, J. W., Woo, S. L.-Y., and Kwan, M. K., Application of the u-P finite element method to the study of articular cartilage, *J. Biomech. Eng.*, 113(4), 397–403, 1991.
39 Hughes, T. J. R., *The Finite Element Method: Linear Static and Dynamic Finite Element Analysis*, Prentice-Hall, Englewood Cliffs, NJ, 1987.
40 Spilker, R. L. and Suh, J.-K., Formulation and evaluation of a finite element model of soft hydrated tissue, *Comput. Structures*, 35(4), 425–439, 1990.
41 Spilker, R. L., Suh, J.-K., and Mow, V. C., A finite element formulation of the nonlinear biphasic model for articular cartilage and hydrated soft tissues including strain-dependent permeability, in *Computational Methods in Bioengineering, BED-9*, Spilker, R. L. and Simon, B. R., Eds., ASME. New York, 1988, pp. 81–92.
42 Suh, J.-K., Spilker, R. L., and Holmes, M. H., A penalty finite element analysis for nonlinear mechanics of biphasic hydrated soft tissue under large deformation, *Int. J. Numer. Methods Eng.*, 32. 1411–1439, 1991.
43 Spilker, R. L. and Maxian, T. A., A mixed-penalty finite element formulation of the linear biphasic theory for soft tissues, *Int. J. Numer. Methods Eng.*, 30, 1063–1082, 1990.
44 Holmes, M. H. and Mow, V. C., The nonlinear characteristics of soft polyelectrolyte gels and hydrated connective tissues in ultrafiltration, *J. Biomech.*, 23(11), 1145–1156, 1990.
45 Suh, J.-K., Finite Element Formulations for the Nonlinear Deformation of Soft Hydrated Tissues Using a Biphasic Model, *Ph.D. dissertation*, Rensselaer Polytechnic Institute, Troy, NY, 1989.
46 Bathe, K. J., *Finite Element Procedures in Engineering Analysis*, Prentice-Hall, Englewood Cliffs, NJ, 1982.

47 Baehmann, P. L., Wittchen, S. L., Shepard, M. S., Grice, K. R., and Yerry, M. A., Robust geometrically-based automatic two-dimensional mesh generation, *Int. J. Numer. Methods Eng.*, 24, 1043–1078, 1987.

48 Baehmann, P. L. and Shephard, M. S., Adaptive multiple-level h-refinement in automated finite element analysis, *Eng. Comput.*, 5, 235–247, 1989.

49 Babuska, I. and Yu, D., Asymptotically exact a posteriori error estimation for biquadratic elements, *Finite Elements Anal. Design*, 3, 341–345, 1987.

50 Baehmann, P. L., Shephard, M. S., and Flaherty, J. E., A posteriori error estimates for triangular and tetrahedral quadratic elements, using interior residuals, *Int. J. Numer. Methods Eng.*, 34, 1992.

51 Szabo, B. A., Mesh design for p-version of the finite element method, *Appl. Mech. Eng.*, 55(1–2), 181–197, 1986.

52 Shephard, M. S., Niu, Q., and Baehmann, P. L., Some results using stress projectors for error indication and estimation, in *Adaptice Methods for Partial Differential Equations*, Flaherty, J. E., et al., Eds., Society for Industrial and Applied Mathematics, Philadelphia, 1989.

53 Niu, Q. and Shephard, M. S., Transfer of Solution Variables for Finite Element Meshes, *Report 4–1990*, Scientific Computation Research Center, Rensselaer Polytechnic Institute, Troy, NY, 1990.

54 Vermilyea, M. E. and Spilker, R. L., Hybrid and mixed-penalty finite elements for 3D analysis of soft hydrated tissue, *Int. J. Numer. Methods Eng.*, submitted.

55 Oden, J. T. and Brauchli, H. J., On the calculation of consistent stress distributions in finite element approximations, *Int. J. Numer. Methods Eng.*, 3, 317–325, 1971.

56 Hinton, E. and Campbell, J. S., Local and global smoothing of discontinuous finite element functions using a least squares method, *Int. J. Numer. Methods Eng.*, 8, 461–480, 1974.

57 Zienkiewicz, O. C., Zhu, J. Z., Craig, A. W., and Ainsworth, A., Simple and practical error estimation and adaptivity: h and h-p version procedures, in *Adaptive Methods for Partial Differential Equations*, Flaherty, J. E., et al., Eds., Society for Industrial and Applied Mathematics, Philadelphia, 1989.

58 Zienkiewicz, O. C. and Zhu, J. Z., The three R's of engineering analysis and error estimation and adaptivity, *Comput. Methods Appl. Math.*, 82, 94–113, 1990.

59 Cantin, G., Loubignac, G., and Touzot, G., An iterative algorithm to build continuous stress and displacement solutions, *Int. J. Numer. Methods Eng*, 12, 1493–1506, 1978.

1 *NIH Consensus Development Conf* Vol. 4.4, 1982.

2 Horzack, W., Rothman, R., Booth, R., Balderston, R., Cohn, J., and Pickens, G., Survivorship analysis of 1041 Charnley total hip arthroplasties, *J. Arthroplasty*, 5(1), 41–47, 1990.

3 Collis, D., Long-term (twelve to eighteen year) follow-up of cemented total hip replacements in patients who were less than fifty years old, *J. Bone Joint Surg.*, 73A(4), 593–597, 1991.

4 Blacker, F. and Charnley, J., Changes in the upper femur after low friction arthroplasty, *Clin. Orthop. Rel Res.*, 137, 15–23, 1978.

5 Galante, J., Clinical results with the HGP cementless total hip prosthesis, in*Non-Cemented Total Hip Arthroplasty*, Fitzgerald, Jr., R., Ed., Raven Press, New York, 1987, pp. 427–432.

6 Donaldson, T., Huddleston, T., Swenson, T., Evans, R., and Rubash, H., Minimum 3 year clinical and radiographic analysis of uncemented Harris-Galante total hip arthroplasty, *J. Bone Joint Surg.*, submitted for publication,October 1991.

7 Callaghan, J., Salvati, E., Pellicci, P., Wilson, P., and Ranawat, C., Results of revision for the mechanical failure after cemented total hip replacement 1979–1982, *J. Bone Joint Surg.*, 67A(7), 1074–1085, 1985.

8 Engelbreth, D., Weber, F., Sweet, M., and Jakim, I., Long term results of revision total hip arthroplasty, *J. Bone Joint Surg.*, 72B(1), 41–45, 1990.

9 Kavanagh, B., Ilstrup, D., and Fitzgerald, R., Revision total hip arthroplasty, *J. Bone Joint Surg.*, 67A(4), 517–526, 1985.

10 Rubash, H. and Harris, W., Revision THA of cemented femoral components: Six year follow-up study, *J. Arthroplasty*, 3(3), 241–248, 1989.

11 Rohlmann, A., Cheal, E., and Hayes, W., *Influence of porous coating thickness and elastic modulus on stress distributions in hip prostheses, presented at the Fifth Meeting of the European Society of Biomechanics*, 1986.

12 Engh, C. and Bobyn, D., The influence of stem size and extent of porous coating on femoral bone resorption after cementless primary hip arthroplasty, *Clin. Orthop. Rel. Res.*, 231, 7–28, 1988.

13 Sumner, D. and Turner, T., The effects of femoral component design features on femoral remodeling, in *Non-Cemented Total Hip Arthroplasty*, Fitzgerald, Jr., R., Ed., Raven Press, New York, 1987, pp. 143–158.

14 Bobyn, J. and Engh, C., Bone ingrowth and remodeling in canine and human porous-coated hip replacements, in *Non-Cemented Total Hip Arthroplasty*, Fitzgerald, Jr., R., Ed., Raven Press, New York, 1987, pp. 49–68.

15 Kang, J., McKernan, D., Kruger, M., Mutschler, T., Thompsen, W., and Rubash, H., Ingrowth and formation of bone in defects in an uncemented fiber-metal total hip replacement model in dogs, *J. Bone Joint Surg.*, 73A(1), 93–105, 1991.

16 Greis, P., Silvaggio, V., Kim, K., Klein, A., Kang, J., and Rubash, H., A long term comparative study of defect filling and bone ingrowth in a canine fiber metal total hip model, in *Proc. 37th Annual Meeting, Orthopaedic Research Society*, 1991, p. 33.

17 Marstnelli, G., Fornasier, V., Binnington, A., McKenzie, K., Sessa, V., and Harrington, I., Effect of stem modulus in a total hip arthroplasty model, *J. Bone Joint Surg.*, 73B(1), 43–46, 1991.

18 Galante, J., Lemons, J., Spector, M., Wilson, P., and Wright, T., The biologic effects of implant materials, *J. Orthop. Res.*, 9, 760–775, 1991.

19 Bobyn, J., Glassman, A., Goto, H., Krygier, J., Miller, J., and Brooks, C., The effect of stem stiffness on femoral bone resorption after canine porous-coated total hip arthroplasty, *Clin. Orthop. Rel. Res.*, 261, 196–213, 1990.
20 Cheal, E., Spector, M., and Hayes, W., Role of loads and material properties on the mechanics of the proximal femur after total hip arthroplasty, in *Proc. 37th Annual Meeting, Orthopaedic Research Society*, 1991, p. 512.
21 Koeneman, J. and Hansen, T., Finite element analysis of a composite materials dog femoral prosthesis, in *Proc. 35th Annual Meeting, Orthopaedic Research Society*, 1989, p. 528.
22 Kareh, J., Jasty, M., Bragdon, C., Stracher, M., O'Connor, D., and Harris, W., Stress transfer around porous coated uncemented titanium femoral components compared to composite plastic femoral components, in *Proc. 37th Annual Meeting, Orthopaedic Research Society*, 1991, p. 519.
23 Ritter, M. and Fechtman, R., Distal cortical hypertrophy following total hip arthroplasty, *J. Arthroplasty*, 3, 117–121, 1988.
24 Schmalzried, T. and Finerman, G., Osteolysis in aseptic failure, in *Non-Cemented Total Hip Arthroplasty*, Fitzgerald, Jr., R., Ed., Raven Press, New York, 1987, pp. 303–318.
25 Wolff, J., Ueber die Bedeutung der Architektur der spongiosen Substanz, *Zent hi. med. Wiss*, VI, 223–234, 1869.
26 Thompson, D., *On Growth and Form*, Cambridge University Press, 1919.
27 Hart, R. and Davy, D., Theories of bone modeling and remodeling, in *Bone Mechanics*, Cowin, S., Ed., CRC Press, Boca Raton, FL, 1989, pp. 253–276.
28 Beaupre, G., Orr, T., and Carter, D., An approach for time dependent bone modeling and remodeling —Theoretical development, *J. Orthop. Res.*, 8, 651–661, 1990.
29 Fyhrie. D. and Carter, D., A unifying principle relating stress to trabecular bone morphology. *J. Orthop. Res.*, 4, 304–317, 1986.
30 Orr, T., Beaupre, G., Carter, D., and Schurmen, D., Computer predictions of bone remodelling around porous-coated implants, *J. Arthroplasty*, 5(3), 191–200, 1990.
31 Cowin, S. and Hegedus, D., Bone remodelling. I. Theory of adaptive elasticity, *J. Elasticity*, 6, 313–326, 1976.
32 Firoozbakhsh, K. and Cowin, S., Evolution of inhomogeneities in bone structure — Predictions of adaptive elasticity, *J. Biomech. Eng.*, 102, 287–295, 1980.
33 Cowin, S., Bone remodeling of diaphyseal surfaces by torsional loads: Theoretical predictions, *J. Biomech.*, 20(11/12), 1111–1120, 1987.
34 Hart, R., Davy, D., and Heiple, K., A computational method for the stress analysis of adaptive elastic materials with a view toward applications in strain-induced bone remodeling, *J. Biomech. Eng.*, 106, 342–350, 1984.
35 Frost, H., Skeletal structural adaptations to mechanical usage (SATMU). 1. Redefining Wolff's law: The bone modeling problem, *Anatom. Rec.*, 226, 403–413, 1990.
36 Huiskes, R., Weinans, H., and Dalstra, M., Adaptive bone remodeling and biomechanical design considerations for noncemented total hip arthroplasty, *Orthop.*, 12(9), 1255–1267, 1989.
37 Huiskes, R., Weinans, H., Grootenboer, H., Dalstra, M., Fudala, B., and Slooff, T., Adaptive boneremodelling theory applied to prosthetic-design analysis, *J. Biomech.*, 20(11/12), 1135–1150, 1987.
38 Carter, D., Mechanical loading histories and cortical bone remodeling, *Calcif. Tissue Int.*, 36, S19–S24, 1984.
39 Zienkiewicz, O., *The Finite Element Method*, 3rd ed., McGraw-Hill, New York, 1977.
40 Huiskes, R. and Chao, E., A survey of finite element analysis in orthopedic biomechanics: The first decade, *J. Biomech.*, 16(6), 385–409, 1983.
41 Estok, D., Harrigan, T., and Harris, W., Finite element analysis of cement strains at the tip of an idealized cemented femoral component, in *Proc. 37th Annual Meeting, Orthopaedic Research Society*, 1991, p. 504.
42 Crowninshield, R., Brand, R., Johnson, R., and Milroy, J., The effect of femoral stem cross-sectional geometry on cement stresses in total hip reconstruction, *Clin. Orthop. Rel. Res.*, 146, 71–77, 1980.
43 Natarajan, R., andriacchi, Y., Freeman, P., and Galante, J., A relationship between the extent of porous coating and micromotion in a cementless femoral stem of a total hip replacement, in *Proc. 37th Annual Meeting, Orthopaedic Research Society*, 1991, p. 551.
44 Wang, C., Cheal, E., and Spector, M., The effects of porous coating distribution on the femoral component of a total hip replacement, in *Proc. 37th Annual Meeting, Orthopaedic Research Society*, 1991, p. 268.
45 Orr, T., Beaupre, G., Fyhrie, D., Schurman, D., and Carter, D., Application of a bone remodeling theory to femoral and tibial prosthetic components, in *Proc. 34th Annual Meeting, Orthopaedic Research Society*, 1988, p. 100.
46 Huiskes, R., Weinans, H. v., Rietbergen, B., Sumner, D., Turner, T., and Galante, J., Validation of strain adaptive bone-remodelling analysis to predict bone morphology around noncemented THA, in *Proc. 37th Annual Meeting, Orthopaedic Research Society*, 1991, p. 105.
47 Huiskes, R., Weimans, H., Sumner, D., Fudala, B., Turner, T., Grootenboer, H., and Galante, J., Stress-shielding, stress-bypassing and bone resorption around press-fit and bone-ingrowth THA, in *Proc. 35th Annual Meeting, Orthopaedic Research Society*, 1989, p. 529.
48 Bergmann, G., Siraky, J., Rohlmann, A., and, Koelbel, R., A comparison of hip joint forces in sheep, dog and man, *J. Biomech.*, 17, 907–921, 1984.
49 Steinberg, G., Kearns McCarthy, C., and Baran, D., Quantification of bone loss of the proximal femur after total hip arthroplasty, in *Proc. 37th Annual Meeting, Orthopaedic Research Society*, 1991, p. 221.
50 Kiratli, B., Heiner, J., McKinley, N., Wilson, M., and McBeath, A., Bone mineral density of the proximal femur after uncemented total hip arthroplasty, in *Proc. 36th Annual Meeting, Orthopaedic Research Society*, 1991, p. 545.
51 Edidin, A., Taylor, D., and Bartel, D., Automatic assignment of bone moduli from CT data: A 3-D finite element study, in *Proc. 37th Annual Meeting, Orthopaedic Research Society*, 1991, p. 491.

1 Allen, R. D., David, G. B., and Nomarski, G., The Zeiss-Nomarski differential interference equipment for transmitted light microscopy, *Z. wiss. Mikrosk.*, 69, 193–221, 1969.
2 Beeler, G. W. and Reuter, H., Reconstruction of the action potential of ventricular myocardial fibers, *J. Physiol. (London)*, 268, 177–210, 1977.
3 Bishop, S. P. and Drummond, J. L., Surface morphology and cell size measurement of isolated rat cardiac myocytes, *J. Molec. Cell. Cardiol.*, 11, 423–433, 1979.
4 Burt, J. M. and Spray, D. C., Single-channel events and gating behavior of the cardiac gap junction channel, *Proc. Nad. Acad. Sci. USA*, 85, 3431–3434, 1988.
5 Clerc, L., Directional differences of impulse spread in trabecular muscle from mammalian heart, *J. Physiol. (London)*, 255, 335–346, 1976.
6 Cole, W. C., Picone, J. B., and Sperelakis, N., Gap junction uncoupling and discontinuous propagation in the heart, *Biophys. J.*, 53, 809–818, 1988.
7 Conte, S. D. and de Boor, C., *Elementary Numerical Analysis, An Algorithmic Approach*, 3rd ed., McGraw-Hill, New York, 1980, pp. 153–156.
8 Crank, J. and Nicolson, P., A practical method for numerical evaluation of solutions of partial differential equations of the heat conduction type, *Proc. Cambridge Phil. Soc.*, 43, 50–67, 1947.
9 Ebihara, L. and Johnson, E. A., Fast sodium current in cardiac muscle. A quantitative description, *Biophys. J.*, 32, 779–790, 1980.
10 Fawcett, D. W. and McNutt, N. S., The ultrastructure of the cat myocardium, *J. Cell Biol*, 42, 1–45, 1969.
11 Gerald, C. F. and Wheatley, P. O., *Applied Numerical Analysis*, 4th ed., Addison-Wesley, Reading, MA, 1989, pp. 132–136, 356–360.
12 Gerdes, A. M., Kreseman, J., and Bishop, S. P., Morphometric study of cardiac muscle: The problem of tissue shrinkage, *Lab. Invest.*, 46, 271–274, 1982.
13 Gourdie, R. G., Green, C. R., and Severs, N. J., Gap junction distribution in adult mammalian myocardium revealed by anti-peptide antibody and laser scanning confocal microscopy, *J. Cell Sci.*, 99, 41–55, 1991.
14 Hodgkin, A. L. and Huxley, A. F., A quantitative description of membrane current and its application to conduction and excitation in nerve, *J. Physiol. (London)*, 117, 500–544, 1952.
15 Hoyt, R. H., Cohen, M. L., and Saffitz, J. E., Distribution and three-dimensional structure of intercellular junctions in canine myocardium, *Circ. Res.*, 64, 563–574, 1989.
16 Jacobson, S. L., Culture of spontaneously contracting myocardial cells from adult rats, *Cell Struct. Fund.*, 2, 1–9, 1977.
17 Johnson, E. A., The generation of the cardiac action potential: After the first millisecond, *Ann. Biomed. Eng.*, 11, 159–176, 1983.
18 Joyner, R. W., Ramon, F., and Moore, J. W., Simulation of action potential propagation in an inhomogeneous sheet of coupled excitable cells, *Circ. Res.*, 36, 654–661, 1975.
19 Kamiyana, A. and Matsuda, K., Electrophysiological properties of the canine ventricular fiber, *Japan J. Physiol*, 16, 407–420, 1966.
20 Levin, K. R. and Page E. P., Quantitative studies on plasmalemmal folds and caveolae of rabbit ventricular myocardial cells, *Circ. Res.*, 46, 244–255, 1980.
21 Leon, L. J. and Roberge, F. A., Directional characteristics of action potential propagation in cardiac muscle. A model study, *Cir. Res.*, 69, 378–395, 1991.
22 Luke, R. A., Beyer, E. C., Hoyt, R. H., and Saffitz, J. E., Quantitative analysis of intercellular connections by immunohistochemistry of the cardiac gap junction protein connexin43, *Circ. Res.*, 65, 1450–1457, 1989.
23 Luo, C. and Rudy, Y., A model of the ventricular cardiac action potential. Depolarization, repolarization, and their interaction, *Circ. Res.*, 68, 1501–1526, 1991.
24 Metzger, P. and Weingart, R., Electric current flow in cell pairs isolated from adult rat hearts, *J. Physiol*, 366, 177–195, 1985.
25 Page, E., Quantitative ultrastructural analysis in cardiac membrane physiology, *Am. J. Physiol*, 235, C147–C158, 1978.
26 Page, E. and McCallister, L. P., Quantitative electron microscopic description of heart muscle cells. Application to normal, hypertrophied, and thryoxin-stimulated hearts, *Am. J. Cardiol.*, 31, 172–181, 1973.
27 Roth, B. J., Action potential propagation in a thick strand of cardiac muscle, *Circ. Res.*, 68, 162–173, 1991.
28 Rudy, Y. and Quan, W., A model study of the effects of the discrete cellular structure on electrical propagation in cardiac tissue, *Circ. Res.*, 61, 815–823, 1987.
29 Simpson, F. O., Rayns, D. G., and Ledingham, J. M., The ultrastructure of ventricular and atrial myocardium, in *Ultrastructure of the Mammalian Heart*, Challice, C. E. and Virogh, S., Eds., Academic Press, New York, 1973, pp. 1–41.
30 Sommer, J. R. and Johnson, E. A., Ultrastructure of cardiac muscle, in *Handbook of Physiology. Section* 2, *The Cardiovascular System*, Vol. 1, Berne, R. M., Sperelakis, N., and Geiger, S. R., Eds., American Physiology Society, Bethesda, MD, 1979, pp. 113–186.
31 Spach, M. S. and Dolber, P. C., Relating extracellular potentials and their derivatives to anisotropic propagation at a microscopic level in human cardiac muscle: Evidence for electrical uncoupling of side-to-side fiber connections with increasing age, *Circ. Res.*, 58, 356–371, 1986.
32 Spach, M. S. and Heidlage, J. F., Models of discontinuous anisotropic propagation in cardiac muscle: A question of size scale, *Comments Theoret. Biol.*, 1, 359–386, 1990.

33 Spach, M. S., Kootsey, J. M., and Sloan, J. D., Active modulation of electrical coupling between cardiac cells of the dog, *Circ. Res.*, 51, 347–362, 1982.
34 Spach, M. S., Miller, I.I.I. W. T., Geselowitz, D. B., Barr, R. C., Kootsey, J., and Johnson, E. A., The discontinuous nature of propagation in normal canine cardiac muscle. Evidence for recurrent discontinuities of intracellular resistance that affect the membrane currents, *Circ. Res.*, 48. 39–54, 1981.
35 Spear, J. F., Michelson, E. L., and Moore, E. N., Reduced space constant in slowly conducting regions of chronically infarcted canine myocardium, *Circ. Res.*, 53, 176–185, 1983.
36 Strang, G., *Introduction to Applied Mathematics*, Wellesley-Cambridge Press, Wellesley, MA, 1986, pp. 403–410.
37 Tanaka, I. and Sasaki, Y., On the electronic spread in cardiac muscle, *J. Gen. Physiol.*, 49. 1089–1110, 1966.
38 Tseng, G.-N., Robinson, R. B., and Hoffman, B. F., Passive properties and membrane currents of canine ventricular myocytes, *J. Gen. Physiol.*, 90, 671–701, 1987.
39 Weidmann, S., Electrical constants of trabecular muscle from mammalian heart, *J. Physiol. (London)*, 210, 1041–1054, 1970.
40 Weingart, R., Electrical properties of the nexal membrane studied in rat ventricular cell pairs, *J. Physiol. (London)*, 370, 267–284, 1986.
41 Weingart, R. and Maurer, P., Action potential transfer in cell pairs isolated from adult rat and guinea pig ventricles, *Circ. Res.*, 63, 72–80, 1988.
42 White, R. L., Campos de Carvalho, A. C., Spray, D. C., Wittenberg, B. A., and Bennett, M. V. L., Gap junctional conductance between isolated pairs of ventricular myocytes from rat, *Biophys. J.*, 41, 217a, 1983.
43 White, R. L., Spray, D. C., Campos de Carvalho, A. C., Wittenberg, B. A., and Bennett, M. V. L., Some electrical and pharmacological properties of gap junctions between adult ventricular myocytes, *Am. J. Physiol.*, 249 (*Cell Physiol.*, 18), C447–C455, 1985.
44 Woodbury, J. W. and Crill, W. E., On the problem of impulse conduction in the atrium, in *Nervous Inhibition*, Florey, E., Ed., Pergamon Press, New York, 1961, pp. 124–135.
1 Clerc, L., Directional differences of impulse spread in trabecular muscle from mammalian heart, *J. Physiol.*, 255, 335–346, 1976.
2 Sano, T., Takayama, N., and Shimamoto, T., Directional differences of conduction velocity in the cardiac ventricular syncitium studied by microelectrodes, *Circ. Res.*, 7, 262–267, 1959.
3 Spach, M. S., Miller, W. T., Miller-Jones, E., Warren, R., and Barr, R. C., Extracellular potentials related to intracellular action potentials during impulse conduction in anisotropic canine cardiac muscle, *Circ. Res.*, 45, 188–204, 1979.
4 Goldstein, S. S. and Rail, W., Changes of action potential shape and velocity for changing core conductor geometry, *Biophys. J.*, 14, 731–757, 1974.
5 Spach, M. S., The discontinuous nature of electrical propagation in cardiac muscle, *Ann. Biomed. Eng.*, 11, 209–261, 1983.
6 Joyner, R. W., Effects of the discrete pattern of electrical coupling on propagation through an electrical syncitium, *Circ. Res.*, 50, 192–200, 1982.
7 Spach, M. S., Kootsey, J. M., and Sloan, J. D., Active modulation of electrical coupling between cardiac cells of the dog, *Circ. Res.*, 51, 347–362, 1982.
8 Victorri, B., Vinet, A., Roberge, F. A., and Drouhard, J. P., Numerical integration in the reconstruction of cardiac action potentials using Hodgkin-Huxley type models, *Comput. Biomed. Res.*, 18, 10–23, 1985.
9 Steinhaus, B. M., Spitzer, K. W., and Isomura, S., Action potential collision in heart tissue; Computer simulations and tissue experiments, *IEEE Trans. Biomed. Eng.*, BME-32, 731–742, 1985.
10 Barr, R. C. and Plonsey, R., Propagation of excitation in idealized anisotropic two-dimensional tissue, *Biophys. J.*, 45, 1191–1202, 1984.
11 Tung, L. A., A Bidomain Model for Describing Ischemic Myocardial D.C. Potentials, *Ph.D. dissertation*, Massachusetts Institute of Technology, Cambridge, 1978.
12 Muler, A. L. and Markin, V. S., Electrical properties of anisotropic neuro-muscle syncytia. I. Distribution of the electrotonic potential, *Biofizika*, 22, 307–312, 1977.
13 Geselowitz, D. and Miller, W. T., A bidomain model for anisotropic cardiac muscle, *Ann. Biomed. Eng.*, 11, 191–206, 1983.
14 Roth, B. J. and Wikswo, Jr., J. P., A bidomain model for the extracellular potential and magnetic field of cardiac tissue, *IEEE Trans. Biomed. Eng.*, BME-33, 467–469, 1986.
15 Sepulveda, N. G. and Wikswo, J. P., Electric and magnetic fields from two-dimensional anisotropic bisyncitia, *Biophys. J.*, 51, 557–568, 1987.
16 Henriquez, C. S., Trayanova, N., and Plonsev, R., A planar slab bidomain model for cardiac tissue, *Ann. Biomed. Eng.*, 18, 367–376, 1990.
17 Plonsey, R., Henriquez, C. S., and Trayanova, N., Extracellular (volume conductor) effect on adjoining cardiac muscle electrophysiology, *Med. Biol. Eng. Comput.*, 26, 126–129, 1988.
18 Barach, J. P., Simulation of action potential in a one-dimensional bidomain, *IEEE Trans. Biomed. Eng.*, BME-35, 340–345, 1988.
19 Roth, B. J., Action potential propagation in a thick strand of cardiac muscle, *Circ. Res.*, 68, 162–173, 1991.
20 Ebihara, L. H. and Johnson, E. A., Fast sodium current in cardiac muscle: A quantitative description, *Biophys. J.*, 32, 779–790, 1980.
21 Beeler, G. W. and Reuter, H., Reconstruction of the action potential of ventricular myocardial fibres, *J. Physiol.*, 268, 177–210, 1977.

22 Drouhard, J. P. and Roberge, F. A., Revised formulation of the Hodgkin-Huxley representation of the sodium current in cardiac cells, *Comput. Biomed. Res.*, 20, 333–350, 1987.
23 Roberge, F. A., Vinet, A., and Victorri, B., Reconstruction of propagated electrical activity with a two-dimensional model of anisotropic heart muscle, *Circ. Res.*, 58, 461–475, 1986.
24 Steinhaus, B. M., Spitzer, K. W., Burgess, M. J., and Abildskov, J. A., Electrotonic interactions in a model of anisotropic cardiac tissue, in *Proc. Society for Computer Simulations, 1986 Summer Computer Simulations Conference*, Reno, NV, pp. 421–426.
25 Lesh, M. D., Pring, M., and Spear, J. F., Cellular uncoupling can unmask dispersion of action potential duration in ventricular myocardium, *Circ. Res.*, 65, 1426–1440, 1989.
26 Leon, J. L. and Roberge, F. A., Directional characteristics of action potential propagation in cardiac muscle. A model study, *Circ. Res.*, 69, 368–395, 1991.
27 Pollard, A. E. and Barr, R. C., Computer simulations of activation in an anatomically based model of the human ventricular conduction system, *IEEE Trans. Biomed. Eng.*, BME-38, 982–996, 1991.
28 Parnas, I. and Segev, I., A mathematical model for conduction of action potentials along bifurcating axons, *J. Physiol*, 295, 323–343, 1979.
29 Moore, J. W. and Ramon, R., On numerical integration of the Hodgkin and Huxley equations for a membrane action potential, *J. Theor. Biol.*, 45, 249–273, 1974.
30 Rush, S. and Larsen, H., A practical algorithm for solving dynamic membrane equations, *IEEE Trans. Biomecl. Eng.*, BME-25, 389–392, 1978.
31 Press, W. H., Flannery, B. P., Zeukolsky, S. A., and Vetterling, W. T., *Numerical Recipes*, 1st ed., Cambridge University Press, 1986.
32 Smith, G. D., *Numerical Solution of Partial Differential Equations*, 2nd ed., Clarendon Press, London, 1978.
33 Bank, R. E., Coughran, W. M., Fichtner, W., Grosse, E. El., Rose, D. J., and Smith, R. K., Transient simulation of silicon devices and circuits, *IEEE Trans. Comput.-Aided Design*, CAD-4. 436–451. 1985.
34 Ortega, J. M. and Rheinboldt, W. C., *Iterative Solution of Nonlinear Equations in Several Variables*, Academic Press, New York, 1970.
35 Sherman, A. H., On Newton-iterative methods for the solution of systems of nonlinear equations. *SIAM J. Numer. Anal.*, 15, 755–771, 1978.
36 Bank, R. E. and Rose, D. J., Global approximate Newton methods, *Numer. Math.*, 37, 279–295, 1981.
37 Duff, I. S., Erisman, A. M., and Reid, J. K., *Direct Methods for Sparse Matrices*, Clarendon Press, London, 1986.
38 Saad, Y. and Schultz, M. A., GMRES: A generalized minimum residual algorithm for solving nonsymmetric linear systems, *SIAM J. Sci. Statist. Comput.*, 7, 856–869, 1986.
39 Elenriquez, C. S., An examination of a computationally efficient algorithm for modeling propagation in cardiac tissue, *Innov. Tech. Biol. Med.*, 10, 25–35, 1989.
40 Dahlquist, G. and Bjorck, A., *Numerical Methods*, Prentice-Hall, Englewood Cliffs, NJ, 1974.
41 Spach, M. S. and Kootsey, J. M., Relating the sodium current and conductance to the shape of the transmembrane and extracellular potential by simulations: Effects of propagation boundaries, *IEEE Trans. Biomed. Eng.*, BME-32, 743–755, 1985.
42 Spach, M. S., Miller, W. T., Geselowitz, D. B., Barr, R. C., Kootsey, J. M., and Johnson, E. A., The discontinuous nature of propagation in normal canine cardiac muscle, *Circ. Res.*, 48, 39–54, 1981.
43 Plonsey, R. and Barr, R. C., Current flow patterns in two-dimensional anisotropic bisyncitia with normal and extreme conductivities, *Biophys. J.*, 45, 557–571, 1984.
44 Hodgkin, A. L. and Huxley, A. S., A quantitative description of membrane current and its application to conduction and excitation in nerve, *J. Physiol.*, 117, 500–544, 1952.
45 Muler, A. L. and Markin, V. S., Electrical properties of anisotropic nerve-muscle syncytia. II. Spread of a flat front of excitation, *Biofizika*, 22, 518–522, 1977.
46 Armour, J. A. and Randall, W. C., Structural basis for cardiac function, *Am. J. Physiol.*, 218, 1517–1523, 1970.
47 Burgess, M. J., Steinhaus, B. M., Spitzer, K. W., and Ershler, P. R., Nonuniform epicardial activation and repolarization properties of in vivo pulmonary conus, *Circ. Res.*, 62, 233–246, 1988.
48 Duthinh, V. and Houser, S. R., Contractile properties of single isolated feline ventriculocytes, *Am. J. Physiol.*, 254, H59–H66, 1988.
49 Babuska, I. and Rheinboldt, W. C., Reliable error-estimation and mesh adaption for the finite element method, in *Computational Methods and Nonlinear Mechanics*, Oden, J. T., Ed., North-Holland, Amsterdam, 1980, pp. 67–109.
50 Arney, D. C. and Flaherty, J. E., An adaptive mesh-moving and local refinement method for time-dependent partial differential equations, *ACM Trans. Math. Software*, 16, 48–71, 1990.
51 Roberts, D., Hersh, L. T., and Scher, A. M., Influence of cardiac fiber orientation on wavefront voltage, conduction velocity and tissue resistivity in the dog, *Circ. Res.*, 44, 701–712, 1979.
52 Henriquez, C. S. and Plonsey, R., Simulation of propagation along a cylindrical bundle of cardiac tissue. II. Results of simulation, *IEEE Trans. Biomed. Eng.*, BME-37, 861–875, 1990.
53 Spach, M. S., Dolber, P. C., Heidlage, J. F., Kootsey, J. M., and Johnson, E. A., Propagation of depolarization in anisotropic human and canine cardiac muscle: Apparent directional differences in membrane capacitance, *Circ. Res.*, 60, 206–219, 1987.
54 Leon, L. J. and Horacek, B. M., Computer model of excitation and recovery in the anisotropic myocardium. I. Rectangular and cubic arrays of elements, *J. Electrocardiol.*, 24, 1–15, 1991.

55 Courtemanche, M., Skaggs, W., and Winfree, A. T., Stable three-dimensional action potential circulation in the FitzHugh-Nagumo model, *Physica D*, 41, 173–182, 1990.
56 FitzHugh, R. A., Impulses and physiologic states in a theoretical model of nerve membrane, *Biophys. J.*, 1, 445–466, 1961.
57 Keener, J. P., An eikonal curvature equation for action potential propagation in myocardium, *J. Math. Biol.*, 29, 629–651, 1991.
58 Colli Franzone, P., Wavefront propagation in an activation model of the anisotropic cardiac tissue: Asymptotic analysis and numerical simulations, *J. Math. Biol.*, 28, 121–176, 1990.
59 Colli Franzone, P., Guerri, L., and Tentoni, S., Mathematical modeling of the excitation process in myocardial tissue: Influence of fiber rotation on wavefront propagation and potential field, *Math. Biosci.*, 101, 155–235, 1990.
60 Taccardi, B., Lux, R. L., Ershler, P. R., Watabe, S., and Macchi, E., Normal and abnormal intramural spread of excitation and associated potential distributions, in *Proc. 17th Int. Congress on Electrocardiology*, Florence, Italy, 1990, p. 12.
61 Lambert, J. D., *Numerical Methods for Ordinary Differential Systems*, Wiley, New York, 1991.
62 Plonsey, R. and Barr, R. C., *Bioelectricity*, Plenum Press, New York, 1988.
1 Adam, D., Propagation of depolarization and repolarization processes in the myocardium—An anisotropic model, *IEEE Trans. Biomed. Eng.*, BME-38, 133–141, 1991.
2 Aoki, M., Okamoto, Y., Musha, T., and Harumi, K., Three-dimensional simulation of depolarization and repolarization processes and body surface potentials: Normal heart and bundle branch block, *IEEE Trans. Biomed. Eng.*, BME-34, 454–462, 1987.
3 Armour, J. A. and Randall, W. C., Structural basis for cardiac function, *Am. J. Physiol.*, 218(6), 1517–1523, 1970.
4 Aronson, D. G. and Weinberger, H. F., Nonlinear diffusion in population genetics, combustion and nerve propagation, in *Partial Differential Equations and Related Topics*, Goldstein, J. A., Ed., *Lecture Notes in Mathematics*, Vol. 446, Springer-Verlag, Berlin, 1975, pp. 5–49.
5 Axelsson, O., A generalized SSOR method, *BIT*, 13, 443–467, 1972.
6 Axelsson, O., A survey of preconditioned iterative methods for linear systems of algebraic equations, *BIT*, 25, 166–187, 1985.
7 Axelsson, O. and Barker, V. A., *Finite Element Solution of Boundary Value Problems. Theory and Computation*, Academic Press, New York, 1984.
8 Barr, R. C. and Plonsey, R., Propagation of excitation in idealized anisotropic two dimensional tissue, *Biophys. J.*, 45, 1191–1202, 1984.
9 Barta, E., Adam, D., Salant, E., and Sideman, S., 3-D ventricular myocardial electrical excitation: A minimal orthogonal pathway model, *Ann. Biomed. Eng.*, 15, 443–456, 1987.
10 Baruffi, S., Spaggiari, S., Stilli, D., Musso, E., and Taccardi, B., The importance of fiber orientation in determining features of the cardiac electric field, in *Modem Electrocardiology*, Anatoczy, Z., Ed., Excerpta Medica, Amsterdam, 1978, pp. 89–92.
11 Baruffi, S., Spaggiari, S., Arisi, G., Malanca, A., Macchi, E., and Taccardi, B., The effect of myocardial anisotropy on epicardial potential distribution in the dog heart in situ, in *Adrances in Body Surface Potential Mapping*, Yamada, K., Harumi, K., and Musha, T., Eds., The University of Nagoya Press, Tokyo, 1983, p. 151.
12 Baruffi, S., Spaggiari, S., Colli Franzone, P., Tentoni, S., Viganotti, C., and Taccardi, B., The influence of myocardial anisotropy on tridimensional potential distribution generated by isolated dog hearts during epicardial stimulation, *Pfluger Arch. Eur. J. Phys.*, 414, S53—abstr. 45, 1989.
13 Berkenblit, M. B., Kovalev, S. A., Smolyaninov, V. V., Chailakhyan, L. M., and Shura-Bura, T. H., Spread of excitation in anisotropic syncytia, *Biofizika*, 19(6), 1057–1061, 1974; English transl: *Bio-physics*, 22, 1079–1083, 1975.
14 Brebbia, C. A., Telles, J., and Wrobel, L., *Boundary Element Techniques—Theory and Applications in Engineering*, Springer-Verlag, Berlin, 1984.
15 Brown, A. M., Lee, K. S., and Powell, T., Sodium current in single rat heart muscle cells, *J. Physiol. (London)*, 318, 479–500, 1981.
16 Burgess, M. J., Steinhaus, B. M., Spitzer, K. W., and Ershler, P. R., Nonuniform epicardial activation and repolarization properties of the in vivo canine pulmonary conus, *Circ. Res.*, 62, 233–246, 1988.
17 Casten, R., Cohen, H., and Lagerstrom, P., Perturbation analysis of approximation to Hodgkin–Hux-ley theory, *Quart. Appl. Math.*, 32, 365–402, 1975.
18 Ciarlet, P. G., *The Finite Element Method for Elliptic Problems*, North–Holland, Amsterdam, 1978.
19 Clerc, L., Directional differences of impulse spread in trabecular muscle from mammalian heart, *J. Physiol*, 255, 335–346, 1976.
20 Cohen, H., Mathematical developments in Hodgkin-Huxley theory and its approximation, in *Lectures on Mathematics in the Life Sciences*, Levin, S. A., Ed., Vol. 8, Am. Math. Soc., Providence, 1975, pp. 89–124.
21 Colatsky, T. J., Voltage clamp measurements of sodium channel properties in rabbit cardiac Purkinje fibres, *J. Physiol. (London)*, 305, 215–234, 1980.
22 Colli Franzone, P. and Guerri, L., Spreading of the excitation in 3-D models of the anisotropic cardiac tissue, *Math. Biosci.*, to appear.
23 Colli Franzone, P. and Magenes, E., On the inverse problem of electrocardiology, *Calcolo*, XVI, 459–538, 1979.
24 Colli Franzone, P., Guerri, L., and Magenes, E., Oblique dipole layer potentials for the direct and inverse problems of electrocardiology, *Math. Biosci.*, 68, 23–55, 1984.

25 Colli Franzone, P., Guerri, L., and Rovida, S., Model studies of three-dimensional distribution of the electric cardiac potential, in *Advances in Biomagnetism, Functional Localization: A Challenge for Biomagnetism*, Erne, S. N. and Romani, G. L., Eds., World Scientific, Singapore, 1989, pp. 3–12.
26 Colli Franzone, P., Guerri, L., and Rovida, S., Wavefront propagation in an activation model of the anisotropic cardiac tissue: asymptotic analysis and numerical simulations, *J. Math. Biol.*, 28, 121–176, 1990.
27 Colli Franzone, P., Guerri, L., and Tentoni, S., Mathematical modeling of the excitation process in the myocardial tissue: Influence of the fiber rotation on the wavefront propagation and the potential field, *Math. Biosci.*, 101, 155–235, 1990.
28 Colli Franzone, P., Guerri, L., and Viganotti, C., Oblique dipole layer potentials applied to electrocardiology, *J. Math. Biol*, 17, 93–114, 1983.
29 Colli Franzone, P., Guerri, L., Rovida, S., and Tentoni, S., A model of excitation wavefronts spreading in the anisotropic cardiac tissue, in *Nonlinear Wave Processes in Excitable Media*, Holden, A. V., Markus, M., and Othmer, H. G., Eds., Plenum Press, New York, 1991, pp. 313–326.
30 Colli Franzone, P., Guerri, L., Viganotti, C., Macchi, E., Baruffi, S., Spaggiari, S., and Taccardi, B., Potential fields generated by oblique dipole layer modeling excitation wavefronts in the anisotropic myocardium. Comparison with potential fields elicited by paced dog hearts in a volume conductor, *Circ. Res.*, 51, 330–346, 1982.
31 Corbin, L. V. I.I., and Scher, A. M., The canine heart as an electrocardiographic generator: Depending on cardiac cell orientation, *Circ. Res.*, 41, 58–67, 1977.
32 Diaz, P. J., Rudy, Y., and Plonsey, R., The intercalated disc as a cause for discontinuous propagation in cardiac muscle: A theoretical simulation, *Ann. Biomed. Eng.*, 11, 177–190, 1983.
33 Di Franceso, D. and Noble, D., A model of cardiac electrical activity incorporating ionic pumps and concentration changes, *Phil. Trans. Roy. Soc. London B*, 307, 353–398, 1985.
34 Draper, M. H. and Mya-Tu, M., A comparison of the conduction velocity in cardiac tissues of various mammals, *Q. J. Exp. Physiol.*, 44, 91–109, 1959.
35 Drouhard, J. P. and Roberge, F. A., Revised formulation of the Hodgkin–Huxley representation of the Na^+ current in cardiac cells, *Comput. Biomed. Res.*, 20, 333–350, 1987.
36 Ebihara, L. and Johnson, E. A., Fast sodium current in cardiac muscle, *Biophys. J.*, 32, 779–790, 1980.
37 Eifler, W. J., Macchi, E., Ritsema von Eck, H. J., Horacek, B. M., and Rautaharju, P. J., Mechanism of generation of body surface electrocardiographic *P*-wave in normal, middle and lower sinus rhythms, *Circ. Res.*, 48, 168–182, 1980.
38 Fife, P. C., Asymptotic analysis of reaction–diffusion wavefronts, *Rocky Mountain J. Math.*, 7, 389–415, 1977.
39 Fife, P. C., Mathematical aspects of reacting and diffusing systems, in *Lecture Notes in Biomathematics*, Vol. 28, Springer-Verlag, Berlin, 1979.
40 Forsythe, G. E. and Wasow, W. R., *Finite Difference Methods for Partial Differential Equations*, Wiley, New York, 1960, pp. 376–377.
41 Frazier, D. W., Krassowska, W., Chen, P. S., Wolf, P. D., Danieley, N. D., Smith, W. M., and Ideker, R. E., Transmural activations and stimulus potentials in three-dimensional anisotropic canine myocardium, *Circ. Res.*, 63, 135–146, 1988.
42 Geselowitz, D. B., Barr, R. C., Spach, M. S., and Miller, W. T., Ill, The impact of adjacent isotropic fluids on electrograms from anisotropic cardiac muscle: A modeling study, *Circ. Res.*, 51, 602–613, 1982.
43 Geselowitz, D. B. and Miller, W. T., Ill, A bidomain model for anisotropic cardiac muscle, *Ann. Biomed. Eng.*, 11, 191–206, 1983.
44 Golub, G. F.I. and Van Loan, C. F., *Matrix Computations*. The Johns Hopkins University Press, Baltimore, 1983.
45 Gomatam, J. and Grindrod, P., Three-dimensional waves in excitable reaction–diffusion systems, *J. Math. Biol.*, 25, 611–622, 1987.
46 Guerri, L. and Magenes, E., On the inverse problem of electrocardiology, in *Proc. USSR Colloquium on Recent Problems in Numerical Analysis and Applied Mathematics*, Nauka, Moscow, 1983, pp. 59–72 (in Russian); English translation: I.A.N.-C.N.R., Pavia, 290, 1983.
47 Greenbaum, R. A., Ho, S. Y., Gibson, D. G., Becker, A. E., and Anderson, R. H., Left ventricular fibre architecture in man, *Br. Heart J.*, 45(3), 248–263, 1981.
48 Gulko, F. B. and Petrov, A. A., Mechanism of the formulation of closed pathways of conduction in excitable media, *Biofizika*, 17(2), 261–270, 1970; English transl.: *Biophysics*, 17, 271–282, 1972.
49 Hageman, L. A. and Young, D. M., *Applied Iterative Methods*, Academic Press, New York, 1981.
50 Harumi, K., Tsumakawa, H., Nishiyama, G., Wei, D., Yamada, G., Okamoto, Y., and Musha, T., Clinical application of electrocardiographic computer model, *J. Electrocardiology*, 22, Suppl., 54–63, 1990.
51 Henriquez, C. S. and Plonsey, R., Effect of resistive discontinuities on waveshape and velocity in a single cardiac fiber, *Med. Biol. Eng. Comput.*, 25, 428–438, 1987.
52 Henriquez, C. S. and Plonsey, R., Simulation of propagation along a bundle of cardiac tissue. Part I: Mathematical formulation, *IEEE Trans. Biomed. Eng.*, BME-37, 850–860, 1990; Part II: Results of simulation, *IEEE Trans. Biomed. Eng.*, BME-37, 861–875, 1990.
53 Henriquez, C. S., Trayanova, N., and Plonsey, R., Potential pattern and current distributions in a cylindrical bundle of cardiac tissue, *Biophys. J.*, 53, 907–918, 1988.
54 Hestenes, M. R., *Conjugate Direction Methods in Optimization*, Springer-Verlag, New York, 1980.
55 Hodgkin, A. L. and Huxley, A. F., A quantitative description of membrane current and its application to conduction and excitation in nerve, *J. Physiol. (London)*, 117, 500–544, 1952.

56 Hunter, P. J., McNaughton, P. A., and Noble, D., Analytical models of propagation in excitable cells, *Prog. Biophys. Molec.*, 30, 99–144, 1975.
57 Hunter, P. J. and Smaill, B. H., The analysis of cardiac function: A continuum approach, *Prog. Biophys. Molec. Biol.*, 52, 101–164, 1988.
58 Jack, J. J. B., Noble, D., and Tsien, R. W., *Electric Current Elow in Excitable Cells*, Clarendon, Oxford, 1983.
59 Joyner, R. W., Ramon, R., and Moore, J. W., Simulation of action potential propagation in an inhomogeneous sheet of coupled excitable cells, *Circ. Res.*, 36, 654–661, 1975.
60 Radish, A., Shinnar, M., Moore, E. N., Levine, J. H., Balke, C. W., and Spear, J. F., Interaction of fiber orientation and direction of impulse propagation with anatomic barriers in anisotropic canine myocardium, *Circulation*, 78, 1478–1494, 1988.
61 Kaplan, D. T., Smith, J. M., Saxberg, B. E. H., and Cohen, R. J., Nonlinear dynamics in cardiac conduction, *Math. Biosci.*, 90, 19–48, 1988.
62 Keener, J. P., A geometrical theory for spiral waves in excitable media, *SIAM J. Appl. Math.*, 46(6), 1039–1056, 1986.
63 Keener, J. P., An eikonal-curvature equation for action potential propagation in myocardium, *J. Math. Biol.*, 29, 629–651, 1991.
64 Krassowska, W., Pilkington, T. C., and Ideker, R. E., The closed form solution to the periodic core-conductor model using asymptotic analysis, *IEEE Trans. Biomed. Eng.*, BME-34, 519–531, 1987.
65 Krassowska, W., Pilkington, T. C., and Ideker, R. E., Potential distribution in three-dimensional periodic myocardium. Part I: Solution with two-scale asymptotic analysis, *IEEE Trans. Biomed. Eng.*, 37, 252–265, 1990.
66 Leon, L. J. and Horáček, B. M., Excitation in three-dimensional anisotropic cardiac tissue: A model study, in *Proc. IEEE Eng. in Med. and Biol. Soc. 1st Annu. Int. Conf.*, 1989, pp. 83–84.
67 Leon, L. J. and Horáček, B. M., Computer model of excitation and recovery in the anisotropic myocardium. I: Rectangular and cubic arrays of excitable elements, *J. Electrocardiol.*, 24(1), 1–14, 1991; II: Excitation in the simplified left ventricle, *J. Electrocardiol.*, 24(1), 17–31, 1991; III: Arrhyth- mogenic conditions in the simplified left ventricle, *J. Electrocardiol.*, 24(1), 33–41, 1991.
68 Leon, L. J. and Roberge, F. A., Directional characteristics of action potential propagation in cardiac muscle. A model study, *Circ. Res.*, 69, 378–395, 1991.
69 Lorange, M. and Gulrajani, R. M., Computer simulation of the Wolf–Parkinson–White preexcitation syndrome with a modified Miller–Geselowitz heart model, *IEEE Trans. Biomed. Eng.*, BME-33, 862–873, 1986.
70 Luo, C. and Rudy, Y., A model of the ventricular cardiac action potential. Depolarization, repolarization and their interaction, *Circ. Res.*, 68, 1501–1526, 1991.
71 Lynn, M. S. and Timlake, W. P., The use of multiple deflations in the numerical solution of singular systems of equations with application to potential theory, *SIAM J. Numer. Anal.*, 5, 303–322, 1968.
72 Miller III, W. T. and Geselowitz, D. B., Simulation studies of the electrocardiogram. I: The normal heart, *Circ. Res.*, 43(2), 301–314, 1978.
73 Moe, G. K., Rheinboldt, W. C., and Abildskov, J. A., A computer model of atrial fibrillation, *Am. Heart J.*, 67, 200–220, 1964.
74 Muler, A. L. and Markin, V. S., Electrical properties of anisotropic nerve-muscle syncytia. I: Distribution on the electrotonic potential, *Biofizika*, 22, 307–312, 1977 (English transl.: *Biophysics*, 22, 315–321, 1978); II; Spread of flat front of excitation, *Biofizika*, 22, 518–522, 1978 (English transl.: *Bio-physics*, 22, 536–541, 1978); III: Steady form of the excitation front, *Biofizika*, 22, 671–675, 1977 (English transl.: *Bio-physics*, 22, 698–704, 1977).
75 Murphy, C. R., Clark, J. W., Giles, W. R., Rasmusson, R. L., Halter, J. A., Hicks, K., and Hoyt, B., Conduction in bullfrog atrial strand: Simulations of the role of disc and extracellular resistance, *Math. Biosci.*, 106, 39–84, 1991.
76 yerburg, R. J., Cameron, J. S., Lodge, N. J., Kimura, S., Kozlovskis, P. L., and Basset, A. L., The papillary muscle preparation in the study of cardiac electrophysiology, electropharmacology and disease models, in *Cardiac Electrophysiology and Arrhythmias*, Zipes, D. P. and Jalife, J., Eds., Grune & Stratton, Orlando, FL, 1985, pp. 225–231.
77 Nielson, P. M. F., LeGrice, I. L., Smaill, B. H., and Hunter, P. J., A mathematical model of the geometry and fibrous structure of the heart, *J. Physiol.*, 260, HI365–1378, 1991.
78 O'Carrol, M. J., Inconsistencies and S.O.R. convergence for the discrete Neumann problem, *J. Inst. Math. Applic.*, 11, 343–350, 1973.
79 Ohta, T., Mimura, M., and Kobayashi, R., Higher–Dimensional localized patterns in excitable media, *Physica D*, 34, 115–144, 1989.
80 Okajima, H., Fujino, T., Kobayashi, T., and Yamada, K., Computer simulation of the propagation process in excitation of the ventricles, *Circ. Res.*, 23, 203–211, 1968.
81 Ortega, J. M., *Introduction to Parallel and Vector Solution of Linear Systems*, Plenum Press, New York, 1988.
82 Osher, S. and Sethian, J. A., Fronts propagating with curvature-dependent speed: Algorithms based on Hamilton–Jacobi formulation, *J. Comput. Phys.*, 79, 12–49, 1988.
83 Peskin, C. S., Fiber architecture of the left ventricular wall: An asymptotic analysis, *Commun. Pure Appl. Math.*, XLII, 79–113, 1989.
84 Pilkington, T. C., Morrow, M. N., and Stanley, P. C., A comparison of finite element and integral equation formulations for the calculation of electrocardiographic potentials:Part I, *IEEE Trans. Biomed. Eng.*, BME-32, 166–173, 1985.

85 Pilkington, T. C., Morrow, M. N., and Stanley, P. C., A comparison of finite element and integral equation formulations for the calculation of electrocardiographic potentials: Part II, *IEEE Trans. Biomed. Eng.*, BME-34, 258–260, 1987.
86 Plonsey, R., The use of a bidomain model for the study of excitable media, in *Some Mathematical Questions in Biology*, Othmer, H. G., Ed., A.M.S., Providence, 1989.
87 Plonsey, R., Bioelectric sources arising in excitable fibers (Alza Lecture), *Ann. Biomed. Eng.*, 16, 519–546, 1988.
88 Plonsey, R. and Barr, R. C., Current flow patterns in two-dimensional anisotropic bisyncytia with normal and extreme conductivities, *Biophys. J.*, 45, 557–571, 1984.
89 Blonsey, R. and Barr, R. C., Effect of microscopic and macroscopic discontinuities on the response of cardiac tissue to defribrillating (stimulating) currents, *Med. Biol. Eng. Comput.*, 24, 130–136, 1986.
90 Plonsey, R. and Barr, R. C., Mathematical modeling of the electrical activity of the heart, *J. Electrocardiol.*, 20, 219–226, 1987.
91 Plonsey, R. and Barr, R. C., Interstitial potentials and their change with depth into cardiac tissue, *Biophys. J.*, 51, 547–555, 1987.
92 Plonsey, R. and Heppner, D., Considerations of quasi-stationarity in electrophysiological systems, *Bull. Math. Biophys.*, 29, 657–664, 1967.
93 Plonsey, R. and Rudy, Y., Electrocardiogram sources in a two-dimensional anisotropic activation model, *Med. Biol. Eng. Comput.*, 18, 87–94, 1980.
94 Pollard, A. E. and Barr, R. C., The construction of an anatomically based model of the human ventricular conduction system, *IEEE Trans. Biomed. Eng.*, BME-37, 1173–1185, 1990.
95 Pollard, A. E. and Barr, R. C., Computer simulations of activation in an anatomically based model of the human ventricular conduction system, *IEEE Trans. Biomed. Eng.*, BME-38, 982–996, 1991.
96 Rawling, D. A. and Joyner, R. W., Characteristics of junctional regions between Purkinje and ventricular muscle cells of canine ventricular subendocardium, *Circ. Res.*, 60, 580–585, 1987.
97 Rawling, D. A., Joyner, R. W., and Overholt, E. D., Variation in the functional electrical coupling between the subendocardial Purkinje and ventricular layers of the canine left ventricle, *Circ. Res.*, 57, 252–261, 1985.
98 Roberge, F. A., Vinet, A., and Victorri, B., Reconstruction of propagated electrical activity with a two-dimensional model of anisotropic heart muscle, *Circ. Res.*, 58, 461–475, 1986.
99 Roberts, D., Hersch, L. T., and Scher, A. M., Influence of cardiac fiber orientation of wavefront voltage, conduction velocity and tissue resistivity in the dog, *Circ. Res.*, 44, 701–712, 1979.
100 Roberts, D. and Scher, A. M., Effect of tissue anisotropy on extracellular potential fields in canine myocardium in situ, *Circ. Res.*, 50, 342–351, 1982.
101 Roth, B. J., The electrical potential produced by a strand of cardiac muscle: A bidomain analysis, *Ann. Biomed. Eng.*, 16, 609–637, 1988.
102 Roth, B. J., Action potential propagation in a thick strand of cardiac muscle, *Circ. Res.*, 68, 162–173, 1991.
103 Roth, B. J. and Wikswo, J. P., A bidomain model for the extracellular potential and magnetic field of cardiac tissue, *IEEE Trans. Biomed. Eng.*, BME-33, 467–469, 1986.
104 Rudy, Y. and Quan, W. L., A model study of the effects of the discrete cellular structure on electrical propagation in cardiac tissue, *Circ. Res.*, 61, 815–823, 1987.
105 Saad, Y., Krylov subspace methods on supercomputers, *SIAM J. Sci. Statist. Comput.*, 10(10), 1200–1232, 1989.
106 Sano, T., Takayama, N., and Shimamoto, T., Directional difference of conduction velocity in the cardiac ventricular syncytium studies by microelectrodes, *Circ. Res.*, 7, 262–267, 1959.
107 Semitt, O. H., Biological information processing using the concept of interpenetrating domains, in *Information Processing in the Nervous System*, Leibovich, K. N., Ed., Springer-Verlag, New York, 1969, p. 329.
108 Scher, A. and Spach, M. S., Cardiac depolarization and repolarization and the electrocardiogram, in *Handbook of Physiology*, Vol. 1; The Heart, Sect. 2: The cardiovascular system, Berne, R. M., Ed., *Am. Physiol. Soc.*, Bethesda, MD, 1979, pp. 357–392.
109 Sepulveda, N. G., Roth, B. J., and Wikswo, J. P., Current injection into a two-dimensional anisotropic bidomain, *Biophys. J.*, 55, 987–999, 1989.
110 Sethian, J. A., Numerical algorithms for propagating interfaces: Hamilton–Jacobi equations and conservation laws, *J. Diff. Geom.*, 31, 131–161, 1990.
111 Sethian, J. A. and Strain, J., Crystal growth and dendritic solidification, *preprint*, 1990.
112 Solomon, J. C. and Selvester, R. H., Myocardial activation sequence simulation, in *Vectorcardiography*, Vol. 2, Hoffman, I., Ed., North-Holland, Amsterdam, 1971, pp. 175–182.
113 Solomon, J. C. and Selvester, R. H., Simulation of measured activation sequence in the human heart, *Am. Heart J.*, 85, 518–523, 1973.
114 Spach, M. S., The discontinuous nature of electrical propagation in cardiac muscle, *Ann. Biomed. Eng.*, 11, 207–261, 1983.
115 Spach, M. S., and Dolber, P. C., The relation between discontinuous propagation in anisotropic cardiac muscle and the "vulnerable period" of reentry, in *Cardiac Electrophysiology and Arrhythmias*, Lipes, D. P. and Jalife, J., Eds., Grune & Stratton, London, 1985, pp. 241–252.
116 Spach, M. S. and Kootsey, J. M., The nature of electrical propagation in cardiac muscle, *Am. J. Physiol.*, 244, H3–H22, 1983.
117 Spach, M. S., Miller, I.I.I. W. T., Miller-Jones, E., Warren, R. R., and Barr, R. C., Extracellular potentials related to intracellular action potentials during impulse conduction in anisotropic canine cardiac muscle, *Circ. Res.*, 45, 188–204, 1979.

118 Spach, M. S., Miller, I.I.I. W. T., Geselowitz, D. B., Barr, R. C., Kootsey, J. M., and Johnson, E. A., The discontinuous nature of propagation in normal canine cardiac muscle. Evidence for recurrent discontinuities of intracellular resistance that affect membrane currents, *Circ. Res.*, 48, 39–54, 1981.
119 Spaggiari, S., Baruffi, S., Arisi, G., Macchi, E., and Taccardi, B., Effect of intramural fiber direction on epicardial isochrone and potential maps (abstract), *Circulation*, 76(Suppl. II), IV–241, 1987.
120 tanley, P. C. and Pilkington, T. C., The combination method: A numerical technique for electrocardiographic calculations, *IEEE Trans. Biomed. Eng.*, BME-36, 456–461, 1989.
121 Streeter, D., Gross morphology and fiber geometry of the heart, in *Handbook of Physiology*, Vol. 1: The heart, Sect. 2: The cardiovascular system, Berne, R. M., Ed., Williams and Wilkins, Baltimore, 1979, pp. 61–112.
122 Taccardi, B., Three-dimensional spread of excitation in the heart, in *IV Giomate Intemazionali di Chirurgia, E. Malan*, Botta, G. C., Ed., Provincia di Parma, Italy, 1991, pp. 47–49.
123 Taccardi, B., Lux, R. L., Ershler, P. R., Watabe, S., and Macchi, E., Normal and abnormal intramural spread of excitation and associated potential distributions, in *Abstract Book of the XVII. Int. Congr. Electrocardiology and 31st Int. Symp. Vectorcardiology*, O.I.C. Medical Press, Firenze, Italy, 1990, p. 12.
124 Taccardi, B., Watabe, S., Ershler, P. R., Lux, R. L., and Macchi, E., A method for separating the axial and transverse contribution of excitation wavefronts to the cardiac electric field (abstract), *Circulation*, 78(Suppl. II), 11–412, 1988.
125 Taccardi, B., Watabe, S., Lux, R. L., Ershler, P. R., and Macchi, E., Effect of myocardial anisotropy and non-homogeneous conducting media on intracardiac and epicardial potential fields, in *Abstract Book of the XVII. Int. Congr. Electrocardiology and 31st Int. Symp. Vectorcardiology*. O.I.C. Medical Press, Firenze, Italy, 1990, p. 8.
126 Tyson, J. J. and Keener, J. P., Singular perturbation theory of traveling waves in excitable media (a review), *Physica D*, 32, 327–361, 1988.
127 Van Capelle, F. J. L. and Durrer, D., Computer simulation of arrhythmias in a network of coupled excitable elements, *Circ. Res.*, 47, 454–466, 1980.
128 Van der Vorst, H. A., High performance preconditioning, *SIAM J. Sci. Statist. Comput.*, 10(6), 1174–1185, 1989.
129 Watabe, S., Taccardi, B., Lux, R. L., and Ershler, P. D., Effect of non-transmural necrosis on epicardial potential fields: Correlation with fiber direction, *Circulation*, 82, 2115–2127, 1990.
130 Wei, D., Yamada, G., Musha, T., Tsunakawa, H., Tsutsumi, T., and Harumi, K., Computer simulation of superventricular tachycardia with the Wolff-Parkinson-White syndrome using three-dimensional heart models, *J. Electrocardiology*, 23(3), 261–273, 1990.
131 Wei, D., Yamada, G., Hasegawa, K., Nakamura, T., and Musha, T., Evaluation of the rotating anisotropy of the ventricular myocardium: A simulation study, in *IEEE Eng. Med. Biol. Soc., 11th Annu. Int. Conf*, 1989, pp. 186–187.
132 Weidmann, S., Electrical constant of trabecular muscle from mammalian heart, *J. Physiol.*, 210, 1041–1054, 1970.
133 Zienkiewicz, O. C., Kelly, D. W., and Bettes, P., The coupling of the finite element method and boundary solution procedure, *Int. J. Numer. Methods Eng.*, 2, 355–375, 1977.
134 Weiner, N. and Rosenblueth, A., The mathematical formulation of the problem of conduction of impulses in a network of connected excitable elements, specifically in cardiac muscle, *Arch. Inst. Cardiol. Mexico*, 16, 205, 1946.
135 Zykov, V. S. and Petrov, A., Role of the inhomogeneity of an excitable medium in the mechanism of self-sustained activity, *Biofizika*, 22(2), 300–306, 1977; English transl.: *Biophysics*, 22, 307–314, 1977.
136 Zykov, V. S. Analytical evaluation of the dependence of the speed of an excitation wave in a two-dimensional excitable medium on the curvature of its front, *Biofizika*, 25(5), 888–892, 1980; English transl.: *Biophysics*, 25, 906–911, 1980.
137 Zykov, V. S. *Simulation of Wave Processes in Excitable Media*, Manchester University Press, Manchester, 1987.
138 Green, L. S., Taccardi, B., Ershler, P. H., and Lux, R. L., Epicardial potential mapping. Effects of conducting media on isopotential and isochrone distributions, *Circulation*, 84, 2513–2521, 1991
1 Miller, III. W. T. and Geselowitz, D. B., Simulation studies of the electrocardiogram, *Circ. Res.*, 43, 301–315, 1978.
2 Geselowitz, D. and Miller, III, W. T., A bidomain model for anisotropic cardiac muscle, *Ann. Biomed. Eng.*, 11, 191–206, 1983.
3 Tung, L., A Bidomain Model for Describing Ischemic Myocardial dc Potentials, *Ph.D. dissertation*, Massachusetts Institute of Technology, Cambridge, 1978.
4 Eisenberg, R. S., Barcolin, V., and Mathias, R. T., Electrical properties of spherical syncytia, *Biophys. J.*, 45, 1191–1202, 1979.
5 Plonsey, R. and Rudy, Y., Electrocardiogram sources in a 2-dimensional anisotropic activation model, *Med. Biol. Eng. Comput.*, 18, 87–94, 1980.
6 Henriquez, C. S., Trayanova, N., and Plonsey, R., Potential and current distributions in a cylindrical bundle of cardiac tissue, *Biophys. J.*, 53, 907–918, 1988.
7 Henriquez, C. S., Trayanova, N., and Plonsey, R., A planar slab bidomain model for cardiac tissue, *Ann. Biomed. Eng.*, 18, 367–376, 1990.
8 Henriquez, C. S. and Plonsey, R., Simulation of propagation along a bundle of cardiac tissue. I. Mathematical formulation, *IEEE Trans. Biomed. Eng.*, 37, 850–860, 1990.
9 Henriquez, C. S. and Plonsey, R., Simulation of propagation along a bundle of cardiac tissue. II. Results of simulation, *IEEE Trans. Biomed. Eng.*, 37, 861–875, 1990.
10 Trayanova, N. and Henriquez, C. S., Modification of a cylindrical bidomain model for cardiac tissue, *Math. Biosci.*, 104, 59–72, 1991.

11 Henriquez, C. S., Trayanova, N., and Papazoglou, A., Modeling conduction as a function of depth in cardiac muscle, *IEEE Trans. Biomed. Eng.*, submitted.
12 Plonsey, R. and Barr, R. C., The four-electrode resistivity technique as applied to cardiac muscle, *IEEE Trans. Biomed. Eng.*, BME-29, 541–546, 1982.
13 Geselowitz, D. B., Barr, R. C., Spach, M. C., and Miller, III. W. T., The impact of adjacent isotropic fluids on electrograms from anisotropic cardiac muscle. A modeling study, *Circ. Res.*, 51, 602–613, 1982.
14 Barr, R. C. and Plonsey, R., Propagation of excitation in idealized anisotropic two-dimensional tissue, *Biophys. J.*, 45, 1191–1202, 1984.
15 Roth, B. J. and Wikswo, Jr., J. P., A bidomain model for the extracellular potential and magnetic field of cardiac tissues, *IEEE Trans. Biomed. Eng.*, BME-33, 467–469, 1986.
16 Roth, B. J., The electrical potential produced by a strand of cardiac muscle: A bidomain analysis, *Ann. Biomed. Eng.*, 16, 609–637, 1988.
17 Plonsey, R. and Barr, R. C., Interstitial potentials and their change with depth into cardiac tissue, *Biophys. J.*, 51, 547–555, 1987.
18 Plonsey, R. and Barr, R. C., Current flow patterns in two-dimensional anisotropic bisyncytia with normal and extreme conductivities, *Biophys. J.*, 45, 557–571, 1984.
19 Roth, B. J., Action potential propagation in a thick strand of cardiac muscle, *Circ. Res.*, 68, 162–173, 1991.
20 Roth, B. J., Guo, W.-Q., and Wikswo, Jr., J. P., The effects of spiral anisotropy on the electrical potential and magnetic field at the apex of the heart, *Math. Biosci.*, 88, 159–189, 1988.
21 Colli-Franzone, P., Guerri, L., and Rovida, S., Wavefront propagation in an activation model of the anisotropic cardiac tissue: Asymptotic analysis and numerical simulations, *J. Math. Biol.*, 28, 121–176, 1990.
22 Colli-Franzone, P., Guerri, L., and Tentoni, S., Mathematical modeling of the excitation process in myocardial tissue: Influence of fiber rotation on wavefront propagation and potential field, *Math. Biosci.*, 101, 155–235, 1990.
23 Leon, L. J. and Horacek, B. M., Computer model of excitation and recovery in the anisotropic myocardium. I. Rectangular and cubic arrays of excitable elements, *J. Electrocardiol.*, 24, 1–15, 1991.
24 Leon, L. J. and Horacek, B. M., Computer model of excitation and recovery in the anisotropic myocardium. II. Excitation in the simplified left ventricle, *J. Electrocardiol.*, 24, 17–31, 1991.
25 Leon, L. J. and Horacek, B. M., Computer model of excitation and recovery in the anisotropic myocardium. III. Arrhythmogenic conditions in the simplified left ventricle, *J. Electrocardiol.*, 24, 33–41, 1991.
26 Sepulveda, N. G., Roth, B. J., and Wikswo, Jr., J. P., Current injection into a two-dimensional anisotropic bidomain, *Biophys. J.*, 55, 987–999, 1989.
27 Hodgkin, A. L. and Ruston, W. A. H., The electrical constants of crustacean nerve fiber, *Proc. Roy. Soc. London, Biol. Sci.*, 133, 444–479, 1946.
28 Peskoff, A., Electric potential in three-dimensional electrically syncytial tissues, *Bull. Math. Biol.*, 41, 163–181, 1979.
29 Roth, B. J., The bidomain model of cardiac tissue: predictions and experimental verification, in *Neural Engineering*, Kim, Y. and Thakor, N., Eds., submitted.
30 Plonsey, R., The use of a bidomain model for the study of excitable media, *Lectures Math, in Life Sci.*, 21, 123–149, 1989.
31 Roth, B. J., How the anisotropy of the intracellular and extracellular conductivities influences stimulation of cardiac muscle, *J. Math. Biol.*, to be published.
32 Muler, A. L. and Markin, V. S., Electrical properties of anisotropic nerve-muscle syncytia. I. Distribution of the electrotonic potential, *Biofizika*, 22, 307–312, 1977.
33 Wikswo, Jr., J. P., Wisialowski, T. A., Altemeier, W. A., Balser, J. R., Kopelman, H. A., and Roden, D. M., Virtual cathode effects during stimulation of cardiac muscle, *Circ. Res.*, 68, 513–530, 1991.
34 Roth, B. J. and Saypol, J. M., The formation of a reentrant action potential wave front in tissue with unequal anisotropy ratios, *Int. J. Bifurcations Chaos*, to be published.
35 Trayanova, N. and Roth, B. J., The response of a spherical heart to a uniform electric field: A bidomain analysis of cardiac stimulation, *IEEE Trans. Biomed. Eng.*, submitted.
36 Sepulveda, N. G. and Wikswo, Jr., J. P., Bipolar stimulation of cardiac tissue: A bidomain model, in *Proc. 13th Annual IEEE/EMBS Conf*, 1991, pp. 617–618.
37 Sepulveda, N. G., Barach, J. P., and Wikswo, Jr., J. P., A three-dimensional finite element bidomain model for cardiac tissue, in *Proc. 13th Annual IEEE/EMBS Conf*, 1991, pp. 512–514.
38 Suenson, M., Interaction between ventricular cells during the early part of excitation in ferret heart, *Acta Physiol. Scand.*, 125, 81–90, 1985.
39 Press, W. H., Flannery, B. P., Teukolsky, S. A., and Vetterling, W. T., *Numerical Recipes in C*, Cambridge University Press, 1988.
40 Andrews, L. and Shivamoggi, B., *Integral Transforms for Engineers and Applied Mathematicians*, Macmillan, New York, 1988.
41 Clerc, L., Directional differences of impulse spread in trabecular muscle from mammalian heart, *J. Physiol*, 255, 335–346, 1976.
42 Weidmann, S., Electrical constants of trabecular muscle for mammalian heart, *J. Physiol.*, 210, 1041–1054, 1970.
43 Roth, B., A comparison of two boundary conditions used with the bidomain model of cardiac tissue, *Ann. Biomed. Eng.*, 19, 669–678, 1991.
44 Neu, J. and Krassowska, W., Continuous representation of syncytial tissues using homogenization technique *CRC Crit. Rev. Bioeng.*, submitted.

45 Trayanova, N., Pilkington, T., and Henriquez, C. A., A periodic bidomain model for cardiac tissue, in *Proc. 13th Annual IEEE/EMBS Conf*, 1991, pp. 502–503.
46 Trayanova, N. and Pilkington, T., A bidomain model with periodic intracellular junctions. A onedimensional analysis, *IEEE Trans. Biomed. Eng.*, submitted.
47 Plonsey, R. and Barr, R. C., Effect of microscopic and macroscopic discontinuities on the response of cardiac tissue to defibrillating (stimulating) currents, *Med. Biol. Eng. Comput.*, 24, 130–136, 1986.
48 Plonsey, R. and Barr, R. C., Inclusion of junction elements in a linear cardiac model through secondary sources: Application to defibrillation, *Med. Biol. Eng. Comput.*, 24, 137–144, 1986.
49 Plonsey, R., Barr, R. C., and Witkowski, F. X., One-dimensional model of cardiac defibrillation, *Med. Biol. Eng. Comput.*, 29, 465–469, 1991.
50 Krassowska, W., Pilkington, T., and Ideker, R., The closed form solution to the periodic core-conductor model using asymptotic analysis, *IEEE Trans. Biomed. Eng.*, BME-34, 519–531, 1987.
51 Krassowska, W., Pilkington, T., and Ideker, R., Periodic conductivity as a mechanism for cardiac stimulation and defibrillation, *IEEE Trans. Biomed. Eng.*, BME-34, 555–559, 1987.
1 Levoy, M., Display of surfaces from volume data, *IEEE Comput. Graphics AppL*, 8(3), 29–37,May 1988.
2 Sabella, P., A rendering algorithm for visualizing 3D scalar fields, *Comput. Graphics*, 22(4), 51–58, 1988.
3 Upson, C. and Keeler, M., Vbuffer: Visible volume rendering, *Comput. Graphics*, 22(4), 59–64, 1988.
4 Drebin, R. A., Carpenter, L., and Hanrahan, P., Volume rendering, *Comput. Graphics*, 22(4), 65–74, 1988.
5 Westover, L., Interactive volume rendering, in *Chapel Hill Workshop on Volume Visualization*, ACM SIGGRAPH,May 1989, pp. 9–16.
6 Fuchs, H., Kedem, Z. M., and Uselton, S. P., Optimal surface reconstruction from planar contours, *Commun. ACM*, 20(10), 693–702, 1977.
7 Wyvill, G., McPheeters, C., and Wyvill, B., Data structures for soft objects, *Visual Comput.*, 2(4), 227–234, 1986.
8 Lorensen, W. E. and Cline, H. E., Marching cubes: A high resolution 3D surface construction algorithm, *Comput. Graphics*, 21(4), 163–169, 1987.
9 Cline, H. E. and Lorenson, W. E., Two algorithms for the thee-dimensional reconstruction of tomograms, *Med. Phys.*, 15(3), 320–327, 1988.
10 Ney, D. R., Fishman, E. K., Magid, D., and Drebin, R. A., Volumetric rendering of computed tomography data: Principles and techniques, *IEEE Comput. Graphics AppL*, 10(2), 24–32, March 1990.
11 Phong, B. T., Illumination for computer generated images, *Commun. ACM*, 18(6), 311–371, June 1975.
12 Blinn, J. F., Light reflection functions for simulation of clouds and dusty surfaces, *Comput. Graphics*, 16(3), 21–29, 1982.
13 Kajiya, J. T., Ray tracing volume densities, *Comput. Graphics*, 18(3), 165–174, 1984.
14 Porter, T. and Duff, T., Compositing digital images, *Comput. Graphics*, 18(3), 253–259, 1984.
15 Novins, K. L., Sillion, F. X., and Greenberg, D. P., An efficient method for volume rendering using perspective projection, *Comput. Graphics*, 24(5), 95–100, 1990.
16 Levoy, M., Efficient ray tracing of volume data, *ACM Trans. Graphics*, 9(3), 245–261, 1990.
17 Levoy, M., A hybrid ray tracer for rendering polygon and volume data, *IEEE Comput. Graphics Appl.*, 10(2), 33–40, March 1990.
18 Levoy, M., Design for a real-time high-quality volume rendering workstation, in *Chapel Hill Workshop on Volume Visualization*, ACM SIGGRAPH,May 1989, pp. 85–90.
19 Laur, D. and Hanrahan, P., Hierarchical splatting: A progressive refinement algorithm for volume rendering, *Comput. Graphics*, 25(4), 285–288, 1991.
20 Goodsell, D. S. and Olson, A. J., Molecular applications of volume rendering and 3-D texture maps, in *Chapel Hill Workshop on Volume Visualization*, ACM SIGGRAPH,May 1989, pp. 27–31.
21 Hu, X., Tan, K. K., Levin, D. N., Galhotra, S. G., Pelizzari, C. A., Chen, G. T. Y., Beck, R. N., Chen, C.-T., and Cooper, M. D., Volumetric rendering of multimodality, multivariable medical imaging data, in *Chapel Hill Workshop on Volume Visualization*, ACM SIGGRAPH,May 1989, pp. 45–49.
22 Andrews, L. T., Klingler, J. W., Begeman, M. S., Zeiss, J., and Leighton, R. F., Visualization of cardiac magnetic resonance images with color encoded 2D and 3D functional images, in *Proc. 1st Conf, Visualization in Biomedical Computing*, IEEE,May 1990, pp. 172–178.
23 Valentino, D. J., Mazziotta, J. C., and Huang, H. K., Volume rendering of multimodal images: Application to MRI and PET imaging of the human brain, *IEEE Trans. Med. Imaging*, 10(4), 554–562, December 1991.
24 Palmer, T. C., A language for molecular visualization, *IEEE Comput. Graphics Appl.*, 12(3), 23–32, 1992.
25 Crawfis, R. A. and Allison, M. J., A scientific visualization synthesizer, in *Proc. Visualization VI*, IEEE,October 1991, pp. 262–267.
26 Smith, W. M., Wharton, J. M., Blanchard, S. M., Wolf, P. D., and Ideker, R. E., Direct cardiac mapping, in *Cardiac Electrophysiology, From Cell to Bedside*, Zipes, D. P. and Jalife, J., Eds., Saunders, Philadelphia, 1990, pp. 849–858.
27 Sepulveda, N. G. and Wikswo, Jr., J. P., Electric and magnetic fields from two-dimensional anisotropic bisyncytia, *Biophys. J.*, 51, 557-568, 1987.
28 Hill, J. L. and Gettes, L. S., Ion-sensitive plunge wire electrodes for intramyocardial pH and K + determinations, in *Ion Measurement in Physiology and Medicine*, Kessler, M., Harrison, D. K., and Hoper, J., Eds., Springer-Verlag, New York, 1985, pp. 85–89.
29 Kavanagh, K. M., Kabas, J. S., Rollins, D. L., Melnick, S. B., Smith, W. M., and Ideker, R. E., High-current stimuli to the spared epicardium of a large infarct induce ventricular tachycardia, *Circulation*, 85, 680–698, 1992.

30 Shibata, N., Chen, P.-S., Dixon, E. G., et al., Influence of shock strength and timing on induction of ventricular arrhythmias in dogs, *Am. J. Physiol.*, 255, H891–H901, 1988.
31 Chen, T. C. K., Parson, I. D., and Downar, E., The construction of endocardial balloon arrays for cardiac mapping, *PACE*, 14, 470–479, 1991.
32 Tang, A. S. L., Wolf, P. D., Claydon, III. F. J., Smith, W. M., Pilkington, T. C., and Ideker, R. E., Measurement of defibrillation shock potential distributions and activation sequences of the heart in three dimensions, *Proc. IEEE*, 76, 1176–1186, 1988.
33 Wolf, P. D., Rollins, D. L., Blitchington, T. F., Ideker, R. E., and Smith, W. M., Design for a 512 channel cardiac mapping system, in *Biomedical Engineering: Opening New Doors, Proc. Fall 1990 Annual Meeting of the Biomedical Engineering Society*, Mikulecky, D. C. and Clarke, A. M., Eds., New York University Press, 1990, pp. 5–13.
34 Witkowski, F. X., Penkoske, P. A., and Plonsey, R., Mechanism of cardiac defibrillation in open-chest dogs with unipolar dc-coupled simultaneous activation and shock potential recordings, *Circulation*, 82, 244–260, 1990.
35 Wharton, J. M., Wolf, P. D., Smith, W. M., et al., Cardiac potential and potential gradient fields generated by single, combined, and sequential shocks during ventricular defibrillation, *Circulation*, 85, 1510–1523, 1992.
36 Laxer, C., Ideker, R. E., Kavanagh, K. M., Simpson, E. V., Johnson, G. A., and Smith, W. M., An interactive graphics system for locating plunge electrodes in cardiac MRI images, in *Proc. Conf. Image Capture, Formatting and Display*, 1991, pp. 190–195.
37 Barr, R. C., Gallie, T. M., and Spach, M. S., Automated production of contour maps for electrophysiology, I. Problem definition, solution strategy, and specification of geometric model, *Comput. Biomed. Res.*, 13, 142–153, 1980.
38 Barr, R. C., Gallie, T. M., and Spach, M. S., Automated production of contour maps for electrophysiology, II. Triangulation, verification, and organization of the geometric model, *Comput. Biomed. Res.*, 13, 154–170, 1980.
39 Barr, R. C., Gallie, T. M., and Spach, M. S., Automated production of contour maps for electrophysiology, III. Construction of contour maps, *Comput. Biomed. Res.*, 13, 171–191, 1980.
40 Bartram, F. R., Ideker, R. E., and Smith, W. M., A system for the parametric description of the ventricular surface of the heart, *Comput. Biomed. Res.*, 14, 533–541, 1981.
41 Mallet, J.-L., Discrete smooth interpolation, *ACM Trans. Graphics*, 8, 121–144, 1989.
42 Simpson, E. V., Wolf, P. D., Ideker, R. E., and Smith, W. M., Three-dimensional visualization of electrical variables in the ventricular wall of the heart, in *Proc. 1st Conf. Visualization in Biomedical Computing*, IEEE,May 1990, pp. 190–194.
43 Simpson, E. V., Ideker, R. E., and Smith, W. M., Discrete smooth interpolation as an aid to visualizing electrical variables in the heart wall, in *Proc. Comput. Cardiol.*, 1991, pp. 409–412.
1 Vajda, S., Jafri, M. S., Sezerman, O. S., and DeLisi, C., Necessary conditions for avoiding incorrect peptide folds in conformational search by energy minimization, *submitted Biopolymers*, 1992.
2 DeLisi, C.,Computer aided prediction of protein structure and function, in *Computers in Endocrinology: Recent Advances*,Guardobasso, V., Rodbard, D., and Forti, G., Eds., Raven Press, New York, 1990.
3 See, for example,Branden, C. and Tooze, J., *Introduction to Protein Structure*, Garland Publishing, New York, 1991.
4 For example,Chothia, C., et al., The predicted structure of immunoglobulin D 1.3 and its comparison with the crystal structure, *Science*, 233, 7755-7758, 1986.
5 Vajda, S., Margolit, H., Cornette, J., Ryoichi, K., Berzofsky, J., and DeLisi, C., Molecular structure and vaccine design, *Annu. Rev. Biophys. Biochem.*, 19, 69-82, 1990.
6 Zheng, Q., Rosenfeld, R., Vajda, S., and DeLisi, C., Loop closure via bond scaling and relaxation, *Protein, submitted*, 1992.
7 Figure 4 from Grand Challenge, High Performance Computing and Communications. *A Report by the Committee on Physical, Mathematical, and Engineering Sciences, OTS, FY* 1992.
8 Born, M. and Oppenheimer, J. R., *Ann. Physik*, 84, 457, 1927.
9 Iori, G., Marinari, E., and Parisi, G., Random Self-Interacting Chains: A Mechanism for Protein Folding, *Preprint ROM2F-91-4*, 1991.
10 Gibson, K. D. and Scheraga, H. A., in *Structure and Expression, Vol. I: From Proteins to Ribosomes*,Sarma, M. H. and Sarma, R. H., Eds.Adenine Press, Guilderland, NY, 1988, p.67.
11 Brower, R. C., Vasmatzis, G., Silverman, M., and DeLisi, C., Protein folding on a lattice by exhaustive search and simulated annealing, *Biopolymers, submitted*, 1992.
12 Bouzida, D., Kumar, S., and Swendsen, R. K., *Almost Markov Processes*, Springer-Verlag, New York, 1990.
13 Swendsen, R. H., Wang, J.-S., and Ferrenberg, A. M., in *Monte Carlo Methods in Condensed Matter Physics*,Binder, K., Ed., Springer, Berlin, 1991.
14 Sokal, A., *New Numerical Algorithms for Critical Phenomena (Multi-Grid Methods and All That)*, Springer-Verlag, Berlin, 1988.
15 Brower, R. C. and Tamayo, P., Embedded dynamics for ϕ^4 theory, *Phys. Rev. Lett.*, 62, 1087, 1989.
16 Swendsen, R. H. and Wang, J.-S., *Phys. Rev. Lett.*, 58, 86, 1987.
17 Batrouni, G. G., Katz, G. R., Kronfeld, A. S., Lepage, G. P., Svetitsky, B., and Wilson, K. G., *Phys. Rev. D*, 32, 2736, 1985.
18 Amit, D. J., *Field Theory, the Renormalization Group, and Critical Phenomena*, McGraw-Hill, New York, 1978;Itzykson, C. and Drouffe, J.-M., *Statistical Field Theory, Vols. 1 and 2*, Cambridge University Press, 1989.
19 Miyazawa, S. and Jernigan, R. L., Estimation of effective interresidue contact energies from protein crystal structures: Quasi-chemical approximation, *Macromolecules*, 18, 534, 1985.

20 Sokal, A., *Monte Carlo Methods in Statistical Mechanics: Foundations and New Algorithms*, Cours de Troisieme Cycle de la Physique ne Suisse Romande, 1989.
21 Honig, B. H., Hubbell, W. L., and Flewelling, R. F., Electrostatic interactions in membrane and proteins, *Annu. Rev. Biophys. Chem.*, p.163, 1986;Rashin, A. and Nambooriri, K., A simple method for the calculation of hydration enthalpies of polar molecules with arbitrary shapes, *J. Phys. Chem.*, 91, 6003, 1987;Lim, C., Bashford, D., and Karplus, M., Absolute p*Ka* calculations with continuum dielectric methods, *J. Phys. Chem.*, p.95, 1991.
22 Hill, T. L., *Statistical Mechanics*, McGraw-Hill, New York, 1956.
23 Brower, R. C. and Banks, J., A dynamic continuum model for solvation of macromolecules, *in preparation*, 1992.
24 Jorgensen, W. L., Chandrasekhar, J., and Madura, J. D., Comparison of simple potential functions for simulating liquid water, *J. Chem. Phys.*, 79, 298, 1983.
25 Hockney, R. W. and Eastwood, J. W., *Computer Simulation Using Particles*, IOP Publishing, Bristol, 1988.
26 Jain, A., Rodriguez, R., Vaidel, N., Mathiowetz, A. M., and Goddard III, W. A., The Newton-Euler inverse mass operator method for internal coordinate molecular dynamics simulation, JPL preprint, *J. Comp. Phys.*, submitted.
27 Brower R. C., Tamayo, P., and York, B., Parallel multigrid algorithm for percolation clusters, *J. Stat. Phys.*, 63, 73, 1991.
1 Rosenman, J. G., Chaney, E. L., Sailer, S., Sherouse, G. W., and Tepper, J. E., Recent advances in radiotherapy treatment planning, *Cancer Invest.*, 9, 465–481, 1991.
2 Fuchs, H., Poulton, J., Eyles, J., et al., Pixel-Planes 5: A heterogeneous multiprocessor graphics system using processor-enhanced memories, *Computer Graphics, Proc. SIGGRAPH '89*, 23, 79–88, 1989.
3 Sherouse, G. W. and Chaney, E. L., The portable virtual simulator, *Int. J. Rad. Oncol. Biol. Phys.*, 21, 475–482, 1991.
4 Niemierko, A. and Goitein, M., The use of variable grid spacing to accelerate dose calculations, *Med. Phys.*, 16, 357–365, 1989.
5 Rosenman, J. G., Chaney, E. L., Cullip, T. J., Symon, J. R., Fuchs, H., and Stevenson, D., VISTAnet: Interactive realtime calculation and display of 3D radiation dose: An application of gigabit networking, *Int. J. Rad. Oncol. Biol. Phys.*,in press.
1 Hennessy, J. L. and Patterson, D. A., *Computer Architecture: A Quantitative Approach*, Morgan Kaufman, San Mateo, CA, 1990.
2 Gotoh, O. and Tagashira, Y., Sequence search on a supercomputer, *Nucleic Acids Res.*, 14, 57–64, 1986.
3 Gilbert, B. K. et al., Application of optimized parallel processing digital computers and numerical approximation methods to the ultra high-speed three-dimensional reconstruction of the intact thorax, *Int. J. Biomed. Comput.*, 10, 317–329, 1979.
4 Dongarra, J. J., Performance of Various Computers Using Standard Linear Equations Software, *Tech. Rep. CS-89-85, version of Feb. 6, 1992*, Oak Ridge National Laboratory, Oak Ridge, TN, 1992.
5 Carriero, N. and Gerlernter, D., *How to Write Parallel Programs: A First Course*, MIT Press, Cambridge, MA, 1990.
6 Sunderam, V. S., PVM: a framework for parallel distributed computing, *Concurrency: Practice and Experience*, 2, 315–339, 1990.
7 van Mulligen, E. M., Timmers, T., Langhout, A., and Leao, B. de F., CW 2000: a medical workstation to support research in cardiology, in *Computers in Cardiology*, IEEE Computer Society Press, Los Alamitos, CA, 1990, pp. 203–206.
8 Johnston, W. E. et al., High-performance computing, high-speed networks, and configurable computing environments: progress toward fully distributed computing, in *High-Performance Computing in Biomedical Research*, Pilkington, T. et al., Eds., CRC Press, Boca Raton, FL, 1993.
9 Rosenman, J. and Cullip, T., High-performance computing in irradiation cancer treatment, in *High-Performance Computing in Biomedical Research*, Pilkington, T. et al., Eds., CRC Press, Boca Raton, FL, 1993.
10 Jadvar, H., Jenkins, J. M., Stewart, R. W., Schwaiger, M., and Arzbaecher, R. C., Computer analysis of the electrocardiogram during esophageal pacing cardiac stress, *IEEE Trans. Biomed. Eng.*, 38, 1089, 1991.
11 Miller, C. E. and Henriquez, C. S., Three-dimensional finite element solution for biopotentials: erythrocyte in an applied field, *IEEE Trans. Biomed. Eng.*, 35, 712–718, 1988.
12 Flurchick, K. and Loftis, B., Modeling: current and next generation;A look at computational methods for solving problems in biomedical research, *presented at Symp. on High-Performance Computing in Biomedical Research*, North Carolina Supercomputing Center, Research Triangle Park,October 14 to 15, 1992.
13 Barach, J. P. and Wikswo, J. P., Jr., The effect of action potential propagation on a numerical simulation of a cardiac fiber subjected to secondary external stimulus, *Comput. Biomed. Res.*, 24, 435–452, 1991.
14 Pollard, A. E., Hooke, N., and Henriquez, C. S., Cardiac propagation simulation, in *High-Performance Computing in Biomedical Research*, Pilkington, T. et al., Eds., CRC Press, Boca Raton, FL, 1993.
15 Hunter, P. J., Nielsen, P. M. F., Smaill, B. H., LeGrice, I. J., and Hunter, I. W., An anatomical heart model with applications to myocardial activation and ventricular mechanics, in *High-Performance Computing in Biomedical Research*, Pilkington, T. et al., Eds., CRC Press, Boca Raton, FL, 1993.
16 Rudy, Y. and Oster, H. S., The electromagnetic inverse problem, in *High-Performance Computing in Biomedical Research*, Pilkington, T. et al., Eds., CRC Press, Boca Raton, FL, 1993.
17 Colli Franzone, P. and Guerri, L., Models of the spreading of excitation in myocardial tissue, in *High-Performance Computing in Biomedical Research*, Pilkington, T. et al., Eds., CRC Press, Boca Raton, FL, 1993.
18 McCulloch, A., Guccione, J., Waldman, L., and Rogers, J., Large-scale finite element analysis of the beating heart, in *High-Performance Computing in Biomedical Research*, Pilkington, T. et al., Eds., CRC Press, Boca Raton, FL, 1993.

19 Meijs, J. W. H. and Peters, M. J., The EEG and MEG, using a model of eccentric spheres to describe the head, *IEEE Trans. Biomed. Eng.*, 34, 913–920, 1987.
20 Cuffin, B. N., Eccentric spheres models of the head, *IEEE Trans. Biomed. Eng.*, 38, 871–878, 1991.
21 Hämäläinen, M. S. and Sarvas, J., Realistic conductivity geometry model of the human head for interpretation of neuromagnetic data, *IEEE Trans. Biomed. Eng.*, 36, 165–171, 1989.
22 Kazarnovskaya, M. I. et al., 3-d computer model of subcortical structures of human brain, *Comput. Biol. Med.*, 21, 451–457, 1990.
23 Smith, S. R. and Wheeler, B. C., A real-time multiprocessor system for acquisition of multichannel neural data, *IEEE Trans. Biomed. Eng.*, 35, 875, 1988.
24 Chaudhary, A. M. and Trachtenberg, E. A., Blackout detection as a multiobjective optimization problem, *Ann. Biomed. Eng.*, 19, 743–766, 1991.
25 Wawrzynski Nicoletti, D. and Onaral, B., The application of delta modulation to EEG waveforms for database reduction and real-time signal processing, *Ann. Biomed. Eng.*, 19, 1–14, 1991.
26 Messinger–Rappaport B. J. and Rudy, Y., Computational issues of importance to the inverse recovery of epicardial potentials in a realistic heart-torso geometry, *Math. Biosci.*, 97, 85–120, 1989.
27 Colli Franzone, P., et al., A mathematical procedure for solving the inverse problem of electrocardiology, *Math, Biosci.*, 77, 353–396, 1985.
28 Oster, H. S. and Rudy, Y., The use of temporal information in the regularization of the inverse problem of electrocardiology, *IEEE Trans. Biomed. Eng.*, 39, 65–75, 1992.
29 Nenonen, J., et al., Magnetocardiographic functional localization using a current dipole in a realistic torso, *IEEE Trans. Biomed. Eng.*, 38, 658–663, 1991.
30 Oostendorp, T. F. and van Oosterom, A., Source parameter estimation in inhomogeneous volume conductors of arbitrary shape, *IEEE Trans. Biomed. Eng.*, 36, 382–391, 1989.
31 Stanley, P. C., Pilkington, T. C., Morrow, M. N., and Ideker, R. E., An assessment of variable thickness and fiber orientation of the skeletal muscle layer on electrocardiographic calculations, *IEEE Trans. Biomed. Eng.*, 38, 1069–1075, 1991.
32 Stanley, P. C. and Pilkington, T. C., The combination method: a numerical technique for electrocardiographic calculations, *IEEE Trans. Biomed. Eng.*, 36, 456–461, 1989.
33 Leon, L. J. and Roberge, F. A., Structural complexity effects on transverse propagation in a two-dimensional model of myocardium, *IEEE Trans. Biomed. Eng.*, 38, 997–1009, 1991.
34 Pollard, A. E. and Barr, R. C., Computer simulations of activation in an anatomically based model of the human ventrical conduction system, *IEEE Trans. Biomed. Eng.*, 38, 982–996, 1991.
35 Pollard, A. E., Hooke, N., and Henriquez, C. S., Cardiac propagation simulation, in *High-Performance Computing in Biomedical Research*, Pilkington, T. et al., Eds., CRC Press, Boca Raton, FL, 1993.
36 Thompson, J. F. and Weatherhill, N. P., Structured and unstructured grid generation, in *High-Performance Computing in Biomedical Research*, Pilkington, T. et al., Eds., CRC Press, Boca Raton, FL, 1993.
37 Breau, C., Shirazi-Adl, A., and de Guise, J., Reconstruction of a human ligamentous lumbar spine using CT images—A three-dimensional finite element mesh generation, *Ann. Biomed. Eng.*, 19, 291–302, 1991.
38 Hawkins, D. A. and Hull, M. L., A computer simulation of muscle-tendon mechanics, *Comput. Biol. Med.*, 21, 369–382, 1991.
39 Spilker, R. L., de Almeida, E. S., and Donzelli, P. S., Finite element methods for the biomechanics of soft hydrated tissues: nonlinear analysis and adaptive control of meshes, in *High-Performance Computing in Biomedical Research*, Pilkington, T. et al., Eds., CRC Press, Boca Raton, FL, 1993.
40 Smolinski, P. and Rubash, H. E., Bone remodeling around total hip implants, in *High-Performance Computing in Biomedical Research*, Pilkington, T. et al., Eds., CRC Press, Boca Raton, FL, 1993.
41 Sharan, M., Singh, B., Singh, M. P., and Kumar, P., Finite-element analysis of oxygen transport in the systemic capillaries, *IMA J. Math. Applied Med. Biol.*, 8, 107–123, 1991.
42 Baker, D. A., Holte, J. E., and Patankar, S. V., Computationally two-dimensional finite-difference model for hollow-fibre blood-gas exchange devices, *Med. Biol. Eng. Comput.*, 29, 482–488, 1991.
43 Verbraak, A. F. M., Bogaard, J. M., Beneken, J. E. W., Hoorn, E., and Versprille, A., Serial lung model for simulation and parameter estimation in body plethysmography, *Med. Biol. Eng. Comput.*, 29, 309, 1991.
44 Segadal, L., Velocity distribution model for normal blood flow in the human ascending aorta, *Med. Biol. Eng. Comput.*, 29, 489–492, 1991.
45 Gustin, M.-P., Cerutti, C., and Paultre, C. Z., Heterogeneous computer network for real-time hemodynamic signal processing, *Comput. Biol. Med.*, 20, 205–215, 1990.
46 Belardinelli, E. and Cavalcanti, S., A new nonlinear two-dimensional model of blood motion in tapered and elastic vessels, *Comput. Biol. Med.*, 21, 1–13, 1991.
47 McQueen, D. M. and Peskin, C. S., Computational studies of blood flow in the heart in two and three dimensions (and references therein), in *17th Annu. Northeast Bioeng. Conf*, IEEE Press, New York, 1991, pp. 77–78.
48 Chowdhury, D. Q. and Hill, S. C., Numerical optimization of 3-d sar distributions in cylindrical models for electromagnetic hyperthermia, *IEEE Trans. Biomed. Eng.*, 38, 1246–1255, 1991.
49 Charny, C. K. and Levin, R. L., A three-dimensional thermal and electromagnetic model of whole limb heating with a MAP A, *IEEE Trans. Biomed. Eng.*, 38, 1030–1038, 1991.
50 Shaw, J. A., Durney, C. H., and Christensen, D. A., Computer-aided design of two-dimensional electric-type hyperthermia applicators using the finite-difference time-domain method, *IEEE Trans. Biomed. Eng.*, 38, 861–869, 1991.

51 Ebbini, E. S. and Cain, C. A., A spherical-section ultrasound phased array applicator for deep localized hyperthermia, *IEEE Trans. Biomed. Eng.*, 38, 634–643, 1991.
52 Morris, L. R. and Barszczewski, P., Algorithms, hardware, and software for a digital signal processor microcomputer-based speech processor in a multielectrode cochlear implant system, *IEEE Trans. Biomed. Eng.*, 36, 573–584, 1989.
53 Zierhofer, C. M. and Hochmair, E. S., High-efficiency coupling-intensive transcutaneous power and data transmission via an inductive link, *IEEE Trans. Biomed. Eng.*, 37, 716–722, 1990.
54 Veltink, P. H., et al., A modeling study of nerve fascicle stimulation, *IEEE Trans. Biomed. Eng.*, 36, 683–692, 1989.
55 Durand, D., Ferguson, A. S., and Dalbasti, T., Effect of surface boundary on neuronal magnetic stimulation, *IEEE Trans. Biomed. Eng.*, 39, 58–64, 1992.
56 Roth, B. J. et al., A theoretical calculation of the electric field induced by magnetic stimulation of a peripheral nerve, *Muscle Nerve*, 13, 734–741, 1990.
57 Ueno, S., Tashiro, T., and Harada, K., Localized stimulation of neural tissues in the brain by means of a paired configuration of time-varying magnetic fields, *J. Appl. Phys.*, 64, 5862–5864, 1988.
58 Liang, D. H., Kovacs, G. T. A., Storment, C. W., and White, R. L., A method for evaluating the selectivity of electrodes implanted for nerve stimulation, *IEEE Trans. Biomed. Eng.*, 38, 443–449, 1991.
59 Campbell, P. K. et al., A silicon-based, three-dimensional neural interface: manufacturing processes for an intracortical electrode array, *IEEE Trans. Biomed. Eng.*, 38, 758, 1991.
60 Bourne, P. E. and Hendrickson, W. A., A cpu benchmark for protein crystallographic refinement, *Comput. Biol. Med.*, 20, 219–230, 1990.
61 Brower, R. C. and DeLisi, C., Impact of massively parallel computation on protein structure determination, in *High-Performance Computing in Biomedical Research*, Pilkington, T. et al., Eds., CRC Press, Boca Raton, FL, 1993.
62 Boehncke, K., Heller, H., Grubmuller, H., and Schulten, K., Molecular dynamics simulation on a systolic ring of transputers, in *Transputer Research and Applications 3*, Wagner, A. S., Ed., NATUG, IOS Press, Washington, DC, 1990, p. 83.
63 Auerbach, D. J., Paul, W., and Bakkers, A. F., A special purpose computer for molecular dynamics: motivation, design, and application, *J. Phys. Chem.*, 91, 4881, 1987.
64 Scott, H. L., Lipid–cholesterol interactions, Monte Carlo simulations and theory, *Biophys. J.*, 59, 445–455, 1991.
65 Bartol, T. M., Jr., et al., Monte Carlo simulation of miniature endplate current generation in the vertebrate neuromuscular junction, *Biophys. J.*, 59, 1290–1307, 1991.
66 Office of Science and Technology, *Grand Challenges: High Performance Computing and Communications, The FY 1992 U.S. Research and Development Program*, Committee on Physical, Mathematical, and Engineering Sciences, National Science Foundation, Washington, DC, 1991.
67 Vogt, G. and Argos, P., Searching for distantly related protein sequences in large databases by parallel processing on a transputer machine, *Comput. Applications Biosci.*, 8, 49–55, 1992.
68 Deshpande, A. S., Richards, D. S., and Pearson, W. R., A platform for biological sequence comparison on parallel computers, *Comput. Applications Biosci.*, 1, 237–247, 1991.
69 Sittig, D. F. et al., A parallel computing approach to genetic sequence comparison: the master-worker paradigm with interworker communication, *Comput. Biomed. Res.*, 24, 152–169, 1991.
70 Miller, P. L., Nadkarni, P. M., and Carriero, N. M., Parallel computation and fasts: confronting the problem of parallel database search for a fast sequence comparison algorithm, *Comput. Applications Biosci.*, 1, 71–78, 1991.
71 Barton, G. J., Scanning protein sequence databanks using a distributed processing workstation network, *Comput. Applications Biosci.*, 1, 85–88, 1991.
72 Roberts, L., New chip may speed genome analysis, *Science*, 244, 655, 1989.
73 Baker, J. R. et al., Generalized approach to inverse problems in tomography: image reconstruction for spatially variant systems using natural pixels, in *High-Performance Computing in Biomedical Research*, Pilkington, T. et al., Eds., CRC Press, Boca Raton, FL, 1993.
74 Shaw, P. J. and Rawlins, D. J., Three-dimensional fluorescence microscopy, *Prog. Biophys. Molec. Biol.*, 56, 187–213, 1991.
75 Guardo, R., Boulay, C., Murray, B., and Bertrand, M., An experimental study in electrical impedance tomography using backprojection reconstruction, *IEEE Trans. Biomed. Eng.*, 38, 617–626, 1991.
76 Yorkey, T. J., Webster, J. G., and Tompkins, W. J., Comparing reconstruction algorithms for electrical impedance tomography, *IEEE Trans. Biomed. Eng.*, 34, 843–852, 1988.
77 Bhargava, V. and Hagan, G., High resolution parametric imaging for the assessment of organ blood perfusion and its dynamics, in *Computers in Cardiology*, IEEE Computer Society Press, Los Alamitos, CA, 1990, pp. 129–132.
78 Spero, L. A. et al., A multiuser networked system for the large scale study of coronary artery restenosis using quantitative and qualitative coronary angiography, in *Computers in Cardiology*, IEEE Computer Society Press, Los Alamitos, CA, 1990, pp. 195–198.
79 Bosch, J. G. et al., Developments towards real-time frame-to-frame automatic contour detection on echocardiograms, in *Computers in Cardiology*, IEEE Computer Society Press, Los Alamitos, CA, 1990, pp. 435–438.
80 Windyga, P., et al., Knowledge-based approach to the management of serious arrythmia in the CCU, *Med. Biol. Eng. Comput.*, 29, 254–260, 1991.
81 Kuncheva, L. I., Fuzzy multi-level classifier for medical applications, *Comput. Biol. Med.*, 20, 421–431, 1990.
82 Kaplan, D. T. et al., Aging and the complexity of cardiovascular dynamics, *Biophys. J.*, 59, 945–949, 1991.

83 Kaplan, D. T., Chaotic statistics of biomedical time series, in *17th Annu. Northeast Bioeng. Conf*, IEEE Press, New York, 1991, pp. 33–34.
84 Hsia, P.-W. E., Hellmann, K. W., and Mahmud, R., Variation of cycle length in epicardial electrograms: a quantification of chaos of ventricular fibrillation using a sock electrode array, in *Computers in Cardiology*, IEEE Computer Society Press, Los Alamitos, CA, 1990, pp. 421–424.
85 Bollacker, K. D., Alferness, C. A., Smith, W. M., and Ideker, R. E., A cellular automata model of electrical propagation in cardiac tissue, in *Computers in Cardiology*, IEEE Computer Society Press, Los Alamitos, CA, 1990, pp. 525–528.
86 Saxberg, B. E. H. and Cohen, R. J., Global analysis of self-sustained reentry by cellular automata models, in *Computers in Cardiology*, IEEE Computer Society Press, Los Alamitos, CA, 1990, pp. 31–34.
87 Tai, S. C., Slope—A real-time ECG data compressor, *Med. Biol. Eng. Comput.*, 29, 175–179, 1991.